THE ROLE OF *NRG3* IN MENTAL ILLNESS AND NEURODEVELOPMENT:

PREDISPOSITION TO "DELUSION" PHENOTYPE

by

Mariela A. Zeledón A.

A dissertation submitted to Johns Hopkins University in conformity with the requirements for the degree of Doctor of Philosophy

Baltimore, Maryland

January, 2014

© Mariela A. Zeledón A. 2014

All rights reserved

Abstract

Background

Schizophrenia (SZ) is a chronic, common, disabling neuropsychiatric disease that affects about 1% of the population. Despite evidence for a prominent genetic contribution to risk for SZ, there are relatively few replicated positive results. Among the genes that have been identified as possible SZ susceptibility genes are *ErbB4*, *NRG1*, and the topic of my dissertation, *NRG3*.

In 2003, Fallin *et al.* reported a linkage signal in chromosome 10q22 in a rigorously-phenotyped homogeneous Ashkenazi Jewish (AJ) population, and a follow-up association study across the linkage peak identified a strong association of several intronic SNPs in *NRG3* (rs60827755, rs10883866 and rs10748842) with the a factor designated "Delusion." This was one of 9 factors derived from a principal component analysis of 73 phenotypic features.

Methods

We used next-generation sequencing in a population of patients that ranked at the extremes of the delusion score distribution in order to identify those variants in the 162 Kb that were most associated with delusion score. Of the top-ranking SNPs, five were chosen for dual-luciferase reporter assays to test for regulatory potential.

In order to test for nuclear protein binding, we used electrophoretic mobility shift assays (EMSAs). We compared binding patterns between alleles and determined relative binding strength by competing with unlabeled probe. Using an *in silico* approach, we predicted which known proteins may bind our regions of interest, and proceeded to test one by supershift.

We also characterized a *Nrg3* knockout mouse developed by our laboratory. We performed a battery of behavioral tests relevant to models of schizophrenia. In order to test whether our mouse has the interneuron migration deficits predicted by previous publications, we assayed neuronal migration by labeling cells born at E12.5 with EdU, and then immunostaining for age-appropriate GABAergic interneuron markers at various developmental and postnatal ages.

Results and Conclusions

We identified three SNPs that exhibit regulatory potential and are most-highly associated with our delusion phenotype. We show that all three SNPs bind to nuclear proteins and that two of them do so differentially. We then show evidence for possible binding of CNOT4 to a 21-bp region of DNA centered around rs60827755. Further experiments are required to confirm this observation, but we believe that elucidating the pathway whereby *NRG3* mediates its effect on the SZ phenotype will be beneficial in understanding the neuronal basis of delusions.

The *Nrg3*$^{-/-}$ animals exhibit a pervasive hyperactivity phenotype, with more subtle deficits in pre-pulse inhibition and startle response. Additional findings include decreased anxiety, pre-pulse inhibition and startle response deficits, fear and/or emotional- based learning or memory deficits, and perturbed working memory. Since these findings are consistent and comparable to those of other mouse models for schizophrenia developed by knocking out other genes in the NRG/ErbB4 pathway, we conclude that this is a useful model for schizophrenia research.

Migration assays revealed that the absence of *Nrg3* does not lead to a depletion of interneurons in several regions of the cortex, but there does appear to be a depletion of interneurons in at least one other region (striatum). We surmise that a migratory change concentrates GABAergic interneurons in the cortex at the expense of other regions of the brain.

Advisor: David Valle

Advisor: Akira Sawa

Acknowledgements

Studies in genetics constantly remind us of the importance of family, so I would like to start by acknowledging mine. My mother and father did far more than just pass on their genes to me—they have been (and continue to be) an unwavering source of support for me. Through their example, dedication, love, and foresight, they provided me with every opportunity to pursue my academic and (somewhat quixotic) personal interests. My brother has likewise been a source of encouragement, pride and support, and I am very proud of his accomplishments. My grandparents deeply enriched my childhood and adolescence, showering me with love and affection.

I would also like to thank Dan for all his love and support. From installing thermostats to trips to Shenandoah, I always look forward to his "Hey…I have an idea." His intellectual curiosity is a constant inspiration to me. I am also thankful to him for "co-parenting" our dog, Panda Bear, whose antics make us laugh after a long day, whose "life-hacks" put us to shame and who constantly reminds me to stop, smell, and occasionally eat the flowers. I am also deeply grateful to him for generating scripts to automate gel shift figures.

I would like to thank the many people who have fostered my love of science throughout my education, especially Ms. Vargas and Ms. Carcheri at Country Day School, and Dr. Beth Jones at Carnegie Mellon. Dr. Jones's encouragement and support were critical in my decision to pursue human genetics and I am enormously grateful to her.

I would like to thank my advisors, Dr. Sawa and Dr. Valle. Dr. Sawa has made a point of helping me connect with people, both people whose work I have long admired as well as possible collaborators or mentors. His appreciation for my genetics background and his help with neuroscience have helped me grow as a scientist. His lab has grown tremendously in the years I have been his student, and there are far too many people who have contributed to the development of my thesis to list them all. However, I would like to make special mention of Yu Taniguchi, Dr. Lindsay Hayes, Dr. Hanna Jaaro-Peled and Dr. Shin-ichi Kano. Lindsay and Hanna have been absolutely instrumental in helping me plan and execute the experiments outlined in Chapter 4.

Dr. Valle has been more than a mentor to me. His cutting insight and view of the patient as a whole person have been inspiring, and his willingness to discuss anything from tropical birds to ELSI matters to troubleshooting experiments have been invaluable. The members of the Valle, Vernon and Avramopoulos labs—Gary Steel, Cassandra Obie, Dr. Nara Sobreira, Dr. Yaping Liu, Julie Jurgens, Jing You, Kaitlin Victor, Dr. Megan Szymanski Pierce, Dr. Hilary Vernon, Nicole Eckart, Xuan Pham, Alex Hatzimanolis and Ruihua Wang—have made my time in lab more than enjoyable. And, of course, I must thank Dr. Paylong Chen, on whose doctoral work this dissertation relies on so heavily.

Cassandra Obie has been enormously helpful in teaching me how to grow cells, chastise teenagers and do crossword puzzles, to name a few. Her humor and friendship have brightened up many a breakfast and lunch. She is also responsible for generating the Northern Blot data in chapter 4. Gary Steel

should also be acknowledged for his direct contributions to this work. He has maintained the Valle lab mouse colonies and provided me with all the mice I could want for primary neuron cultures, migration experiments and phenotyping. Additionally, he collected all the behavioral data with the guidance of Dr. Mikhail Pletnikov, who has been extraordinarily patient with me as I tried to better understand statistics. As if that were not enough,Gary and Cassandra stepped in to keep my cells, mice and experiments going every time I went to a conference or had surgery.

Dr. Ann Pulver and her group (especially John McGrath and Paula Wolyniec) have made this research possible by collecting and carefully phenotyping the patients described below. They have always helped me get all the DNA, pedigrees and information I could possible need for my experiments.

My summer student, Gabriela Abril, was very helpful in preparing the brain sections, imaging them, and processing the data.

I would also like to thank my thesis committee members, Dr. Dimitrious Avramopoulos and Dr. Andy McCallion. Dimitri's door has always been open to me, and I have come to see him as a third advisor. I'm thankful for Andy's willingness to pore over raw data with me, and to encourage while pushing me to always do better.

I would also like to thank the Human Genetics program at Johns Hopkins, both the students and the administration for making my time here memorable. I would especially like to thank Sandy Muscelli, David Valle, Andy McCallion and Kirby Smith for their hard work in keeping the program running

and improving, and Juan Calderón and Tara Doucet and Margot Munzel for their friendship and encouragement.

Table of Contents

List of Tables

List of Figures

Chapter 1 : Introduction

Schizophrenia

Schizophrenia (SZ) is a chronic, common disabling neuropsychiatric disease that affects about 1% of the population.[1-3] The age of onset is typically in young adulthood and response to treatment is poor. The symptoms of SZ are generally classified in three domains: a positive symptom domain that includes delusions and hallucinations; a negative symptom domain characterized by apathy, alogia, blunted affect and social withdrawal; and a cognitive symptom domain that encompasses disorganization in speech and thought.[4]

Schizophrenia is a complex genetic disorder, with susceptibility determined by both genes and environment. The evidence for a genetic contribution to SZ is strong, with a sibling relative risk of 10%, and dizygotic and monozygotic twin concordance rates of ~17% and ~50%, respectively.[5] Heritability of SZ is estimated between 60-89%.[6,7]

Despite this evidence for a prominent genetic contribution to risk for SZ, traditional genetic methods of disease gene identification (linkage and association) have produced relatively few replicated positive results, in part because of phenotypic variability and genetic (allelic and locus) heterogeneity.[2,8-18] Among the genes that have been identified as possible SZ susceptibility genes are *ErbB4*[19-21], *NRG1*[22,23], and the topic of my dissertation, *NRG3*.

Neuregulin 3 as a SZ susceptibility gene

Neuregulin 3 *(NRG3)* is a strong biological candidate gene for SZ. It is one of three paralogs of *NRG1*, another replicated SZ susceptibility gene.[22,23] Like *NRG1, NRG3* undergoes extensive alternative splicing and alternate utilization of first exons (Figure 2-1). Expression of N*RG3* is limited to brain, breast, and testis and is higher early in development.[22,24] The protein product of *NRG3* is a single-pass Type I membrane protein with an extracellular N-terminal EGF-like domain that is cleaved and binds ErbB4 receptors[25-27] encoded by *ErbB4*, another gene implicated in SZ.[19-21] Originally thought to function as an attractive signaling protein, NRG3 appears to function as a chemorepellant signal in patterning and migration of GABAergic interneurons in the developing cerebral cortex.[28-30]

In 2003, Fallin *et al.* [31] reported a linkage signal in chromosome 10q22 (nonparametric linkage score of 4.27) in a rigorously-phenotyped homogeneous Ashkenazi Jewish (AJ) population. This result was independently replicated in the Han Chinese population.[32]

A follow-up association study across the linkage peak with 9 factors (heritability ranging from 0.27-0.60) derived from a principal component analysis of 73 phenotypic features was performed in the AJ population and identified a strong association ($p = 1.6 \times 10^{-6} – 2.3 \times 10^{-7}$) of several intronic SNPs in *NRG3* (rs6584400, rs10883866 and rs10748842) with the factor designated "Delusion."[33,34]

This delusion factor is heavily loaded with positive symptoms of SZ, including thought insertion; delusions of influence, guilt and reference;

somatic, olfactory and tactile hallucinations; thought withdrawal; thought broadcasting; thought echo, primary delusions and primary delusional perception.[33] This constellation of symptoms closely resembles Schneiderian first rank symptoms, and was originally given that name.[35] Subjects who score highly in the delusion factor tend to exhibit more of these symptoms than other patients with schizophrenia.

The aforementioned association of SNPs in *NRG3* with a delusion factor was replicated in Western European[36] and in Anglo-Irish cohorts.[37] In the former, the authors suggested a functional role for rs10748842, possibly by regulating relative abundance of *NRG3* isoforms.[36]

Thesis Statement

The thesis of this dissertation is that variants in *NRG3* affect the expression and/or splicing of this gene. Regulatory imbalances in *NRG3* absolute levels or relative isoform abundance lead to a predisposition to a subtype of SZ that exhibits more types of delusions. This effect is mediated by improper neural migration during development and leads to behavioral abnormalities seen in other mouse models of SZ.

Contributions

Despite the replications of the original linkage and association signals, NRG3 remains a poorly-studied gene that presents an interesting opportunity to

study the modulation of the schizophrenia phenotype. This dissertation aims to better understand the genetics of *NRG3* and its association with schizophrenia, and specifically contributes the following:

- New, inclusive nomenclature of all known exons of *NRG3*
- Identification of causative variants in the association of the *NRG3* gene with the delusion factor
- Evidence of the regulatory effect of SNPs in *NRG3*
- Exploration of putative transcription factors that bind regulatory SNPs and thus mediate the effect of *NRG3* on schizophrenia
- Characterization of neurodevelopmental phenotype of a *Nrg3* knockout mouse
- Analysis of results of behavioral experiments conducted on a *Nrg3* knockout mouse

Chapter 2 : Identification and functional studies of regulatory variants in NRG3 associated with a delusion phenotype in schizophrenia

Mariela Zeledón, B.S. [1,2,3], Margaret Taub Ph.D.[5], Nicole Eckart, B.S. [1,2], Hilary Vernon, MD/Ph.D. [1] , Megan Szymanksi, Ph.D. [1,2], Ruihua Wang, MD. [1], Pei-Lung Chen MD, Ph.D. [6] , Gerry Nestadt, MD [3], John A. McGrath, MA [3,4], Akira Sawa, MD/Ph.D.[3], Ann E. Pulver, Sc.D. [3,4], Dimitrios Avramopoulos, MD, Ph.D. [1,3], David Valle, MD [1]

1) McKusick-Nathans Institute of Genetic Medicine, Johns Hopkins University School of Medicine, Baltimore, MD; 2) Predoctoral Training Program in Human Genetics, Johns Hopkins University School of Medicine, Baltimore, MD; 3) Department of Psychiatry and Behavioral Sciences, Johns Hopkins University School of Medicine, Baltimore, MD; 4) Epidemiology-Genetics Program, Bloomberg School of Public Health, Johns Hopkins University, Baltimore, MD; 5) Biostatistics, Bloomberg School of Public Health, Johns Hopkins University, Baltimore, MD; 6) Department of Medical Genetics, National Taiwan University Hospital, Taipei City, Taiwan.

Abstract

Schizophrenia (SZ) is a severely disabling psychiatric disorder affecting 1% of the world's population. It is both phenotypically and genetically heterogeneous. Previously, we reported a linkage peak for SZ (NPL of 4.7) at 10q22 in the Ashkenazi Jewish (AJ) population and, in a follow-up fine mapping association study, found strong evidence of association between the "delusion"

factor score of our phenotypic principal component analysis and three intronic SNPs in the 5' end of Neuregulin 3 (*NRG3)*. Independently, two other groups have replicated these findings. In aggregate, these results indicate variants in *NRG3* confer risk for a subtype of schizophrenia with a multiplicity of delusions, particularly first rank symptoms.

To identify the responsible causative variants, we sequenced the 162 kb linkage disequilibrium (LD) block covering the 5' end of *NRG3* and containing the three associated SNPs in 47 AJ SZ patients at the two extremes of the delusion quantitative trait distribution. We identified 5 noncoding SNPs with minor alleles on the implicated haplotype that were significantly overrepresented in subjects scoring high on the delusion factor. We tested these for regulatory effects and found that risk alleles of rs10883866 and rs60827755 significantly and reproducibly decreased and increased (3-4 fold), respectively, the expression of a reporter gene when compared to the alternative allele in various cell types. Post-mortem RNA quantification experiments suggest the same variants perturb expression of *NRG3* isoforms. In summary, we have identified the regulatory single nucleotide variants responsible for the association of *NRG3* with delusion symptoms in SZ.

Introduction

In 2009, Chen et al. [34] reported an association of several SNPs in *NRG3* with a delusion factor heavily-weighted for traits similar to Schniderian First-rank symptoms. The SNPs with the most significant association (rs10883866, rs10748842 and rs6584400) were located in a 162kb linkage disequilibrium

(LD) block in the 5' end of *NRG3*, which includes the region upstream (5') of the gene, its promoter regions, several exons as well as large introns. This chapter describes the efforts to identify and characterize the functional variants underlying the association with the delusion factor in the LD block containing the associated SNPs.

Materials and Methods

Nomenclature of NRG3 gene

A comprehensive literature search was conducted for nomenclature of known exons as well as reports of novel exons in *NRG3*. Unpublished data from H. Vernon studying the structure of NRG3 cDNA was added to these reports, and the UCSC genome browser (genome.ucsc.edu) was queried for reported exons and alternate exon usage. The exons were compared to determine overlap between sources, and a comprehensive list of exons generated without regard to splicing patterns.

Subject Ascertainment and Factor Analysis

All of the subjects were participants in the Research Program of the JHU Epidemiology-Genetics Program. The ascertainment and assessment of these patients and controls has been previously described.[31,34,38]

The factor analysis derivation has been previously described.[33] For family studies, 10 probands were selected based on their heterozygosity for a 1.8kb

deletion and availability of DNA and psychiatric history from at least one first-degree relative.

Next-generation sequencing, analysis parameters and software

To generate sequencing libraries, we amplified 19 overlapping ~10kb amplicons to cover the entire 162kb LD block using LA Taq (Kyoto, Japan) and the following conditions: 2 min at 94°C, 14 cycles of 10 sec at 98°C and 20 min at 68°C, 16 cycles of 10 sec at 98°C and 20 min at 68°C, where for each additional cycle the time was increased by 15 sec per cycle, and finally a single 20-min step at 72°C. Fragmentation to approximately 250bp was done using a Covaris sonicator (Herts, England). During the library preparation stage, we multiplexed samples for library preparation in groups of 12, each including 6 low delusion and 6 high delusion individuals. Each multiplexed library was then sequenced in one or two lanes obtaining 75bp paired-end reads on the Illumina Genome Analyzer or the Hi-Seq 2000.

We aligned the reads using the BWA aligner (version 0.5.9) with default settings[39] and post-processed aligned reads using the Genome Analysis Toolkit (GATK, version 1.0.5336)[40] to remove duplicate reads, realign around small insertions or deletions (indels) and recalibrate base-call quality scores. We excluded one high delusion subject from the analysis due to low coverage depth (55) relative to the other samples (average coverage of 850). The median fraction of reads that aligned was 90%. We called single-nucleotide variants (SNVs) and indels using samtools mpileup[41] (version 0.1.17) on all samples simultaneously with parameters -C50 -D -S -d 50000, which were chosen to down weight reads

with excessive mismatches and to allow for high depth coverage. We filtered variant calls based on software recommendations and performance on validation data removing a marker if its overall call quality score was less than 99 and set individual calls to missing if their call quality was below 40.

We also assessed quality and depth of coverage differences between our groups of interest at each variant, comparing these quantities between low and high delusion individuals using a t-test to ensure that differences in sequencing effort or variant call quality between the two groups would not produce biased results in genotype comparisons. We removed variants with p-values less than 0.1 on either of these tests, from further consideration.

We validated a total of 790 known variants across the region in all subjects using previously-obtained SNP genotypes at 19 positions[34]. Of these, 773 were correctly called from our unfiltered SNV detection, for an accuracy of 97.8% (95.1% sensitivity, 99.5% specificity using a variant presence/absence criteria). After setting all calls with an individual call quality less than 40 or a variant call quality less than 99 to missing, 6 incorrect calls remained. This accuracy of 99.2% reflects 100% specificity and 98.1% after filtering

Deletion studies

During the amplification process, we identified a 1.8 kb deletion located 23 kb upstream of the *NRG3* transcriptional start site and genotyped it by PCR amplification as follows: 94°C for 3 min, followed by 31 cycles of 94°C for 45 sec, 60°C for 30 sec, and 72°C for 3 min, and afterwards, 10 min at 72°C. We

calculated association of this deletion to the delusion QTL using UNPHASED software[42].

In family studies and in other population studies we genotyped the deletion using a three-primer assay (Figure 2-5) with a single forward primer 5' of the deletion and two reverse primers, one in the deleted region and one 3' of the deletion. In this assay, a deleted chromosome yields a 249 bp amplicon while a non-deleted chromosome yields a 406 bp product. PCR cycling conditions were: 94°C for 2 min, followed by 31 cycles of 30 sec at 94°C, 61°C and 68°C.

Reporter constructs

To determine if the deleted region had regulatory activity, we generated dual-luciferase reporter assay (DLA) reporter constructs of the genomic region of interest by PCR amplification from subjects who were homozygous for either the deleted or non-deleted allele. We generated two PCR amplicons: the "WT" was 3.8kb and included the region of the deletion plus 1kb flanks on both sides; the "Deleted" construct (Del) was 2kb and included only the 1kb regions flanking the deletion. For the WT construct, we used AccuPrime PCR Systems (Invitrogen, Carlsbad, CA) with the following cycling conditions: 94°C for 2 min, 26 cycles of 30 sec at 94°C, 30s at 57°C and 5 min at 68°C, followed by 5 additional min at 68°C. For the Del construct, we used Taq Polymerase (Invitrogen, Carlsbad, CA). The PCR cycling conditions were: 95°C for 1 min, 31 cycles of 95°C for 30 sec, 58°C for 30 sec and 72°C for 4 min 20 sec, followed by a single step at 72°C for 10 min. The products were gel-extracted using the

QIAquick Spin Kit (Qiagen, Hilden, Germany) and concentrated to at least 25ng/µl by ethanol precipitation.

To determine if the deletion had some effect based on spatial characteristics of the region, we also made a "Stuffer" construct (Stu) based on the Del construct. We utilized a 1.8kb segment of an enhancerless zebrafish construct (ZNAS -17.9) previously found to have no enhancer activity in DLAs.[43] To produce the construct we amplified three segments: the 1 kb 5' flank using a reverse primer with an added *BamHI* site; the 3' flank using a forward primer with an added *ClaI* site; and the 1.8kb stuffer with a forward primer that included a *Bam HI* site and a reverse primer that included a *ClaI* site. Cycling conditions were: 94°C for 3 min, followed by 31 cycles of 94°C for 45 sec, 60°C for 30 sec, and then by 72°C for 3 min, and 10 min at 72°C. We gel-purified the amplicons as above, digested, gel extracted again, and ligated equimolar amounts. We amplified ligation products using the following PCR cycling conditions: 94°C for 3 min, followed by 31 cycles of 94°C for 45 sec, 60°C for 30 sec, and 72°C for 4 min, and afterwards, 10 min at 72°C and gel-purified product.

To produce constructs containing the single nucleotide variants to be tested for regulatory effects, we amplified an approximately 320 bp segment including the regions of highest conservation around the variant, using as template subjects heterozygous for the SNPs. PCR cycling conditions were: 94°C for 3 min, followed by 31 cycles of 94°C for 45 sec, 60°C for 30 sec, and 72°C for 3 min, followed by, 10 min at 72°C. The products were gel-purified and cloned. In our sample of individuals, we identified three haplotypes for SNPs

rs10883862 and rs7919976, which are 35 bp apart, and generated single constructs for each of three haplotypes. Also, we produced a 2.7 kb construct combining rs10748842 and rs60827755 by PCR amplification from 2 subjects using the following cycling conditions: 3 min at 94°C, 31 cycles of 45 sec at 94°C, 30 sec at 56.5-63°C, and 3:30 min at 72°C, followed by a single step at 72 for 10 min. The products were gel-purified and cloned as above.

For all constructs, the inserts were cloned using the pCR8/GW/TOPO TA Cloning Kit (Invitrogen, Carlsbad, CA) following addition of A bases (7ul of DNA, 1 ul of Taq Polymerase, 1ul of 10X PCR Buffer and 1ul of a 12:1:27 mixture of 50 mM $MgCl_2$: 100mM ATP: water incubated at 72°C for 10 min). The recombinant plasmids were harvested from 5mL liquid culture with spectinomycin, miniprepped using the QIAprep Miniprep kit (Qiagen, Hilden, Germany), tested by restriction enzyme digest and Sanger sequencing, and the inserts shuttled to pDSMA, a Gateway-modified pGL3-promoter plasmid[44] using LR Clonase Enzyme Mix (Invitrogen, Carlsbad, CA). The transformants were cultured in LB media with carbenicillin, miniprepped, and tested by restriction enzyme digest and Sanger sequencing. We selected clones with no mutations, cultured them in 50 ml LB with carbenicillin, harvested the plasmid by QIAfilter Plasmid Purification Midi Kit (Qiagen, Hilden, Germany) and diluted each to 100ng/ul (SNP constructs) or 200ng/ul (all others).

Dual-luciferase reporter assays

We cultured HT22[45], HEK 293, and Neuro2A lines in Dulbecco's modified Eagle's medium (DMEM) with Glutamax and 10% FBS. Primary cortical neuron

cells from E18 C57BL/6 mice for assays testing the deletion, or E18 SD rat for assays testing SNPs were cultured and maintained as described previously.[46] To minimize cell death, we switched the cultures to medium without antibiotics 24 hr prior to transfection. We co-transfected cells with the pGL3 and Renilla vectors at a 20:1 ratio using lipofectamine-2000 (Invitrogen, Carlsbad, CA) according to the manufacturer's instructions and lysed the cells 24 hours post-transfection in passive lysis buffer according to the manufacturer's instructions (Promega, Madison WI) except that we used 20ul of lysate and 50ul of each reagent for the assays.

Human brain mRNA studies

We extracted DNA and total RNA from subjects without macroscopic pathology from 190 superior temporal gyrus (STG) samples from the Harvard Brain Tissue Resource Center (HBTRC) and 94 dorsolateral prefrontal cortex (DLPFC) samples from the National Institute of Child and Human Development (NICHD). Samples were genotyped for rs10748842 and rs60827755 by TaqMan genotyping assays (Invitrogen, Carlsbad, CA).

Expression of *NRG3* transcripts initiating with exon 1a and exon 1b was measured separately, using exon-specific primers for qPCR of cDNA reverse transcribed from brain RNA , and was quantified by comparison to a standard curve with normalization to the expression of two housekeeping genes, *MRIP* and *ACTB*, as described.[47] The data were log transformed to achieve a normal distribution and outliers were removed.

Using a generalized linear model, we interrogated the expression data for correlations with genotypes at selected SNPs using age, sex, qPCR plate, and post mortem interval as covariates. To examine changes in relative abundance of classes of transcripts, we adjusted expression of transcripts initiating with exon 1b for that of transcripts initiating with exon 1a.

Results and Discussion

Previously, our laboratory had examined 720 AJ SZ probands for association between each of 9 quantitative traits (phenotypic principal component factor scores) and select genotypes around *NRG3*. We found significant association of the Delusion factor with the genotypes of SNPs in a 162 kb LD block covering the 5' end of *NRG3*.[34] Here, we sequenced SZ subjects stratified according to their scores on the Delusion quantitative trait (QT) with the goal of finding the variant(s) responsible for the association signal. High and low delusion subjects differed primarily in the number of types of delusions that they exhibited, with high delusion factor subjects experiencing more kinds of delusions.[33]

Sequencing of the NRG3 5' 162kb LD block

To identify all variants across the LD block, we sequenced subjects in 4 pooled sets of 12 samples (6 from the high and 6 from the low extremes of the Delusion QT distribution). The minimum average depth for samples included in the analysis was 334, and 98.6% of positions in our region of interest were covered by at least 15 reads, which is considered more than sufficient for analysis.[48] There was no difference between the high and low delusion groups in average coverage (t-test p=0.49) or percentage of bases covered by at least 15 reads (t-test p=0.20). This result indicates that between-sample differences in these variables did not bias our subsequent analyses.

A microdeletion upstream of NRG3 is associated with delusions but lacks functional consequences

PCR and sequencing revealed a 1.8 kb microdeletion located 23kb 5' of the predicted transcription start site of *NRG3* (Figure 2-2). This previously unreported microdeletion is in a region with low sequence conservation. There are flanking clusters of transcription factor binding sites (TFBSs), ~ 6kb 5' and ~12kb 3' of the microdeletion.

To determine if the microdeletion itself was a causative variant, we first measured its frequency in various populations (Table 2-1). We found similar frequencies in our sample of AJ SZ (2.65%, n=641), AJ BP (2.57%, n=564) and AJ Control (2.8%, n=642) cohorts. However, when we tested SZ patients at both extremes of the delusion quantitative trait, we found a significant difference in

frequencies (8/138 or 5.8% in the high compared to 0/134 alleles or 0% in low delusion patients; Fisher exact test p=0.013). To investigate this association with delusion scores in a larger SZ cohort, we genotyped the microdeletion in 624AJ SZ subjects across the range of delusion scores and found a strong association with delusion (genotype effects p=0.006895). We did not detect the microdeletion in 346 outbred American European SZ subjects, suggesting that it is specific to Ashkenazim. We also genotyped the microdeletion in 10 unrelated families with heterozygous probands and found that it was inherited and had identical breakpoints in all. From these results, we reasoned that the microdeletion was either causative or marked a haplotype containing a causative variant(s).

To investigate potential regulatory effects of the microdeletion, we performed DLAs in human HEK 293 cells, HT22 cells and cultured mouse cortical neurons. We found no difference in relative expression among our various reporters, even when we corrected for possible spatial effects by introducing an inactive stuffer sequence into our deletion construct (Figure 2-3). These *in vitro* experiments suggested that the microdeletion lacks regulatory consequences and, more likely, marks a haplotype containing causative variant(s).

Identification of variation in cis with the microdeletion

During the course of these studies, we identified two homozygotes for the microdeletion, a BP subject and a non-affected relative of a SZ. The latter, a 66 year old asymptomatic woman (98023-3446), has a brother and a nephew with

SZ. Sequencing of 98023-3446 revealed homozygosity for all SNPs across the entire LD block (Figure 2-2), including the risk alleles of previously identified delusion-associated SNPs.[34] She has 121 homozygous non-reference variants and no heterozygous variants, suggesting that the microdeletion haplotype extends across the entire sequenced region. Genotyping 5 other members in her family and 31 unrelated affected AJ microdeletion heterozygotes allowed us to define three distinct haplotypes across the LD block, one that is marked by the microdeletion and likely contains the risk variants and two others without the microdeletion that likely do not carry the risk variants. Sequencing the LD block in 24 individuals with high delusion QT scores, 23 with low delusion QT score and 98023-3446 identified a total of 620 SNVs in the LD block. Of the 57 SNVs associated with a high delusion score ($p < 0.05$) in the present study, 54 were non-reference alleles homozygous in 98023-3446 and we concluded these made up the microdeletion haplotype.

To assess differences between low and high delusion subjects at each of these 54 SNVs, we ranked them according to p-value as calculated by Fisher's exact test (Figure 2-2C and Table 2-2). While no results withstood correction for multiple testing, the 5 nominally most significant ($p = 0.003$ for all 5, MAF=0.104 -0.424) were located in a ~8kb cluster flanking and including exon 2. Two SNVs (rs10883866 and rs10748842) were among the three previously identified to be most associated with the delusion factor.[34] The third, rs6584400, while not among the most significantly associated SNPs, had a p-value of 0.015 and was included in our functional studies of a total of 6 variants. The risk alleles of all of these variants ($p<0.05$) are on the microdeletion haplotype.

Variants in intronic regions of NRG3 affect NRG3 expression in vitro and ex-vivo

To determine if the variant genotype affected regulatory function of the surrounding sequence, we performed DLAs testing ~320bp surrounding either allele of a SNV in HEK 293, HT22, Neuro2A cell lines, and rat primary cortical neurons.

We tested rs7919976 and rs10883862, which are only 67bp apart (R^2=0.329), in a single construct and detected no discernible regulatory activity (Figure 2-4). Variant rs6584400 had a minimal and inconsistent effect regardless of genotype. For these reasons, we did not perform additional studies on these variants. We observed modest effects for rs10748842 with the minor allele increasing relative expression by ~1.2 fold. For this reason and because this variant was implicated by previous authors based on *in silico* computational analysis, we included it in additional studies. In contrast, we find that rs10883866, located 5 kb 5' of exon 2, has a strong and consistent effect in DLA experiments. The construct containing the common, non-risk variant conferred a 2-3 fold increase in expression over empty vector in all cell lines tested (in primary rat cortical neurons, the effect was more modest but in the same direction) and this effect was completely abrogated by the the risk variant. We conclude that rs10883866 is a causative variant that perturbs the regulatory function of a DNA element in this genomic location and that in these *in vitro* assays, the effect of the risk variant is to decrease expression. Similarly, rs60827755, located 1.5 kb 5' of exon 2, also showed a consistent effect on expression in all cell types tested. In this case, however, the risk allele is

associated with an increased expression ranging from 0.25-2 fold over the empty vector and 2.5-6 fold over constructs with the non-risk variant ($p= 10^{-4}$ - 10^{-11}). We conclude that rs60827755 is also a causative variant but with opposite effects on expression in these *in vitro* assays.

A curious aspect of our results with rs10883866 and rs60827755 is that the minor alleles, which are both on the risk haplotype, direct expression of the reporter in opposite directions. *In vivo,* the effects of these variants will depend on the relative abundance of the trans-acting factors that bind these regions as well as the context beyond the 320 bp inserts in the test plasmids.

SNPs in NRG3 correlated with alternate first exon use

NRG3 undergoes complex alternative splicing with transcripts that originate from at least two alternative first exons, exons 1a and 1b.[24] We hypothesized that the SNPs associated with the "delusion" factor, which are all located in the 5' end of *NRG3,* might alter the relative abundance of transcripts that begin with exon 1a or exon 1b. To test this possibility, we asked if there was a correlation between the genotype of two variants (rs10748842, rs6087755) and the expression of different *NRG3* transcripts in 2 brain regions (Figure 2-7).[36]

After controlling for qPCR plate, age, sex, and post-mortem interval, colleagues in our laboratory found that carriers of the risk allele (C) at rs10748842 have decreased expression of transcripts containing exon 1b in the STG (p=0.026). The effect of the risk allele is highly significant when expression of transcripts initiating with 1b is adjusted for transcripts initiating with exon

1a ($p=5.11 \times 10^{-9}$). Additionally, in the DLPFC, the risk allele is correlated with lower overall expression of transcripts containing exon 1b ($p=1.9 \times 10^{-7}$), as well as expression adjusted for expression of transcripts with exon 1a ($p=4.7 \times 10^{-8}$).

The risk allele at rs60827755 (G) showed a similar correlation in the STG with decreased expression of transcripts with exon 1b overall ($p=0.048$) and when adjusted for expression of transcripts with exon 1a ($p=1.9 \times 10^{-7}$). In the DLPFC, the risk allele is associated with decreased expression of transcripts with exon 1b ($p=1.42 \times 10^{-7}$) and decreased expression adjusted for exon 1a transcripts ($p=6.0 \times 10^{-8}$). This similarity is expected as the two SNPs are in strong LD ($r^2=0.92$).

From these data, we conclude that the effect of the delusion-associated variants involves the relative expression of various *NRG3* transcripts. This suggests a transcript-specific mechanism, in which the risk variant of one SNP affects the utilization of alternative first exons.

It is important to clarify that these SNPs are associated with a patient's score on the delusion factor, and not to risk of developing SZ *per se*. They are modifiers of the SZ phenotype, and, as such, may help to predict clinical presentation within the diagnosis of SZ. While they do not directly influence the risk or the severity of illness, they do increase susceptibility to delusions in SZ patients, suggesting the importance of NRG3 in the biological pathways of SZ. Further studies are required to study whether the same variants have similar effects in other clinically relevant phenotypic features such as functional impairment or response to specific antipsychotics in SZ. Further efforts are also needed to study whether these variants increase risk of developing more types

of delusions only in the context of SZ, or whether they influence the phenotype of other mental illnesses as well.

Conclusion

In summary, we show that alleles of intronic SNPs strongly associated with a delusion QT also modulate gene expression and alternative first exon utilization. The molecular mechanism by which the single base-pair changes exert their effect is unknown, although we surmise that the variants alter binding sites for transcription factors that interact indirectly with the promoter(s). The identity of the proteins that utilize these putative binding sites to control regulation of particular transcripts of *NRG3*, as well as the functional consequences of various splice forms in specific cells types, will shed light on the molecular pathways involved in delusions and psychiatric disease, as well as deepen our understanding of the regulation of this gene.

Table 2-1: Microdeletion Frequency in Populations

Population	Subjects	Deleted Alleles	Alleles tested	Subjects with Genotype			Allelic Frequency
				+/+	+/-	-/-	
High delusion AJ SZ	73	8	146	65	8	0	5.8%
Low delusion AJ SZ	67	0	134	67	0	0	0%
AJ Control	642	36	1284	606	36	0	2.80%
AJ SZ	641	34	1282	1248	34	0	2.65%
Outbred SZ	346	0	692	346	0	0	0%
AJ Bipolar	564	29	1128	536	27	1	2.57%

Table2-1: Frequency of microdeletion in various population, including the extremes of the delusion score distribution in our AJ sample (high delusion AJ SZ and low delusion AJ SZ), a set of subjects with no psychiatric history (AJ Control), and the entire set of AJ SZ subjects regardless of their delusion score (AJ SZ). Additionally, SZ patients of a mixed background (Outbred SZ) and AJ subjects diagnosed with bipolar disorder are included (AJ Bipolar). For each group, the number of subjects tested, number of alleles tested, number of alleles bearing the deletion, number of subjects with each phenotype and the allelic frequency of the deletion is given.

Table 2-2: Variant Identification and Distribution Amongst Low- and High-Delusion Patients

RS ID	Position (hg19)	Ref	Alt	Alt Allele Freq	Low alleles	High alleles	p-value	On Del Hap	Follow-up ID
rs10883862	83642101	T	G	0.11	0/46	9/46	0.003	TRUE	A
rs10883866	83643639	C	G	0.11	0/46	9/46	0.003	TRUE	C
rs60827755	83647518	A	G	0.10	0/46	9/46	0.003	TRUE	D
rs10748842	83649739	T	C	0.11	0/46	9/46	0.003	TRUE	E
rs7919976	83642034	G	A	0.58	5/46	18/46	0.003	TRUE	B
rs74885547	83672780	T	C	0.56	8/44	22/46	0.004	TRUE	-
rs10786760	83664575	C	T	0.55	9/44	23/46	0.004	TRUE	-
rs1018484	83665670	T	C	0.56	8/44	20/42	0.005	TRUE	-
rs10884019	83757021	G	A	0.15	3/46	13/44	0.005	TRUE	-
rs11191757	83667910	G	T	0.56	9/46	22/46	0.008	TRUE	-
rs10786762	83670102	G	A	0.58	9/46	22/46	0.008	TRUE	-
rs10883921	83685802	A	C	0.57	8/46	20/46	0.012	TRUE	-
rs7075126	83688159	A	G	0.57	8/46	20/46	0.012	TRUE	-
rs10883898	83670126	C	T	0.53	8/44	20/46	0.012	TRUE	-
rs9943299	83640808	A	G	0.22	1/46	9/46	0.015	TRUE	-
rs6584400	83656526	G	A	0.22	1/46	9/46	0.015	TRUE	F
rs3918483	83668440	C	A	0.53	8/44	18/42	0.018	TRUE	-

Table 2-2: Results of our next-generation sequencing efforts. For each variant, we show the rs number, its position on chromosome 10 (using the hg19 reference genome), the reference and alternate alleles, the minor allele frequency, the number of alternate alleles out of the total alleles sequenced for both high and low delusion groups, the p-value, whether the alternate allele is on the deletion risk haplotype, and how we refer to this

allele in follow-up (if we followed-up). Variants are arranged by p-value, and only the top 17 results are shown.

Figure 2-1: Proposed Nomenclature for Exons of *NRG3*

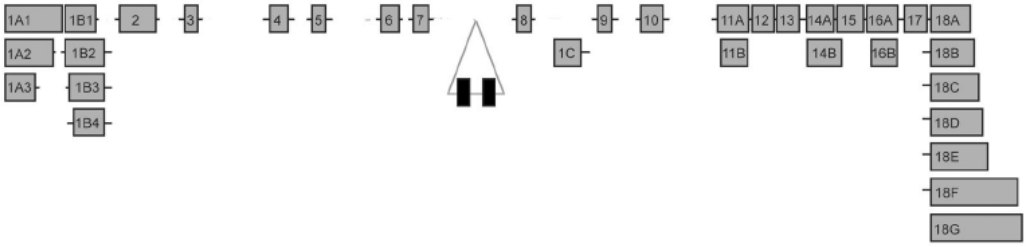

Exon	Kao	Start	Stop	Size
1A1	1	83635070	83635919	849
1A2		83635248	83635919	671
1A3		83635840	83635919	79
1B1	2	83637443	83637776	333
1B2	2ext	83637443	83637851	408
1B3		83637653	83637776	123
1B4		83637717	83637851	134
2	n/a	83648946	83649421	475
3	n/a	83680619	83680710	91
4	3	83926483	83926582	99
5	3A	83992498	83992576	78
6	4	84118495	84118624	129
7	n/a	84128646	84128721	75
8	5	84498333	84498406	73
(1C)		84559498	84559607	109
9	5A	84618889	84618979	90
10*	6	84625167	84625193	26

Exon	Kao	Start	Stop	Size
11A**	7	84711225	84711327	102
11B		84711225	84711297	72
12	7A	84714947	84714989	42
13	8	84718705	84718831	126
14A	9	84733544	84733671	127
14b	n/a	84733544	84733925	381
15*	9A	84738344	84738516	172
16A	10	84738706	84738876	170
16B		84738748	84738876	128
17	11	84744540	84744610	70
18A	12	84744854	84745361	507
18B		84744854	84745401	547
18C		84744854	84745467	613
18D		84744854	84745542	688
18E		84744854	84745589	735
18F		84744854	84746723	1869
18G		84744854	84746935	2081

Figure 2-1: Gene Structure of *NRG3*. A. Proposed nomenclature for validated exons in *NRG3* (grey) and non-*NRG3* transcripts (black). Exons and Introns are not to scale. B. Comparison with previous nomenclature.[36] 1. Shortened versions (3bp) of this exon have been reported[24] 2. Shortened versions (5bp) have been reported.[49]

Figure 2-2: Region of the 5' *NRG3* region of interest

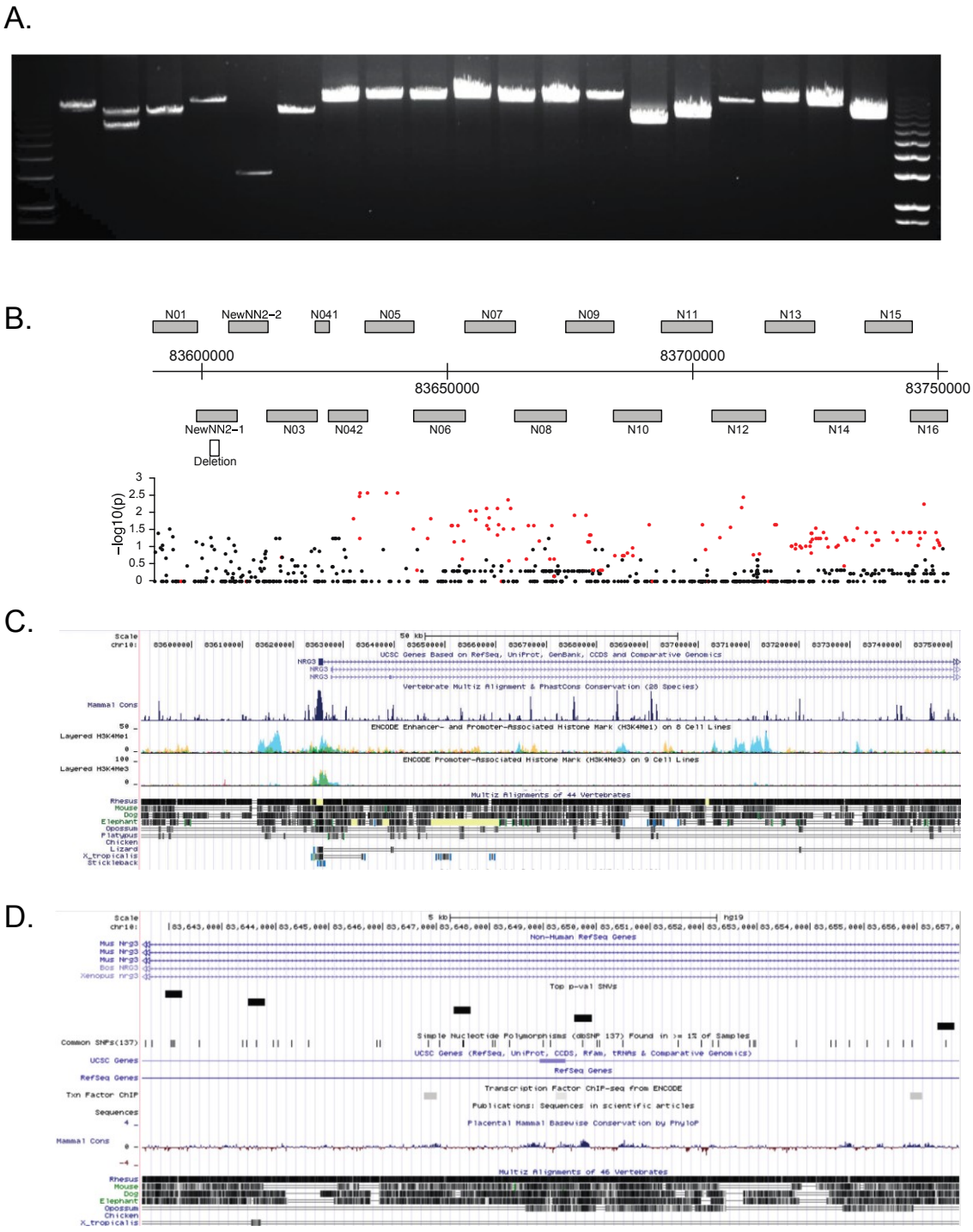

Figure 2-2. A. Gel (0.75%) electrophoresis of amplicons shown in B from a subject heterozygous for a microdeletion (hg19: Chr10: 83 611 664 - 83

613 507). B. Quantity of variants observed in low- (black) and high- (red) delusion patients by amplicon. C. UCSC genome browser view of sequenced region in chromosome 10. Tracks, from top to bottom, display genes, vertebrate conservation, histone marks (H3KMe1 and, separately, H3K4Me3), Multiz vertebrate alignment. D. UCSC genome browser view of region of *NRG3* surrounding SNPs chosen for follow-up. Tracks, from top to bottom, display non-human Refseq genes, custom track marking regions tested in DLA assays, SNPs in the region, UCSC and Refseq genes, transcription factor binding sites, conservation amongst placental mammals, and vertebrate alignment.

Figure 2-3: Dual-luciferase assays testing deleted region of *NRG3*

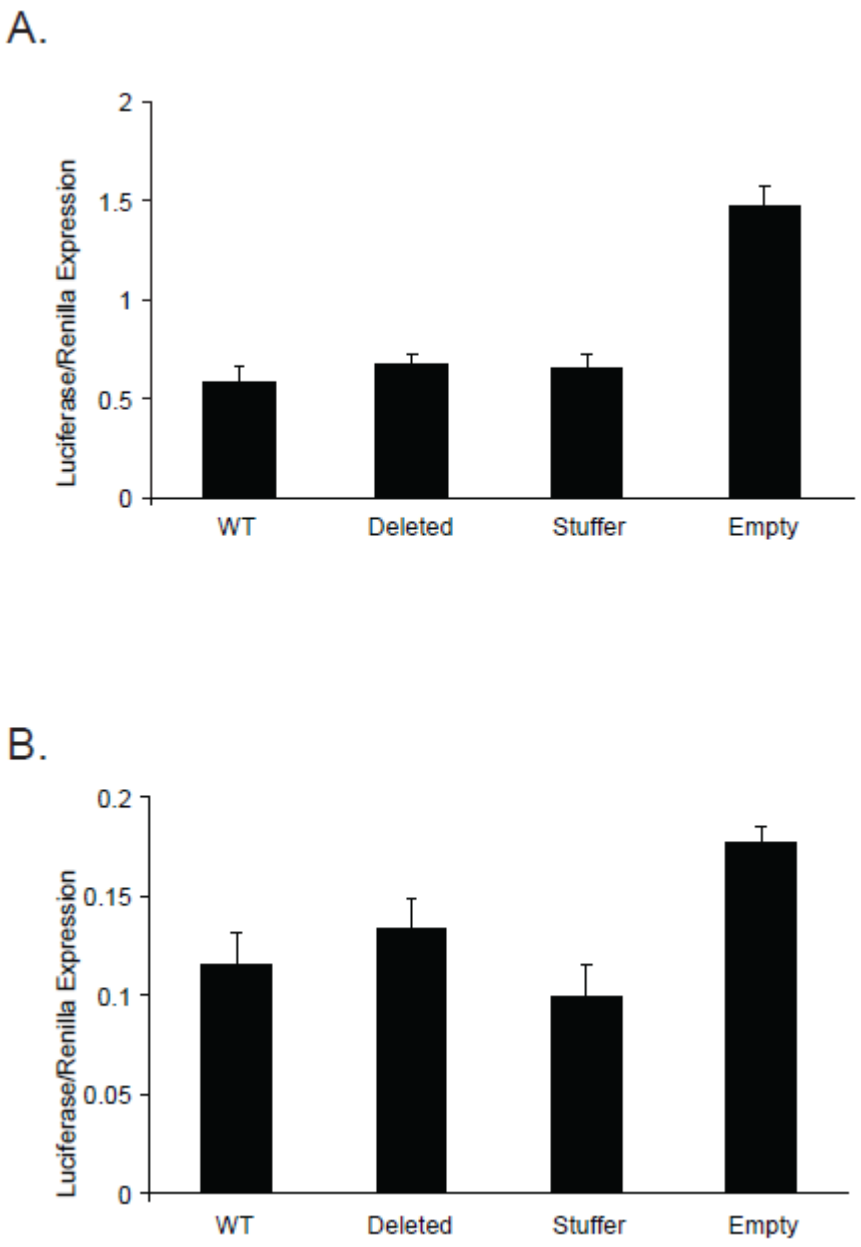

Figure 2-3. Representative results from DLAs of the deleted region in A.HEK293 and B. HT22 cell lines. Each construct was tested in 6 biological replicates per experiment.

Figure 2-4: Dual-luciferase assays testing *NRG3* SNPs

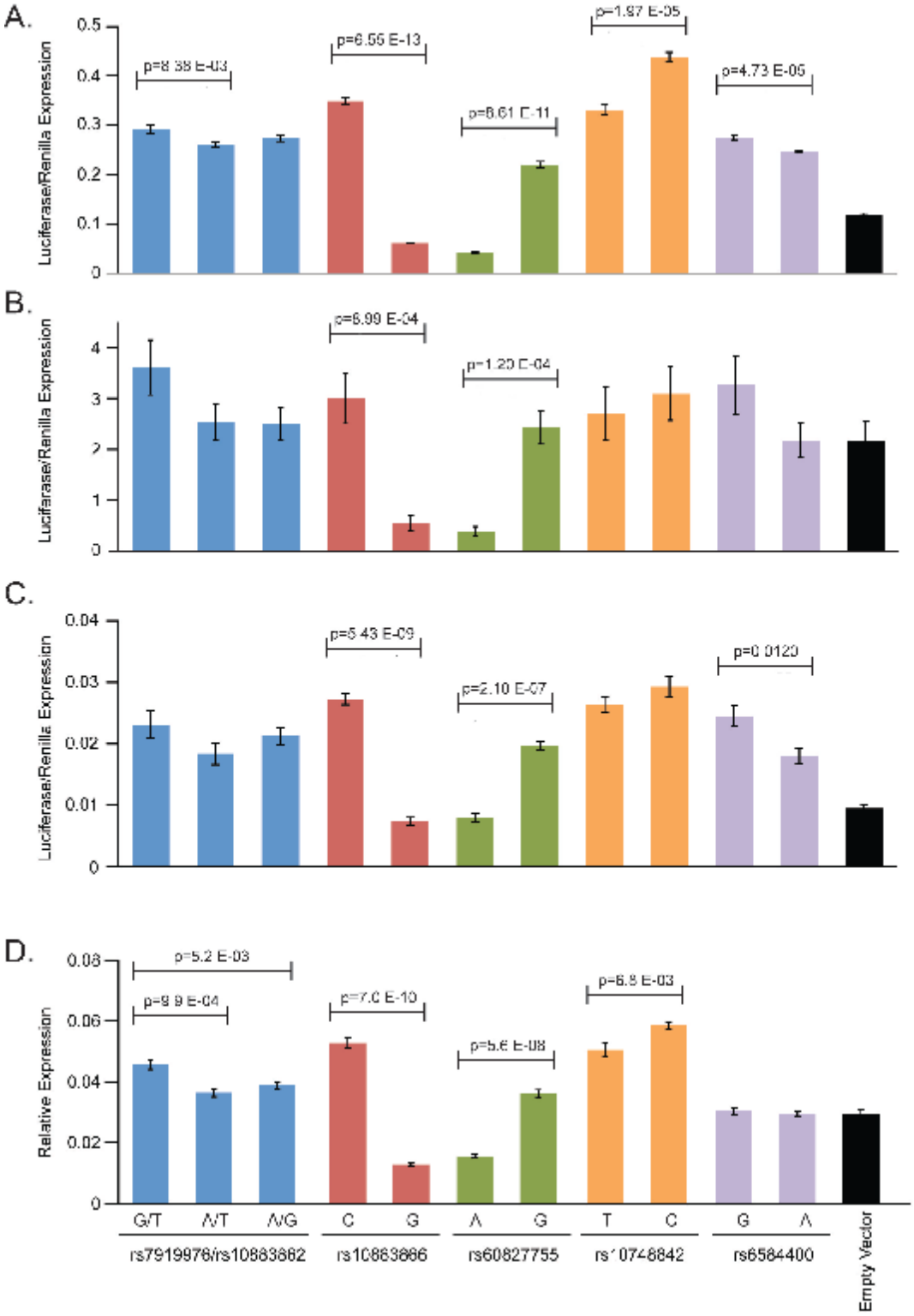

Figure 2-4. DLAs of short regions surrounding SNPs in A. HEK293 cells, B. Cultured rat primary cortical neurons, C. HT22 and D. Neuro-2A cells. Statistically significant results from two-tailed t-tests are shown. Each SNP (or pair of SNPs, in the case of rs7919976 and rs10883862) is represented by a different color; the first bar in each set represents major alleles and the second, minor alleles. Each construct was tested in six biological replicates per experiment.

Figure 2-5: Schematic of 3-Primer Assay design

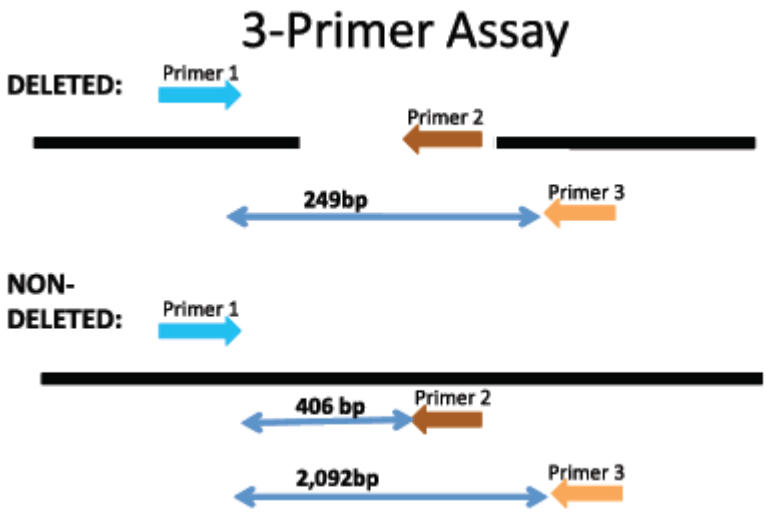

Figure 2-5: Microdeletion genotyping by three-primer PCR assay using a single forward primer 5' of the microdeletion and two reverse primers, one in the deleted region and one 3' of the microdeletion. PCR cycling conditions were: 94°C for 2 min, followed by 31 cycles of 30 sec at 94°C, 61°C and 68°C. Amplifying from the deleted chromosome will preclude binding of the first reverse primer, so only a 249bp product will amplify from the second reverse primer and the common forward primer. The undeleted chromosome would theoretically amplify from both the reverse primers, but the second primer will generate a 2092bp fragment that is not seen due to the short extension time, so only a 406bp product from the primer within the deleted region is produced. Heterozygotes exhibit both bands upon agarose gel electrophoresis.

Figure 2-6: Inheritance of deletion in AJ families

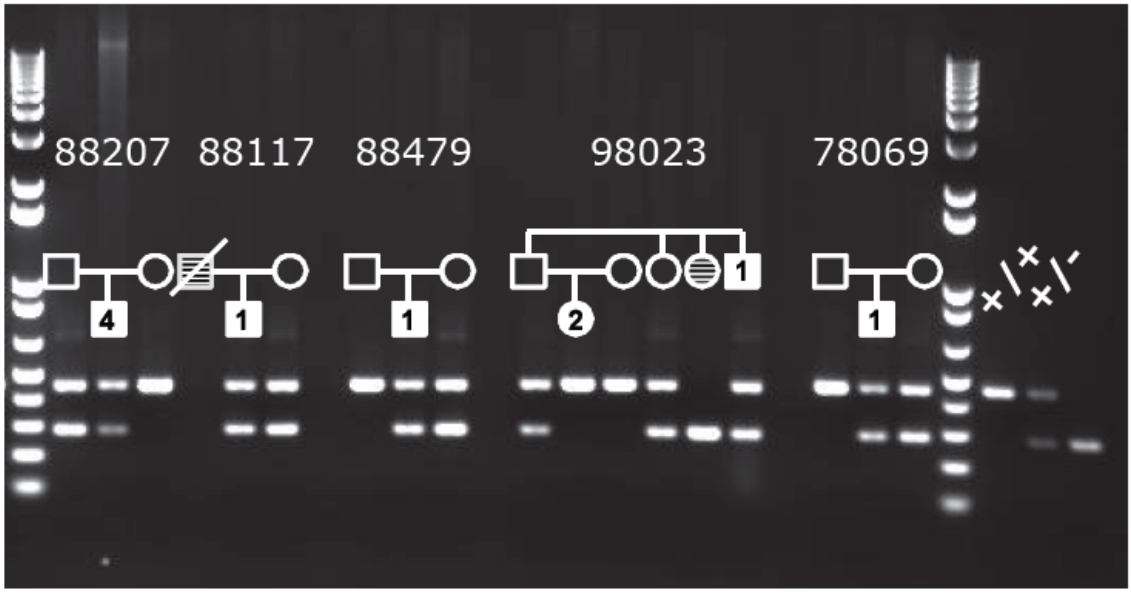

Figure 2-6: Representative sample of AJ family studies. Family ID and pedigree are shown above a 1.5% agarose gel electrophoresis of three-primer assay amplicons. Controls for each genotype are shown at the far right. Pedigree symbols shaded white represent individuals with SZ, shaded symbols represent the presence or possible presence of other psychiatric disorders. Numbers in the symbols for the affected individuals represent the quartiles of the delusion score for that individual. The first quartile contains individuals with the highest delusion scores, and the fourth contains individuals with the lowest delusion scores.

Figure 2-7: Effects of rs1078842 on *NRG3* alternative transcripts

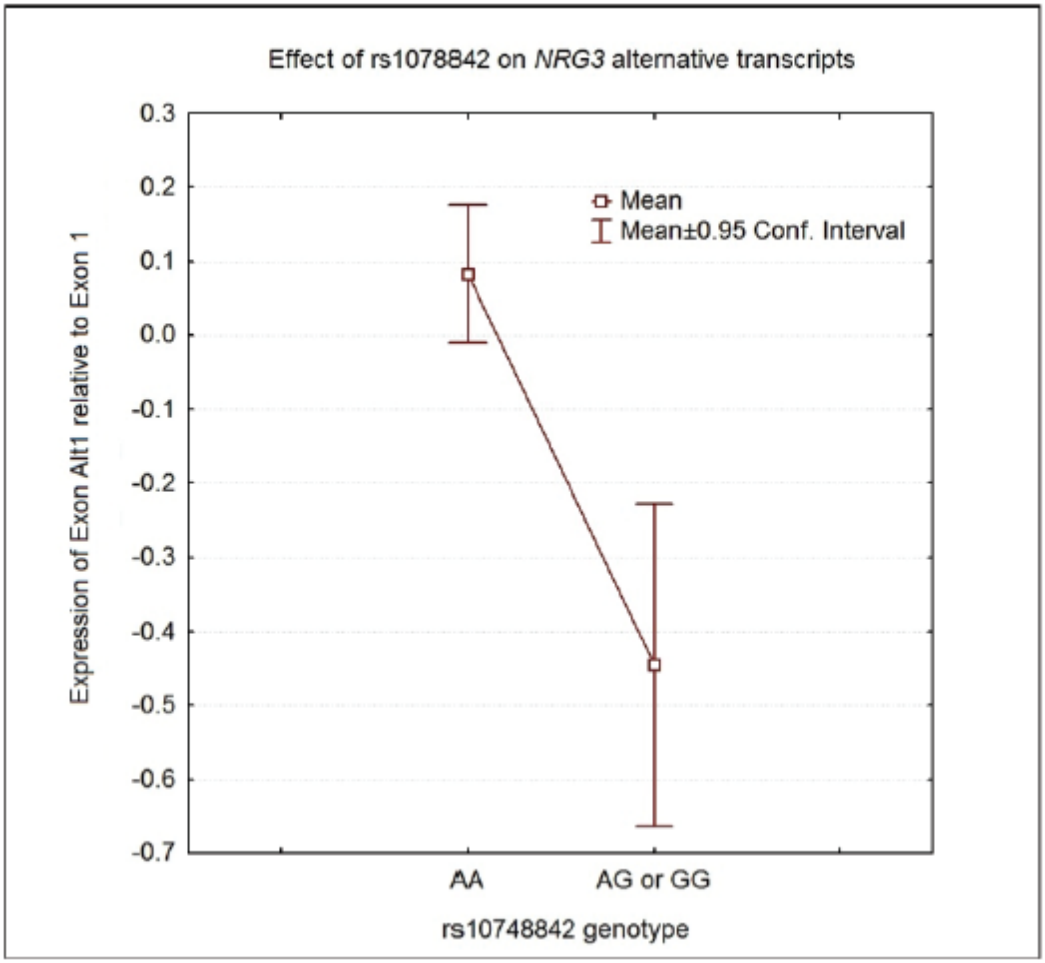

Figure 2-7. Log_2 transformed expression of *NRG3* transcripts initiating with Exon 1B grouped by genotype. A, samples from STG grouped by genotype for rs10748842. B, samples from STG grouped by genotype for rs60827755. C, samples from DLPFC grouped by genotype for rs10748842. D, samples from DLPFC grouped by genotype for rs60827755. Note, expression is not relative to transcripts initiating with exon 1A, nor is it corrected for covariates such as age, sex, pmi, or qPCR plate.

Chapter 3 : Identification of transcription factors binding regulatory regions in *NRG3*

Abstract

Human *NRG3* has been implicated in a "delusion" phenotype of schizophrenia (SZ). Three intronic SNPs in *NRG3* have been shown to have regulatory potential, but no proteins are known to bind to those regions of the genome. To assess whether nuclear proteins bind to the 21-bp region centered around each of these SNPs, I conducted Electrophoretic Mobility Shift Assays (EMSAs) using cell types in which my previous dual luciferase reporter assays indicated the SNPs had regulatory effect. I found that all DNA probes generated a shifted band, but only rs10748842 and rs60827755 showed a noticeable allele-specific difference in shifted band pattern or intensity. Using a computational approach, we have identified candidate proteins potentially binding the DNA region including these 2 SNPs. We tested CNOT4 binding to rs60827755 by supershift and determined that CNOT4 binding to rs60827755 may be responsible for the modification of the SZ phenotype.

Introduction

Chapter 2 of this dissertation details the identification of SNPs in *NRG3* intronic regions that are associated with the delusion factor in SZ.

Furthermore, DLAs provided evidence for their regulatory function. In this chapter, I hypothesize that one or more regulatory DNA-binding proteins recognize and bind to the region of DNA including the SNP, and that protein's or proteins' ability to bind to the locus is affected by the allele of the SNP. The protein in question would be able to interact with other proteins to form an enhancer complex that may regulate temporal and regional expression of *NRG3*.

In order to better elucidate the mechanism(s) whereby SNPs affect *NRG3* expression, and in turn, delusional manifestations in SZ, I sought to identify DNA-binding proteins that preferentially bound to regions including one of the alleles of the SNPs by testing hypotheses generated by *in silico* transcription factor predictions.

Materials and Methods

Electrophoretic Mobility Shift Assays (EMSAs)

Nuclear extracts were collected from HEK-293, Neuro2A and HT22 cell lines using the Nuclear Extraction Kit (EMD Millipore Corporation, Billerica, MA) according to the manufacturer's instructions and stored in single-use aliquots at -80°C.

Probes were generated using 21bp oligonucleotides containing the SNP at the center position. Forward and reverse oligonucleotides for each allele of each SNP were treated with shrimp alkaline phosphatase (Affymetrix, Santa Clara,

CA) to remove end phosphate units (37°C for 1 hour, followed by a 15 minute inactivation step at 65°C), heated to 95°C and allowed to cool at room temperature for 1 hour in order to generate double-stranded oligonucleotides.

To radiolabel the oligonucleotides, I incubated 2µl of the SAPed double-stranded oligos with T4 Polynuclotide Kinase (New England Biolabs, Ipswich, MA) and 2µl of γ^{32}P-ATP at 37°C for 1 hr. The product was purified using QuickClean Enzyme Removal resin (Clontech, Mountain View, CA) and Costar Spin-X centrifuge tube filter (0.22µm, Sigma-Aldrich, St. Louis, MO)column and mixed with 3µl of yeast tRNA. A half volume of ammonium acetate and 2 volumes of cold 100% ethanol were added and the reaction was placed at -80°C overnight to precipitate, then spun for 15 minutes at room temperature. The pellet was washed with 70% ethanol, resuspended in DEPC-treated water, counted and diluted to either 4,000 or 2,000 cpm/µl.

EMSAs were performed as described by Ye *et al*[50], except that probes were made at 2000 cpm/µl, 5.2 ul of 3 mg/ml nuclear extract and precast 5% Mini-Protean TBE gels (Bio-Rad, Hercules, CA) were used.

Competition EMSAs were performed in the same way as EMSAs, except that increasing amounts of unlabeled probe were added to the reactions (50nM, 100nM, 200nM and 300nM unlabeled probe) at the same time as the labeled probes were added.

In silico Prediction of Transcription Factor Binding Sites

Proteins binding loci of interest were identified using a computational model trained on experimental enhancer data, as presented previously.[51]

EMSA supershift assays

In order to test whether shifts seen in EMSAs were due at least in part by binding of the predicted protein (see "*In silico* prediction of transcription factor binding sites" above), EMSA supershift assays were conducted. Nuclear extracts and buffers were prepared in the same way as before, except that they did not contain DTT. After incubation of the reaction buffer, nuclear extract, poly(dI-dC) (Roche, Indianapolis, IN), BSA, and DEPC-treated water on ice for 10 minutes, CNOT4 antibodies (Catalog # 12561-1-AP, Proteintech, Chicago, IL and Catalog #ABIN485359, antibodies-online, Atlanta, GA) or Isotype control (Catalog #NB810-56910, Novus Biologicals, Littleton, CO) were added to appropriate lanes. Final isotype control concentration was matched to the final concentration of antibody. After a 2-hour incubation on ice, oligonucleotide probes were added, and the reaction was allowed to incubate on ice for 30 minutes while the flushed gel was pre-run at 200 V. Samples were loaded and run as before.

Results & Discussion

In order to explore the protein-binding potential of the region including and surrounding our SNPs of interest, I performed a number of EMSA experiments. I chose to limit our study to rs60827755, rs10748842 and rs10883866 for reasons outlined in Chapter 2 (namely, consistent differences in expression between alleles when tested in DLAs).

Nuclear Proteins Bind regions containing SNPs

First, I conducted a series of experiments to ascertain whether nuclear proteins bind the 21bp oligonucleotide centered around the SNP in question. The radiolabeled probe migrates to the bottom of the gel if unbound. If nuclear protein(s) bind the oligonucleotide, the complex exhibits retarded migration which would appear as a band or bands above the free probe.

EMSA competition experiments were also carried out in order to compare the binding strength of the protein-DNA interactions between alleles of the same SNP. For these experiments, equal amounts of radiolabeled probe are competed against increasing amounts of unlabeled probe of the same allele and, separately, of the opposite allele.

rs10883866: Our EMSA testing SNP rs10883866 showed a noticeable shift only in lanes with both radiolabeled probe and nuclear extract (See Figure 3-1). When I used HEK293 nuclear extract, I could see no clear difference in the pattern and intensity of the bands generated by the two alleles of rs10883866 (Figure 3-1, lanes 3 and 8). HT22 nuclear extract generated a slightly less-intense band when the radiolabeled probe contained the G (risk) allele of the

SNP, although the bands were of a different size than those seen with HEK293 nuclear extract (Figure 3-1, lanes 4 and 9). EMSA competition assays revealed no discernible difference in protein binding strength between alleles (Figure 3-2).

I therefore conclude that the 21bp region including rs10883866 appears to bind nuclear proteins. Since there is a difference in the banding pattern generated by the nuclear extracts from the two cell types, the identity of the proteins may be different, or they are orthologs but the divergence between the two species (mouse and human) generates different-sized proteins, or they are orthologs whose splicing patterns differ in the tissues (kidney versus hippocampus). We furthermore conclude that in HEK293 experiments, we have no evidence to support our hypothesis that the alleles of the SNP affect the DNA-protein binding.

rs10748842: SNP rs10748842, on the other hand, shows marked differences between the banding pattern generated by the two alleles of the SNP (Figure 3-3: allele C, lanes 3 and 4; allele T lanes 8 and 9). In experiments including HEK293 nuclear extract, the C (risk) allele generates only one band, which appears to be composed of at least two separate bands that overlap (Figure 3-3, lane 3). The T (protective) allele generates what appears to be the same band, but also generates two higher and one lower band (Figure 3-3, lane 8). Therefore, it appears that some protein or proteins bind this region regardless of the genotype at the SNP, but others bind imperceptively, if at all, to the C (risk) allele. When the experiment was performed using HT22 rather than HEK293 nuclear extract, one clear single band appears only with the C

(risk) allele (Figure 3-3, lane 4). A broader band most likely consisting of several overlapping bands appears regardless of genotype, but appears stronger with the C (risk) genotype (Figure 3-3, lanes 4 and 9). I conclude that the DNA sequence in question appears to bind to one or more nuclear proteins. One allele generates bands not seen with the other, but the allele resulting in more bands are different in different cell types (C in HT22, T in HEK293), suggesting that the effects of this SNP may be cell-type or species-specific.

Furthermore, EMSA competition assays performed in HEK293 cells (Figure 3-4) demonstrate that the shifted bands diminish in intensity at lower concentrations of C allele compared to T allele. This suggests that the C allele is binding most strongly to the protein or proteins generating the band. It is also interesting to note that as the intensity of the strongest band decreases with increasing amounts of cold T allele probe, another, higher, more diffuse band generated by the labeled C allele probe-protein complex seems to increase in strength proportional to the main band at the same time that it appears to migrate further through the gel. This suggests that the C allele may have the ability to bind to a family of proteins of varying molecular weights, with slightly different binding affinities.

rs60827755: EMSAs with SNP rs60827755 and HEK293 nuclear extract generate a doublet which appears more intense when binding the A (protective) allele, as evidenced by the comparisons of the band in the lanes with HEK nuclear extract (Figure 3-5, lanes 3 and 8). HT22 nuclear extract does not generate discernible bands (Figure 3-5, lanes 4 and 9). This may mean that the protein-probe complex is beneath the limit of detection, or that the protein

mediating the effect in the dual-luciferase reporter assays is unable to bind to the DNA probe under the conditions of the assay.

Competition assays performed with HEK nuclear extract (Figure 3-6) demonstrate that the addition of unlabeled oligonucleotide with the A allele causes all bands to diminish in intensity at a lower concentration than oligonucleotide with the G allele. This means that the A (protective) allele appears to bind more strongly than the G (risk) allele to the proteins in question.

CNOT4 as a possible binding protein

In collaboration with Dr. Michael Beer, I used a bioinformatics approach to determine the effect each SNP was expected to have on any protein binding sites overlapping its locus.

rs10883866: The computational analysis predicted that rs10883866 was not expected to change any binding sites. We find this in accordance with our EMSA results, which showed minimal difference in the pattern of shifted bands generated by the two alleles, as well as indiscernible differences in the competition assays testing relative binding affinity.

Since both the *in silico* and the *in vitro* approaches are in agreement, I conclude that rs10883866 does not exhibit differential binding affinity to its protein binding partner. The effects seen in the DLAs presented in the previous chapter suggest that the SNP has some regulatory effect, but we postulate that the mechanism does not include direct protein binding at the DNA level.

rs10748842: Kao *et al.*[36] have previously reported *in silico* experimental results suggesting that rs10748842 lies in a homeodomain binding motif to which a number of protein domains, Hox, LIM, POU and PAX among them, bind. The SNP alters this motif, and so the alleles expected to have differential binding ability. Our computational approach supports this prediction, increasing our confidence in its predictive abilities. However, because of the sheer number of proteins predicted to bind this site, we chose not to approach with EMSA supershift studies using a series of antibodies. Rather, we will wait for the results of a protein microarray experiment which will interrogate differential binding ability for many transcription factors simultaneously.

rs60827755: Our computational analysis predicted that rs60827755 could alter the binding site of a protein known as CNOT4. This protein is a member of the Ccr4-Not complex, a regulator of transcription, particularly by RNA Polymerase II[52]. In addition to its role as a transcription factor complex, mRNA metabolism, ubiquitin ligase and mRNA turnover functions have been assigned to the Ccr4-Not complex[53]. CNOT4 has a RING finger domain, which suggests an ability to bind DNA directly[54].

In order to test whether the CNOT4 protein binds the 21-bp probe around rs60827755, I conducted supershift assays using antibodies against CNOT4. If formed, the protein-DNA probe-antibody complex should generate a "supershift" that is not observed in the absence of antibody, or when the antibody is replaced by an isotype control.

I observed a shift (Figure 3-7, lanes 3 and 8) when the reaction contained HEK293 nuclear extract as well as labeled probe. However, addition of the

antibody did not generate an additional band. It should be noted, however, that there is a marked reduction in the intensity of the shifted band in the lanes containing antibody, nuclear extract and labeled probe (Figure 3-7, lanes 4 and 8). This reduction is not seen with isotype control instead of antibody (Figure 3-7, lanes 5 and 9). These data suggest that it is possible that antibody binding to CNOT4 is causing a reduction of signal by preventing the CNOT4-antibody-DNA probe from migrating through the gel. Alternatively, the antibody may be impeding protein-DNA binding, but in that scenario, I would expect the unlabeled probe signal to be significantly greater in lanes with antibody (Figure 3-7, lanes 4 and 8) than in lanes without it (Figure 3-7, lanes 3 and 7), which I do not observe.

I performed the same experiment using HT22 nuclear extract but found only slight differences between lanes with and without antibody (Figure 3-8, lanes 3, 5, 8 and 10 compared to lanes 4 and 9). As with HEK, no supershifted band was observed.

When I repeated this experiment with Neuro 2A nuclear extract, I observed that lanes without the CNOT4 antibody exhibited the same banding pattern as lanes with CNOT4 antibody (Figure 3-9, lanes 3, 5, 8 and 10 compared to lanes 4 and 9), suggesting no supershift band occurred. There was a reduction in signal intensity of the principal shifted band when antibody was added (Figure 3-9, lanes 4 and 9), but a second band (observed also in lanes without antibody) remained as intense as control lanes (Figure 3-9, lanes 3,5,8 and 10). I therefore cannot conclusively show CNOT4 binding to our DNA region of interest, but neither can I dismiss CNOT4 as being at least partially

responsible for the shifted band observed in EMSAs with rs60827755 and possibly involved in mediating the effect of the SNP on regulation of *NRG3*. In order to confirm or refute involvement of CNOT4 with regulation of *NRG3*, further experiments are warranted, including a protein microarray experiment currently underway.

Conclusions

I have shown that the 21-bp regions containing our 3 SNPs of interest are capable of binding proteins in at least one of the cell types tested. I observe no significant differences in protein binding intensities or patterns for rs10883866, in accordance with our computational predictions. Because of the apparently limited effect of the SNP on differential binding, I chose not to pursue this SNP in our supershift experiments.

My data also show that rs10748842 is responsible for a difference in the binding pattern and intensity in our EMSAs. The multiple bands seen, especially in HEK293 cells, agree with computational predictions performed by us and others[36], suggesting multiple proteins are capable of binding the region containing the SNP. Because of the daunting number of putative binding proteins, I chose not to pursue this approach by supershift.

I found rs60827755 exhibited weak but specific shifting in the presence of HEK293 nuclear extract but bands were below the limit of detection with HT22 nuclear proteins. I notice an allele-specific difference in band intensity.

The experiments described in the latter part of this chapter suggest that there may be an involvement of the CNOT4 protein in the formation of the complex that appears as a shifted band in the EMSAs. However, my experiments were unable to conclusively prove or disprove its ability to bind our region of interest. I continue to test this hypothesis through different experimental means.

Figure 3-1: rs10883866 EMSA using HEK293 and HT22 nuclear extracts

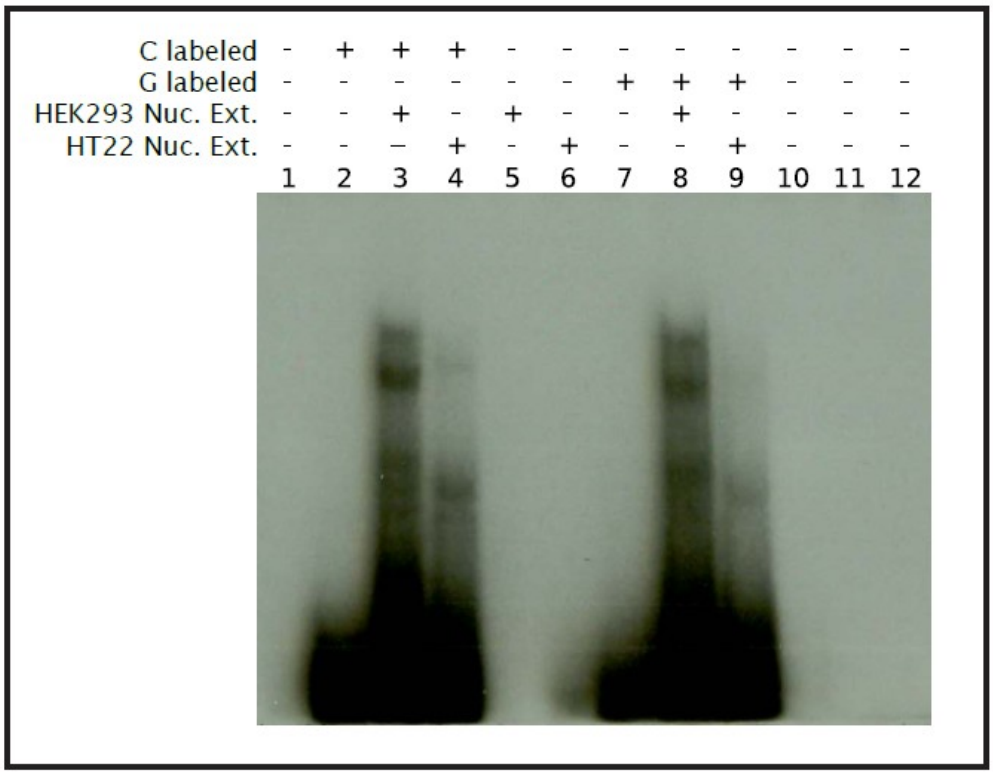

Figure 3-1. Electrophoretic Mobility Shift (EMSA). Radiolabeled probes containing either allele of rs10883866 were tested in the presence and absence of either HEK293 or HT22 nuclear extracts.

Figure 3-2:10883866 EMSA competition with alternate allele using HEK293 nuclear extract

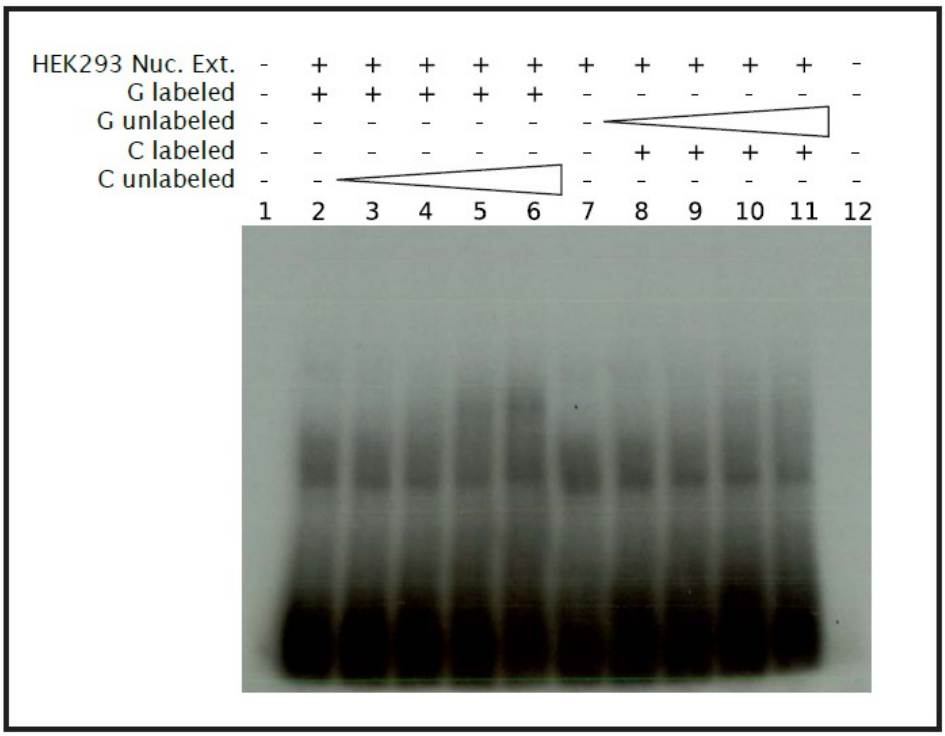

Figure 3-2. Competition Electrophoretic Mobility Shift (EMSA). Radiolabeled probes containing one allele of rs10883866 were incubated with HEK293 nuclear extract in the presence of various amounts of unlabeled probe containing the other allele of the SNP.

Figure 3-3: rs10748842 EMSA using HEK293 and HT22 nuclear extracts

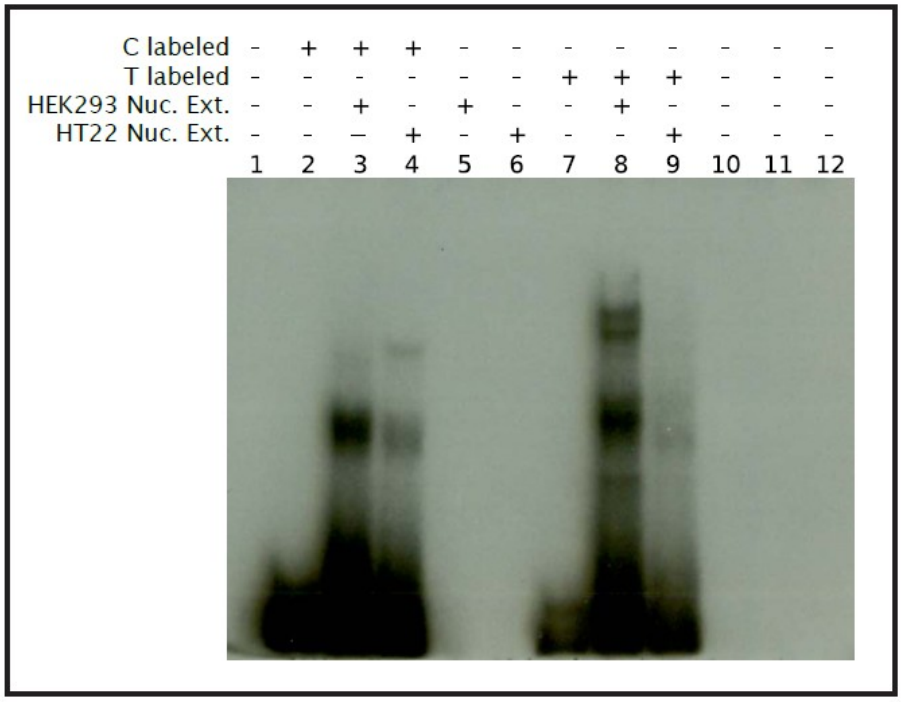

Figure 3-3. Electrophoretic Mobility Shift (EMSA). Radiolabeled probes containing either allele of rs10748842 were tested in the presence and absence of either HEK293 or HT22 nuclear extracts.

Figure 3-4: rs10748842 EMSA competition with alternate allele using HEK293 nuclear extract

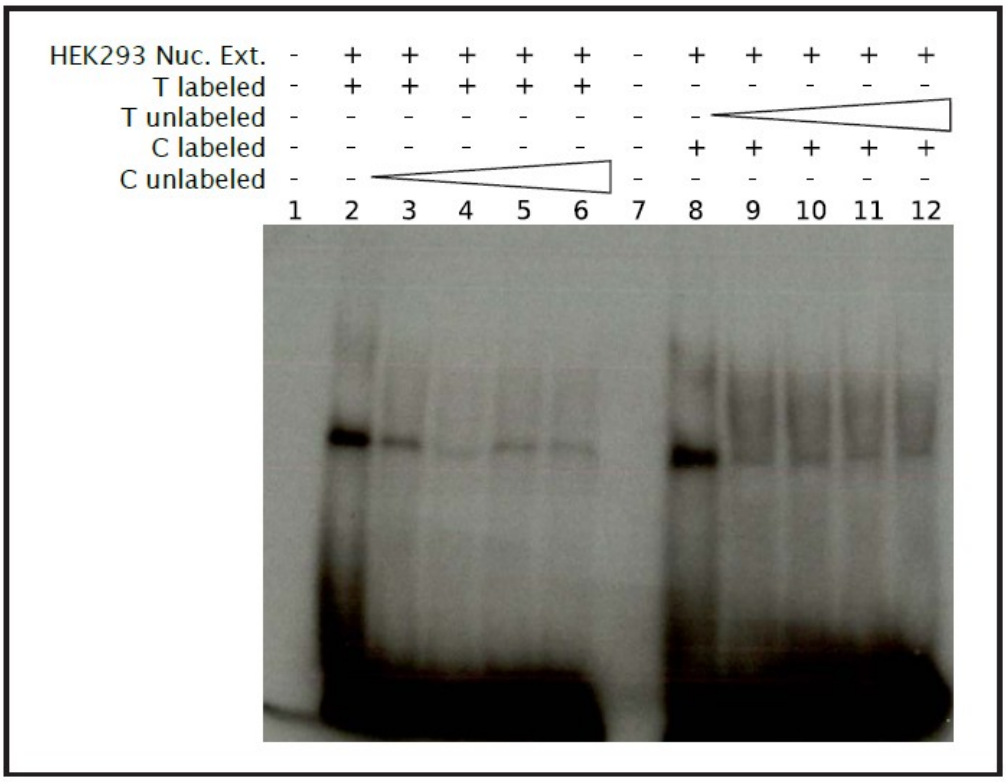

Figure 3-4. Competition Electrophoretic Mobility Shift (EMSA). Radiolabeled probes containing one allele of rs10748842 were incubated with HEK293 nuclear extract in the presence of various amounts of unlabeled probe containing the other allele of the SNP.

Figure 3-5: EMSA with HEK293 and HT22 nuclear extracts

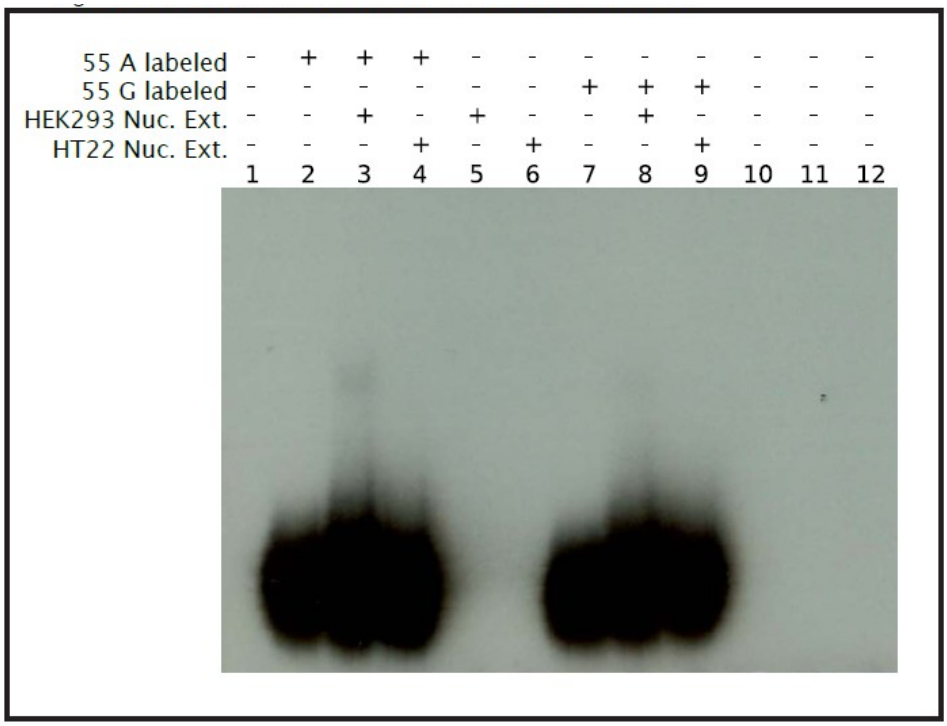

Figure 3-5. Electrophoretic Mobility Shift (EMSA). Radiolabeled probes containing either allele of rs60827755 were tested in the presence and absence of either HEK293 or HT22 nuclear extracts.

Figure 3-6: EMSA competition with alternate allele using HEK293 nuclear extract

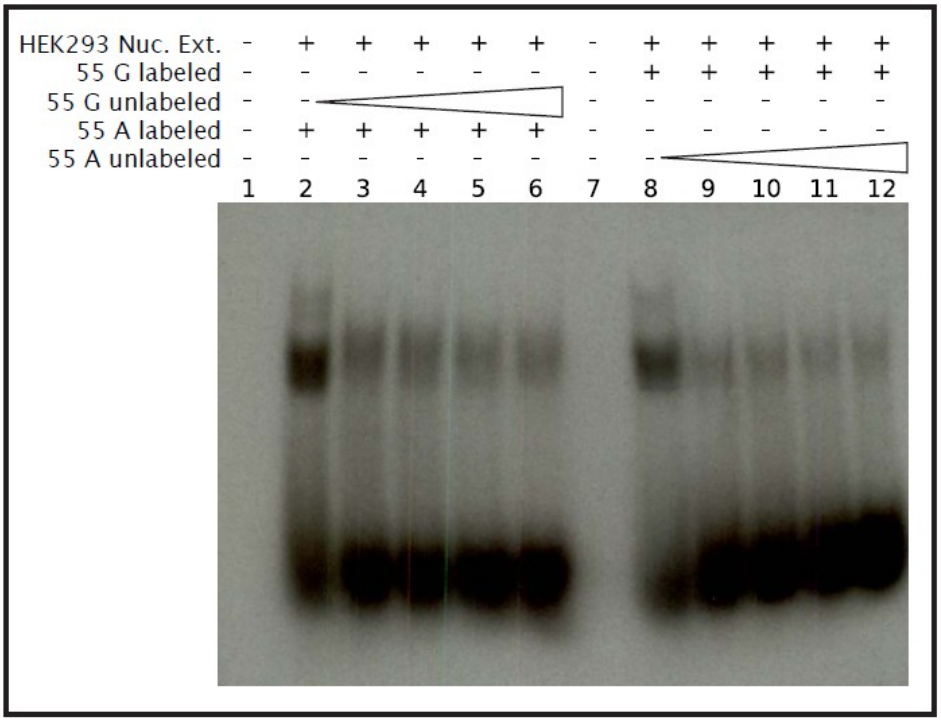

Figure 3-6. Competition Electrophoretic Mobility Shift (EMSA). Radiolabeled probes containing one allele of rs60827755 were incubated with HEK293 nuclear extract in the presence of various amounts of unlabeled probe containing the other allele of the SNP.

Figure 3-7: rs60827755 EMSA supershift with HEK293 nuclear extract

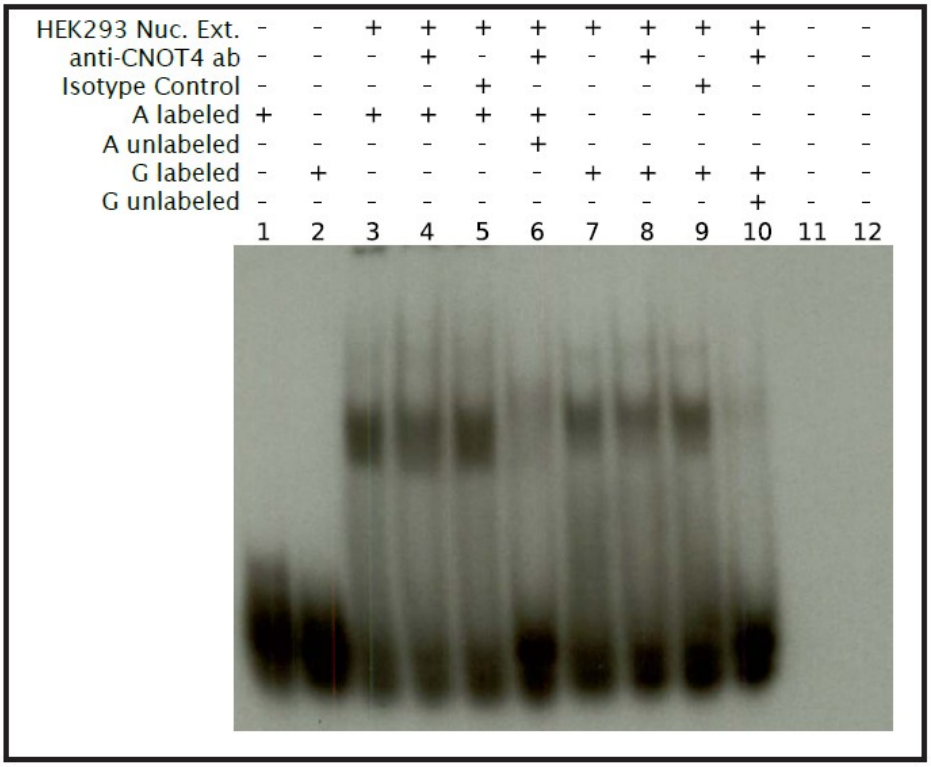

Figure 3-7. Electrophoretic Mobility Shift (EMSA) Supershift. Radiolabeled probes containing one allele of rs60827755 were incubated with HEK293 nuclear extract in the presence of anti-CNOT4 antibody (lanes 4 and 8), isotype control (lanes 5 and 9), or both antibody and an excess of unlabeled probe containing the other allele of the SNP (lanes 6 and 10).

Figure 3-8: rs 60827755 EMSA supershift with HT22 nuclear extract

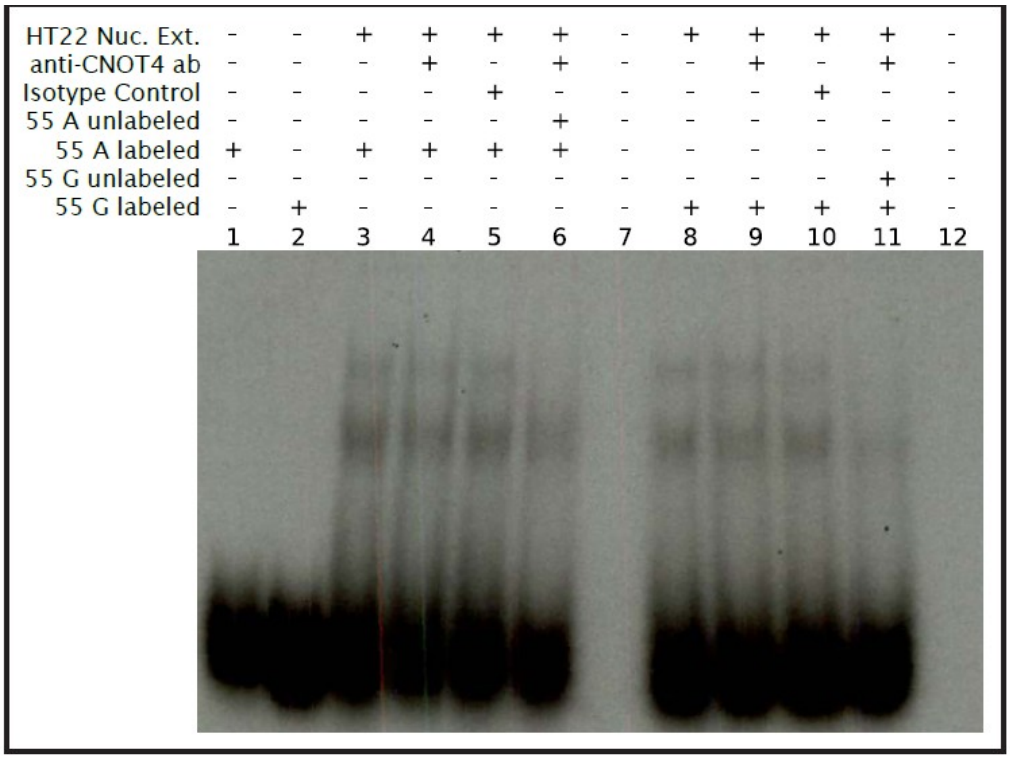

Figure 3-8. Electrophoretic Mobility Shift (EMSA) Supershift. Radiolabeled probes containing one allele of rs60827755 were incubated with HT22 nuclear extract in the presence of anti-CNOT4 antibody (lanes 4 and 8), isotype control (lanes 5 and 9), or both antibody and an excess of unlabeled probe containing the other allele of the SNP (lanes 6 and 10).

Figure 3-9: rs 60827755 EMSA supershift with Neuro2A nuclear extract

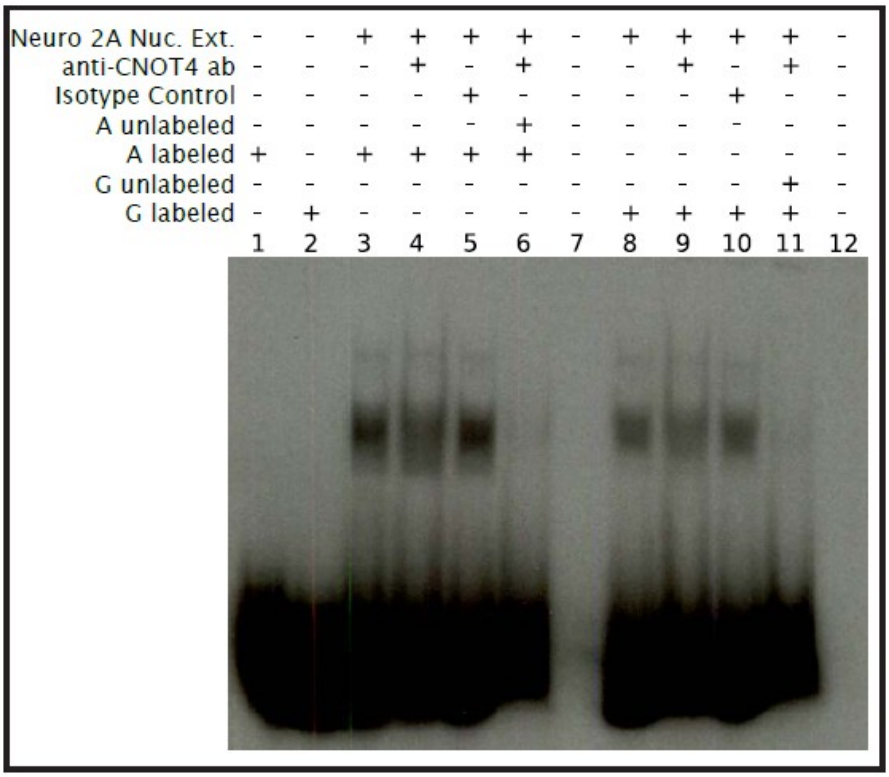

Figure 3-9. Electrophoretic Mobility Shift (EMSA) Supershift. Radiolabeled probes containing one allele of rs60827755 were incubated with Neuro2A nuclear extract in the presence of anti-CNOT4 antibody (lanes 4 and 9), isotype control (lanes 5 and 10), or both antibody and an excess of unlabeled probe containing the other allele of the SNP (lanes 6 and 11).

Chapter 4 : Characterization of a *Nrg3* knockout mouse

Abstract

Stimulated by our data implicating variation in *NRG3* either contributes for risk for schizophrenia or influences the phenotypic manifestations of schizophrenia (SZ), I tested a murine *Nrg3* constitutive knockout mouse developed by our laboratory for both behavioral and neuronal phenotypes relevant to the NRG/ErbB4 pathway. A battery of behavioral tests revealed a pervasive hyperactivity phenotype, even at baseline. Additional findings include decreased anxiety, pre-pulse inhibition and startle response deficits, fear and/or emotional- based learning or memory deficits, and perturbed working memory. At the neuronal level, I tested the hypothesis that *Nrg3*$^{-/-}$ mice may have GABAergic interneuron migration deficits by immunofluorescent staining of brain sections from mice injected with EdU prior to neuronal migration. I conclude that there is no deficit of GABAergic interneurons in the cortical areas assessed in *Nrg3*$^{-/-}$ brains. However, a deficit of GABAergic interneuron precursors during development and depletion of PV+ cells in postnatal brains suggests that migration patterns may be altered in *Nrg3*$^{-/-}$ animals.

Introduction

In this chapter, I focus on experiments aimed at characterizing a *Nrg3* knockout mouse developed in our laboratory. The targeted disruption of *Nrg3* was designed so that exon 2 (present in all four known transcripts of murine *Nrg3*) would be eliminated.

My first research question focuses on the behavioral phenotype of this mouse strain. Although SZ is a human-specific disease, genetic (and other drug-induced or surgical) mouse models *can* display certain facets or endophenotypes of human SZ such as social withdrawal or cognitive deficits. It is by studying SZ in a "piecemeal" fashion, mouse models allow investigators to perform studies that would be impossible, unethical or impractical in humans.[55-57] Just as humans with SZ rarely manifest all known symptoms of SZ, even ideal mouse models likely will only manifest some behavioral changes that may be related to SZ.[58]

Positive symptoms of SZ (including delusions) have classically been tested in mouse models using pre-pulse inhibition (PPI) and locomotor hyperactivity. Locomotor hyperactivity (particularly as a proxy for psychotic agitation) has been used to test for dopaminergic changes, especially after exposure to amphetamines. N-methyl-D-aspartate (NMDA) receptor antagonists such as MK-801 have been used in a similar manner, but to study SZ-like hallucinations.[59]

The startle response is a plastic, unconditioned reflex characteristic of vertebrates, but impaired in subjects with SZ (as well as other psychiatric diseases) and many mouse models of psychiatric disease. Impaired PPI is generally considered to reflect defects in the inhibition of neural circuits critical for sensorimotor gating. Deficient sensorimotor gating can result in cognitive fragmentation and sensory overload, with psychotic and cognitive implications. PPI can model a deficiency in glutamatergic signaling or an increase in dopaminergic activity.[59]

In addition to the literature supporting a PPI deficit in SZ, PPI testing for animal models of psychiatric disease is a choice test because both humans and mice are tested in a similar fashion.[60]

My second research question focuses on the cellular phenotype of knocking out murine *Nrg3*. In 2012, Li *et al.*[30] reported that NRG3 and NRG1 were key chemorepellant signals necessary to guide GABAergic interneurons through their migration via the tangential migratory route. This route leads from the medial ganglionic eminence (MGE), where the interneurons are generated, to their final location in the cortex. The findings of Li *et al.* differed from previous work suggesting chemoattractant properties of NRGs that allow migration of interneurons, such as Flames *et al.*[61] However, the effect of abolishing or diminishing NRG3 in the developing brain has not been tested in a knockout mouse model, nor have the behavioral consequences been studied.

Materials and Methods

Generation of a Nrg3 Knockout (KO) Mouse

A *Nrg3* knockout mouse previously generated in the Valle lab by Lilei Zhang and Pei-lung Chen was utilized in all experiments in this chapter. Exon 2 (GRCm38/mm10 Chr14:39,011,969-39,012,099) was targeted for deletion using a *Neomycin* cassette flanked by both FRT and LoxP sites (see Figure 4-1), as well as genomic regions flanking Exon 2. Successful homologous recombination was tested by Southern Blot and PCR. Chimeric mice were generated by the Johns Hopkins Transgenic Core Laboratory and bred to mice carrying a constitutive *Cre* cassette. Congenic mice were generated by backcrossing a minimum of 10 times to C57BL/6 mice (Jackson Laboratory, Bar Harbor, Maine).

Northern Blot

Northern blots were prepared as described previously[62,63] with 2 ug poly-A RNA extracted from murine brains at ages E14, E16, E18, P1, P3, and P42.

Behavioral Studies

For acoustic startle response experiments[64], 9-10-week-old mice were tested once each. Mice with startle responses below 100 were excluded, for a total of 6 mixed-background *Nrg3*$^{+/+}$ males, 6 mixed-background *Nrg3*$^{-/-}$ males,

9 backcrossed *Nrg3*$^{+/+}$ males, 11 backcrossed *Nrg3*$^{-/-}$ males, 4 mixed-background *Nrg3*$^{+/+}$ females, 2 mixed-background *Nrg3*$^{-/-}$ females, 15 backcrossed *Nrg3*$^{+/+}$ females and 14 backcrossed *Nrg3*$^{-/-}$ females.

Y-maze experiments[65] utilized 5 *Nrg3*$^{-/-}$ females, 7 *Nrg3*$^{+/+}$ females, 2 *Nrg3*$^{-/-}$ males and 7 *Nrg3*$^{+/+}$ males, all from a mixed background and between 10-12 weeks of age.

24-hour circadian rhythm tests[64] used mixed-background mice 10-12 weeks of age (6 male *Nrg3*$^{-/-}$, 6 male *Nrg3*$^{+/+}$, 5 female *Nrg3*$^{-/-}$, 5 female *Nrg3*$^{+/+}$). The dark period persisted from 8pm to 8am.

Fear conditioning was performed as described previously[66] using 9 male mice of each genotype. If data failed normality testing, we calculated least squares means for group by time interaction.

Open field tests were described previously[67] and were performed with and without MK-801 on 6-month old mice. Mice were tested only once, as follows: 30 minute observation period, saline injection, 30 minute observation period, MK801 (0.3 mg/kg) injection, 2 hour observation. 14 mixed-strain male mice of each genotype were tested. Data that failed a normality test was normalized by obtaining least square means.

For hot plate tests[68], mice placed on a Columbus Instruments (Columbus, OH) hot plate analgesia meter set at 55°C and the time to paw-lick response was recorded in seconds. We used 6 *Nrg3*$^{+/+}$ males, 8 *Nrg3*$^{+/+}$ females, 6 *Nrg3*$^{-/-}$ males and 5 *Nrg3*$^{-/-}$ females of mixed-background, as well as 3 *Nrg3*$^{+/+}$

males, 5 *Nrg3*$^{+/+}$ females, 3 *Nrg3*$^{-/-}$ males and 4 *Nrg3*$^{-/-}$ females in a C57BL/6J background. For each mouse, 2 trials were conducted and averaged.

Plus-maze tests[64] were performed on 3-month-old mixed-background mice (5 female *Nrg3*$^{-/-}$, 5 female *Nrg3*$^{+/+}$, 6 male *Nrg3*$^{-/-}$, 6 male *Nrg3*$^{+/+}$) In addition to time spent on the closed and open arms, the following data was collected: number of fecal boli produced, urination (binary), number of times mice leaned over the edge, number of peeks, rearing activity, cleaning activity and stretching. Outliers (3 female *Nrg3*$^{+/+}$, one female *Nrg3*$^{-/-}$, one male *Nrg3*$^{-/-}$ and one male *Nrg3*$^{+/+}$ inactive mice) were eliminated from statistical analysis.

EdU Migration Assays

To track the migration of cells in the developing brain, we mated *Nrg3*$^{+/-}$ heterozygotes to generate a timed pregnancy (E0 designated as midnight on the night of mating). At E12.5, the dam was given a peritoneal injection of 50 ug EdU (Life Technologies, Carlsbad, CA) per g of mouse in a total volume of 500 µl of sterile PBS. Dam and/or offspring were sacrificed at several timepoints (E12.5 1 hour after injection, E17.5, P0, P27 and P61). A cardiac perfusion with PBS and 4% PFA was performed for P27 and P61 mice prior to removal of the brain. For P0, E17.5 and E12.5, the dam was anesthetized and sacrificed, and the pups' brains (E17.5, P0) or heads (E12.5) harvested. All brains were placed in a 4% PFA solution overnight at 4°C overnight. P61 and P27 brains were then placed in PBS and sectioned using a vibratome set to collect 50-micron coronal sections. All others were placed in 15% and then 30% sucrose gradients until

sunk, then embedded in OCT and sectioned using a cryostat. Coronal sections were collected at 14 microns for E12.7 brains and ~35 microns for all others.

Immunohistochemistry

For free-floating vibratome sections (ages P27 and P61), every 12th free-floating section was collected and stained starting four sections from the first section where the hemispheres were joined. For cryostat sections, comparable sections were selected without regards to genotype and stained. All steps were performed at room temperature unless otherwise indicated. Slides or sections were rinsed in PBS for 5 minutes shaking, washed three times for 5 minutes each in PBT (0.2% Triton-X100 in PBS), then blocked in a humid box with 10% normal donkey serum in PBT. A Pap-pen (Sigma-Aldrich, St. Louis, MO) was used to delineate sections in slides. Primary antibodies were diluted in 10% normal donkey serum in PBT to stain overnight at 4°C in the dark. Parafilm coverslips were fashioned for slides. After allowing sections and slides to warm to room temperature, coverslips were removed and the sections or slides washed 3 times with PBT for 5 minutes each. AlexaFluor 568 and/or 680 (Life Technologies, Carlsbad, CA) were used at a dilution of 1:500 in 1% normal donkey serum in PBT for 2 hours in a humid, dark box. Slides and sections were washed in the dark three times for 5 minutes each with PBT, and the EdU Click-IT AlexaFluor 488 (Life Technologies, Carlsbad, CA) reaction performed according to manufacturer's instructions for 30 minutes. Slides and sections were washed as before but with PBS, counterstained with DAPI (1:10,000) for 5 minutes in the dark, and washed twice for 3 minutes each in PBS. Free-floating

sections were arranged on slide, and all slides mounted with PermaFluor Aqueous Mounting Media (Thermo Scientific, Waltham, MA) and left to dry in the dark.

Primary antibodies for all embryonic stages and P0: Anti-Lhx6 (Novus Biologicals, Littleton, CO) and Anti-TTF1 (also known as Nkx2.1) (Upstate Cell Signaling Solutions, Lake Placid, NY) were used at a 1:500 dilution For P27 and P61, Anti-Parvalbumin antibody (Swant PV 25, Switzerland) was used at a 1:2,000 dilution.

Slides were imaged using a Zeiss fluorescent microscope, For P27 and P61, the third, fifth and seventh section (rostral to caudal) were imaged at 200x magnification (20x objective). For P0 and E18, sections imaged corresponded to coronal sections at ~1.3, -0.94, and -2.9 mm from bregma. For adolescent and adult brains, the sections corresponded to ~1.2, -0.9, and -1.9 mm from bregma.

Images were analyzed with the help of either Adobe Photoshop (San Jose, CA, for manual counting and photomerging of multiple images) or Volocity (PerkinElmer, Waltham, MA, for automated counting). Experimenters were blind to genotype while counting. For each image, the number (or intersecting pixels) of cells positive for both Parvalbumin and EdU in the view was counted, as well as the number (or total pixels) of Parvalbumin positive cells, and the number of EdU positive cells.

Results and Conclusions

Generation of the NRG3 Knockout Mouse

Efficiency of the knockout mouse was tested by Northern Blot comparing *Nrg3*$^{-/-}$, *Nrg3*$^{+/-}$, and *Nrg3*$^{-/-}$ littermates. As seen in Figure 4-2, the knockout animals expressed greatly reduced levels of *NRG3* mRNA at every timepoint tested. The mRNA levels of other possible components of the Neuregulin system, *NRG1* and *ErbB4,* however, did not vary according to *Nrg3* genotype.

Prepulse Inhibition and Startle Response

In order to study the effect that an absence or decrease in *NRG3* levels may have on a mouse's PPI phenotype, we tested wildtype and homozygous knockout littermates from heterozygote x heterozygote matings. Two different genetic backgrounds were tested: the original transgenic strain, which is a mixture of 129 and C57BL/6J strains, as well as transgenic mice backcrossed (at least 10 generations) to the C57BL/6J strain.

As expected,[69] genetic background had a significant effect on PPI, so we focused our analyses on within-strain comparisons.

As seen in Figure 4-3A, mixed-strain male *Nrg3*$^{+/+}$ mice displayed a more modest startle response than their *Nrg3*$^{-/-}$ littermates. The difference reached statistical significance (two way repeated measures ANOVA p=0.049). The difference between *Nrg3*$^{+/+}$ and *Nrg3*$^{-/-}$ males was not evident in the backcrossed

mice, perhaps due to an unknown modifier that masks the differences between *Nrg3*$^{+/+}$ and *Nrg3*$^{-/-}$ in the backcrossed strains but not in the mixed-background. This could be discerned by backcrossing the mixed-background mice to a 129 background to compare their PPI to backcrossed C57BL/6J.

Females (Figure 4-3B) did not exhibit a discernible difference between *Nrg3*$^{+/+}$ and *Nrg3*$^{-/-}$ in either strain, although it should be noted that the number of subjects for the mixed-background strain was small after eliminating individuals with startle responses below 100.

The percent of prepulse inhibition (%PPI) was calculated at 5 different prepulses. In the mixed-strain male mice (see Figure 4-3C), the *Nrg3*$^{-/-}$ mice exhibited diminished %PPI at all prepulses (two way repeated measures ANOVA p=0.073). As with the startle response, the *Nrg3*$^{-/-}$ backcrossed males did not significantly differ from the backcrossed controls (p=0.543), nor did the female *Nrg3*$^{+/+}$ and *Nrg3*$^{-/-}$ mice of either background differ from each other.

Therefore, we conclude that there is a trend towards reduced %PPI and increased startle response in *Nrg3*$^{-/-}$ males versus *Nrg3*$^{+/+}$ males, but this phenotype is only evident in a mixed-strain background. Testing more mice, both in the mixed-strain background and in a 129 background, may help support these observations.

Fear conditioning

The fear conditioning paradigm posits that an animal that learns to associate a stimulus (in this case, a tone) to an adverse event (shock) will

exhibit freezing behavior when the stimulus is sensed. Although the freezing behavior is mediated by the amygdala, the hippocampus is responsible for storing the conjunctive representation (in other words, the memory of the association of the stimulus with the adverse event) in the cortex[70]. At the circuitry level, deficits in communication between the three brain regions may be expected to result in poorer performance in the fear conditioning test.

We trained the mice to associate a novel tone with a shock on Day 1, after which we desensitized them to the chamber on Day 2 (no shock, no tone). On Day 3, we tested response to a tone (no shock), measuring the mice's ability to create and remember the association between the shock and the tone.

As seen in Figure 4-4, *Nrg3*$^{-/-}$ males show a decrease in freezing behavior compared to *Nrg3*$^{+/+}$, even at baseline. The difference is more pronounced after the tone and shock (which persists from minute 2 to 2.5) during the first day of testing. During the second day, the *Nrg3*$^{-/-}$ mice are again much more active (less freezing behavior) than the *Nrg3*$^{+/+}$ mice. It should be noted, however, that both genotypes show an increase in freezing behavior in Day 2 compared to their performance on Day 1. On the third day of testing, freezing behavior during the first minute (prior to tone) is comparable to freezing behavior exhibited in Day 2. However, upon hearing the tone, the *Nrg3*$^{+/+}$ mice increase their freezing behavior but the *Nrg3*$^{-/-}$ mice do not. Only after the tone ends does the freezing behavior of the *Nrg3*$^{-/-}$ mice increase.

On Day 1 and Day 3, *Nrg3*$^{-/-}$ mice had a significantly reduced average freezing behavior across the five minutes of the test compared to *Nrg3*$^{+/+}$ mice

(two way repeated measures ANOVA $p<0.001$ and $p=0.003$, respectively). Day 2, when the mice were allowed to habituate to the arena, was not ($p=0.387$).

These may indicate that the *Nrg3*$^{-/-}$ mice failed to correctly form, store and/or recall the association between the tone and the shock. An alternative explanation is that the *Nrg3*$^{-/-}$ mice are hyperactive compared to *Nrg3*$^{+/+}$. If so, they would be expected to exhibit less freezing behavior regardless of context or stimuli. It is important to note that a hyperactivity phenotype is likely to deeply confound this test. Additionally, if the *Nrg3*$^{-/-}$ mice have sensory deficits such that the shock was less painful to them, this would also prove to be a confounding factor in this analysis. For this reason, we tested mice to explore hyperlocomotion and nociception.

Hot Plate Test

The hot plate test is a measure of pain sensation (nociception) and important in understanding whether altered nociception may be a confounding factor in other behavioral tests. For each strain, we saw no differences between sexes or between genotypes (Figure 4-5, 2-tailed t-tests ranged between 0.2 and 0.7). Thus, we conclude that for each strain, there is no differential sensitivity to pain (at least thermal pain).

24-hour circadian rhythm

24-hour circadian rhythm tests were performed in order to explore spontaneous locomotor differences between *Nrg3*$^{+/+}$ and *Nrg3*$^{-/-}$ mice. As seen in Figure 4-6, the KO mice of both sexes exhibit higher locomotive activity, but the results do not reach statistical significance (2-factor ANOVA with replication, males, p=0.208; female, p=0.085). Nonetheless, because of its importance as a confounding factor, this trend should not be ignored and should be further tested.

Open Field

The open field paradigm assesses a number of behaviors: anxiety (although it should be considered only an initial screen), exploration of novel environments (first 5 minutes), habituation, and locomotor actitivy both at baseline and, in our case, under the influence of MK-801.[71]

To study the baseline behavior of the mice, we compared the activity of the mice during the first 30 minutes (prior to any injections). The *Nrg3*$^{-/-}$ mice spent a greater percentage of their time exploring the center of the field (Figure 4-7 E), which mice generally avoid due to thigmotaxis. However, the difference was not statistically significant (2-tailed t-test p=0.18). During this same period, we compared the peripheral, central and total (peripheral plus central) activity of the mice (Figure 4-7F) and found that the central and total activity measures were significantly different between genotypes (two way repeated measures ANOVA p=0.037 and p=0.022, respectively). The data reveal that the difference seen in total activity is driven by the difference in central activity, with the *Nrg3*$^{-/-}$ mouse exploring the center more than the control mice. Therefore, it appears

that *Nrg3*$^{-/-}$ mice are more likely to explore the center and may experience less anxiety in response to this stress. Open Field, however, is not a test designed to measure anxiety, so other tests (including the elevated plus maze) must be conducted in order to claim a difference in anxiety.

In order to explore novel exploratory drive, we compared the total activity in the first five minutes with the total activity during minutes 25-30. We found that in both intervals, the *Nrg3*$^{-/-}$ males were more active than the control males (interval 0-5: 2-tailed t-test p=0.073; interval 25-30: p=0.032, see Figure 4-7. The difference between activity during the two intervals for mice of a given genotype was not significant (2-tailed t-test p=0.385), nor was the difference in percentage of time spent in the center (p=0.861). Thus, we conclude that the *Nrg3*$^{-/-}$ mice appear to be more active than the *Nrg3*$^{+/+}$, but this is not a direct effect of novelty since the change in exploratory behavior was not significantly different between genotypes.

Additionally, we note that after exposure to MK-801, all mice experience hyperlocomotion, as expected (Figure 4-7A). However, the *Nrg3*$^{-/-}$ mice appear to be more sensitive to this drug than their control littermates. The results are nearly significant (two way repeated measure ANOVA p=0.055). Given the confounding factor of genotype-dependent baseline activity, we computed the corrected average difference of the least square means for each genotype at each timepoint (Figure 4-8) and compared the differences between different periods. A comparison of the first 30 minutes (baseline) to the entire 2 hours after MK-801 exposure (overall effect) reveals that there is a statistically-significant difference (p=0.037) not completely accounted for by genotype-specific baseline

activity differences (Figure 4-8A). If, however, instead of comparing the initial 30 minutes of baseline activity to the entire two hours of MK-801 exposure, we compare the 30 minutes of baseline to the first 40 minutes of MK-801 exposure (during which MK-801 induced activity is still increasing), we find that the differences are not statistically significant (p=0.52, Figure 4-8B). Comparison of the 30 minutes of baseline with the last 80 minutes of MK-801 exposure (Figure 4-8C, the period during which MK-801 induced activity begins to wane) reveals that it is the late effects of MK-801 that are driving the difference between genotypes (p=0.0012). We therefore conclude that there is a difference in the response of the *Nrg3*$^{-/-}$ mice to MK-801, that this difference is not completely explained by baseline differences in activity, and that it is driven by the late effects of MK-801.

Elevated Plus Maze

Elevated plus maze experiments are designed to measure anxiety in mice. Anxious mice will prefer to remain in the closed arms, whereas less anxious mice will explore the open arms. The percentage of time the male *Nrg3*$^{-/-}$ mice spent in the open arm was more than twice as much as the *Nrg3*$^{+/+}$ males (19.8% for *Nrg3*$^{-/-}$, 9.8% for *Nrg3*$^{+/+}$), but the differences did not reach statistical significance for any group (Figure 4-9). Therefore, we conclude that the male *Nrg3*$^{-/-}$ mice trend towards decreased anxiety. As before, this would support previously-described evidence for a hyperactive phenotype in the *Nrg3*$^{-/-}$ males. However, if *Nrg3* has unknown consequences on motor ability, urge to explore or recognition memory, this could prove a confounding factor.[71]

Y-maze

Y-maze experiments are commonly used to test spatial working memory in rodents, taking advantage of their tendency to explore novel environments. Mice were scored on the number and type of alterations between the three arms, with "triad" alterations consisting of entering each arm in turn and "non-triad" alterations consisting of any pattern of entry into the arms that does not consist of entering each of the three arms once before repeating an arm. Although the number of non-triad alterations were similar in males of either genotype, the *Nrg3*$^{-/-}$ males had a higher number of triad alterations and a higher number of overall alterations on average, but neither of those comparisons reached statistical significance (2-tailed t-test: total p=0.0866, triads p=0.1311, nontriads p=0.9714) (see Figure 4-10) Females, however, exhibited relatively similar numbers of triad alterations (2-tailed t-test p=0.8923), but *Nrg3*$^{-/-}$ females had close to twice the number of non-triad alterations (2-tailed t-test p=0.00945). The total number of alterations did not reach statistical significance (2-tailed t-test p=0.4172).

As seen in Figure 4-10, the *Nrg3*$^{+/+}$ mice of both sexes, as well as the *Nrg3*$^{-/-}$ females, tended to spend more time exploring the arm that had been previously blocked, compared to the arm that had never been blocked, although only the comparison between time in previously-blocked arm versus time in open arm in *Nrg3*$^{+/+}$ females reached statistical significance (2-tailed t-test p=0.03359). *Nrg3*$^{-/-}$ males averaged more time in the open arm, but it should be noted that for this experiment, the number of male *Nrg3*$^{-/-}$ mice was too small to

draw conclusions. Further experiments with greater number of mice are underway at the time of writing.

Gross Neuroanatomy of Nrg3$^{-/-}$ *mouse*

During preparation of adult brain sections, we noticed a striking difference between the brains of *Nrg3*$^{-/-}$ mice and their control littermates. Prior to any stains, *Nrg3*$^{-/-}$ mice consistently exhibited a region of intense white color in the midline (see Figure 4-11) that was fainter in the *Nrg3*$^{+/+}$ mice. The Johns Hopkins Phenotyping Core examined our mice and reported that differences between mice may be attributable to artifacts, so we are preparing more mice in order to further explore this finding. At this time, however, we are unable to conclude that there is a gross neuroanatomical difference due to genotype, and we are considering alternative imaging techniques to study this question.

Parvalbumin-positive cells in Adult and Adolescent Nrg3$^{-/-}$ *mutant mice*

To assay for migratory changes in GABAergic interneurons, we marked cells exiting the cell cycle at E12.5 with EdU[64], a thymidine analog, and followed them until P27 and P61. At P27 and P61, coronal sections were collected from the extracted brains of *Nrg3*$^{-/-}$ and wildtype control animals and labeled for EdU and parvalbumin (PV). Three sections were selected at different anterior-to-posterior regions (at approximately 1.2, -0.9, and -190 from bregma), and on

each section 2 separate images were recorded, one of the entire cortical thickness from ventricle to pia in the primary or secondary somatosensory cortex and one in the striatum or striatum and internal capsule. For each image, the PV and Edu double positive and total PV positive cells were identified and counted. Two separate measurements were recorded for each image: the total number of PV-positive cells, and the percentage of EdU labeled PV cells. The first measurement was an indication of whether the overall PV cell population was altered, and the percentage a measure of how many of those PV^+ interneurons were born at E12.5.

In the cortical regions, we found a trend towards an increased number of PV+ cells in the cortex in *Nrg3*$^{-/-}$ *mutant* mice (Figure 4-12 D and E, Figure 4-13). These changes reached significance in the posterior-most section at P27 (2-tailed t-test p=0.03) and trended toward significance in the anterior-most section at P61 (p=0.067). Therefore, loss of Nrg3 did not lead to a deficit in PV+ GABAergic interneurons in the cortex, but rather, may have lead to excess when compared to the control. Next, we evaluated the percentage of PV cells exiting the cell cycle at E12.5 in the cortical regions studied (Figure 4-12 A and B). There was a trend towards a greater percentage of the PV+ cells marked at E12.5 in *Nrg3*$^{-/-}$ animals compared to controls at P27. The anterior-most region showed the greatest percentage of PV+/EdU+ double positive cells (p = 0.06). This slight trend was not evident at P61, where the percentage was similar in *Nrg3*$^{-/-}$ and control animals.

Interestingly in the striatum (Figure 4-14), we found fewer PV+ cells in the anterior-most region in *Nrg3*$^{-/-}$ mutants in comparison to the control at P27

(p=0.047). However, this trend was not evident in other sections at P27 or at P61. In addition, there was no change in the percentage of PV+ cells born at E12.5, at P27 or P61.

Together, these data suggest that more PV+ cells were born at E12.5 and migrated to the cortex at the expense of losing cells in the striatum. Altogether, the adolescent and adult timepoints suggested several possible mechanisms mediating the changes observed in the *Nrg3*$^{-/-}$ animals.

First, if the number of GABAergic interneuron precursor cells arising from the MGE is *less*, GABAergic interneuron precursor cells may be migrating in an unchanged fashion, but differentiating such that the smaller cohort of precursors is preferentially contributing to cortical PV+ interneurons perhaps at the expense of other cell fates. Alternatively, if the number of GABAergic interneuron precursor cells arising from the MGE is *greater*, GABAergic interneuron precursor cells may be migrating in an unchanged fashion, but the developing MGE compensated for *Nrg3* depletion early in development by increasing proliferation before E12.5. In this scenario, even though the percentage of MGE cells born at E12.5 would be lower in *Nrg3*$^{-/-}$ mice, the total amount of interneuron progenitor cells overall may be significantly greater in *Nrg3*$^{-/-}$ mice. Finally, if the number of GABAergic interneuron precursor cells arising from the MGE is *unchanged*, GABAergic interneuron precursor cells may be migrating such that they are preferentially converging in the cortex of the *Nrg3*$^{-/-}$ animals and PV+ cells are thus depleted from other brain regions.

Migration of Parvalbumin-positive interneurons during embryogenesis

To test the three hypotheses, we evaluated the GABAergic interneuron progenitors during embryonic and early postnatal development. Since the PV marker was not expressed during the embryonic or early postnatal stages, we used Nkx2.1 as a marker for interneuron precursors. Nkx2.1 is a transcription factor expressed in the MGE in the cells that will become cortical neurons expressing either PV or somatostatin. Nkx2.1 acts on another transcription factor, *Lhx6,* a key player in determining interneuron fate.[65]

In order to study the migration of GABAergic interneuron precursors during embryogenesis, we marked cells exiting the cell cycle at E12.5 as before and sacrificed mice at E18 and P0. Similarly, three sections per animals were chosen at different anterior-to-posterior regions (at approximately 1.3, -0.9, and -2.9 mm from bregma). We labeled sections with Nkx2.1 and EdU and measured the Nkx2.1 and EdU double positive area and the total Nkx2.1 area in each image to calculate the percentage of the interneuron precursors that were born at E12.5. At E18, less Nkx2.1+ area overlapped with EdU in the anterior and posterior cortex, indicating less proliferation of the interneuron progenitors (Figure 4-15 B and D). At P0 (Figure 4-15 C and E), we observed a noticeable decrease in the mid cortex; however, these differences were not statistically significant. Interestingly, when the absolute area of Nkx2.1 and EdU double-positive cells was measured (as opposed to the percentage described above), the difference between *Nrg3*$^{-/-}$ and controls in the mid region of the cortex at P0 became statistically significant (2-tailed t-test p=0.018). Therefore, it appears that there were slightly fewer Nkx2.1-positive cells exiting

the cell cycle at E12.5. Overall in the cortex, the trend was towards fewer Nkx2.1 cells exiting the cell cycle at E12.5 in the *Nrg3*$^{-/-}$ animals. Of course, our experiment only assays cells born at E12.5, so increased proliferation prior to that would not be taken into account and must remain a possibility.

To further narrow down a possible mechanism, we also evaluated the total Nkx2.1+ area (in pixels) in each of the images. The E18 mid-cortical region demonstrated lower total Nkx2.1 expression in the *NRG3*$^{-/-}$ animals (t-test, p= 0.019). But no other regions were different between control and *Nrg3*$^{-/-}$ littermates. Surprisingly, there were not just fewer Nkx2.1+ cells exiting the cell cycle at E12.5, but, at E18 in the mid-cortex region, there are also fewer overall Nkx2.1+ cells.

Given this result, we eliminated the second hypothesis (increased proliferation prior to E12.5), because the *Nrg3*$^{-/-}$ mice did not exhibit greater overall Nkx2.1 expression. To differentiate between the other possible mechanisms, we examined a region of the striatum. In the first hypothesis (a greater number of Nkx2.1-positive cells become interneurons at the expense of other cell fates) migration was not necessarily affected, so we would not have expected to see changes in PV+ cells elsewhere In our third hypothesis (PV-positive cells converge in the cortex), we expected to see a depletion of PV+ cells in some regions in the *NRG3*$^{-/-}$ animal.

At E18 (Figure 4-16 B and D), we found a smaller percentage of the Nkx2.1-positive cells were born at E12.5 in the striatum in *Nrg3*$^{-/-}$ mice (2-tailed t-test p=0.007). The area of Nkx2.1-positive signal was likewise smaller in the

Nrg3$^{-/-}$ animals at E18, but this result was not statistically significant. At P0 (Figure 4-16 C and E), we observed an equal or smaller absolute area of Nkx2.1+ signal in the *Nrg3*$^{-/-}$ mice, although these differences were not significant. However, there was a trend towards a greater percentage of the Nkx2.1 cells that were present at that time to have been born at E12.5 in *Nrg3*$^{-/-}$ mice. This may suggest that there was a slight increase in proliferation near the MGE around P0 that makes up for equal or less proliferation of these cells at E18. In contrast, there were significantly fewer PV+ cells in the same region of the striatum at P27 in the *Nrg3*$^{-/-}$ animals ($p<0.05$). This suggests that even if there was an increase in proliferation in Nkx2.1 cells at P0, the PV-positive cells did not remain in this region as they did in the control littermates. Therefore, these finding support the first hypothesis, that there is a migratory difference in the GABAergic interneurons that populate the cortex. The data suggest that the difference may have been due to a preferential convergence into cortical regions at the expense of other more subcortical regions. Therefore, while we expected to observe fewer PV+ cells in the cortex in the absence of Nrg3 due to migrational deficits, we uncovered a more complex mechanism. We propose that in the absence of Nrg3, the number of GABAergic interneuron precursors born in the MGE remains the same or is slightly lower. During migration (assayed at E18 and P0), the precursors migrate in a tangential fashion to the cortex. However, our data suggest that in the Nrg3-deficient brain, migration may be altered such that GABAergic interneurons converge in the cortical structure at the expense of other subcortical regions.

Discussion

Hyperactivity

Our behavioral studies demonstrate a pervasive hyperactivity phenotype in the *Nrg3*$^{-/-}$ mice. This conclusion is supported by our results in Open Field, Fear Conditioning, and 24-hour Circadian Rhythm tests and is consistent with many mouse models of other NRG/ErbB pathway genes. Gerlai *et al.*[72] reported "findings that suggest a consistent hyperactivity across tests" in a heterozygous mutant *Nrg1* mouse model. Heterozygotes were used because homozygotes did not survive to term. *Nrg1* hypomorph mice also exhibit hyperactivity in tests such as open field and Y-maze.[23]

An *ErbB4* conditional knock-out mouse developed to express no *ErbB4* in neurons and glia, but heterozygous for the *ErbB4* null allele elsewhere to allow viability, also expressed a hyperactive phenotype.[73] Pre-weaned *ErbB4* KO mice scored significantly greater than controls in horizontal activity, and trended towards higher levels of grooming, rearing and sitting, although this effect reversed as adults. A different *ErbB4* conditional knockout mouse, *PV-ErbB4*$^{-/-}$, displayed a hyperactivity phenotype as well.[74]

BACE1catalyzes cleavage of full-length Nrg3 with release of the extracellular EGF domain[75], and *Bace1*-/- mice exhibited reproducible hyperactivity (novelty-induced, in particular) in a number of tests, including Open Field, Plus Maze and Y Maze.[76]

Pre-pulse Inhibition

As mentioned previously, impaired PPI is highly valued as an endophenotype of human SZ that is often observed in mouse models of SZ.[59,60] In our experiments, we see a deficit in pre-pulse inhibition in our *Nrg3*$^{-/-}$ mice of mixed-strain backgrounds.

Similarly, locomotor hyperactivity is also seen in mice deficient in other genes in the NRG/ErbB4 pathway. The *Bace1-/-* mouse model described above exhibits, in addition to hyperactivity, a deficit in PPI.[76] A mouse model engineered to lack both *ErbB2* and *ErbB4* expression in the CNS resulted in decreased PPI in males,[77] as did the the PV-*ErbB4*$^{-/-}$ mouse model.[74] A *Nrg1* hypomorphic mouse[23] has also been reported to be deficient in PPI.

Anxiety and memory

Findings from our Y maze suggest that the Nrg3$^{-/-}$ mice may experience memory deficits in emotional or fearsome conditions. However, further experimentation with a greater number of mice is required to confirm these findings.

Elevated plus maze experiments revealed a trend towards decreased anxiety, but like the memory findings, a greater number of mice are required to confirm the finding. Currently, those experiments are underway.

MK-801 and GABAergic interneurons

As a non-competitive antagonist of the NMDA receptor, MK-801 sensitivity in our mouse model may prove some insight into possible deficiencies in the *Nrg3*$^{-/-}$ mouse, which may have abnormalities in GABAergic interneuron migration.

One possible hypothesis is that reduced NMDA receptor activity affects primarily the function of cortical GABAergic interneurons and may lead to the development of SZ-like symptoms, perhaps through disrupting gamma-frequency oscillations and, in turn, disrupting proper cortical function.[78] This hypothesis is particularly attractive when we take into consideration the early-adulthood age of onset of SZ symptoms, since GABAergic neurons do not complete their innervations until after adolescence.[78]

Nakazawa et al.[78] point out three different lines of evidence for this hypothesis: administration of NMDAR antagonists causes a net excitatory change in the cortex; hippocampal GABAergic hypersensitivity to NMDAR antagonists when compared to pyramidal neurons; and chronic NMDAR antagonist use results in lower expression of GAD67 (an enzyme that converts glutamate to GABA) and PV in GABAergic neurons of the cortex.

Interneuron Migration

We conclude that, as previously reported[30], our *Nrg3*$^{-/-}$mouse exhibits features consistent with abnormal migration of GABAergic interneurons and/or their precursors. However, we hypothesized that the migratory defects would

lead to decreased GABAergic interneurons in the cortex, a finding that we did not observe. We postulate that GABAergic interneuron precursors are born in less or equal numbers in the MGE, but a greater percentage of them migrate to the cortical regions at the expense of subcortical regions. The net effect is an increase in the number of PV+ cells in the cortical regions examined.

GABAergic interneurons and behavioral abnormalities

Yee et al.[79] report that depletion of α3 $GABA_A$ receptors leads to a phenotype reminiscent of our *Nrg3*$^{-/-}$ mouse, with hyperactivity and startle response and prepulse inhibition abnormalities. This finding supports our hypothesis that GABAergic interneuron abnormalities may underlie the behavioral changes seen in *Nrg3*$^{-/-}$ mice.

Figure 4-1:Schematic of knockdown strategy

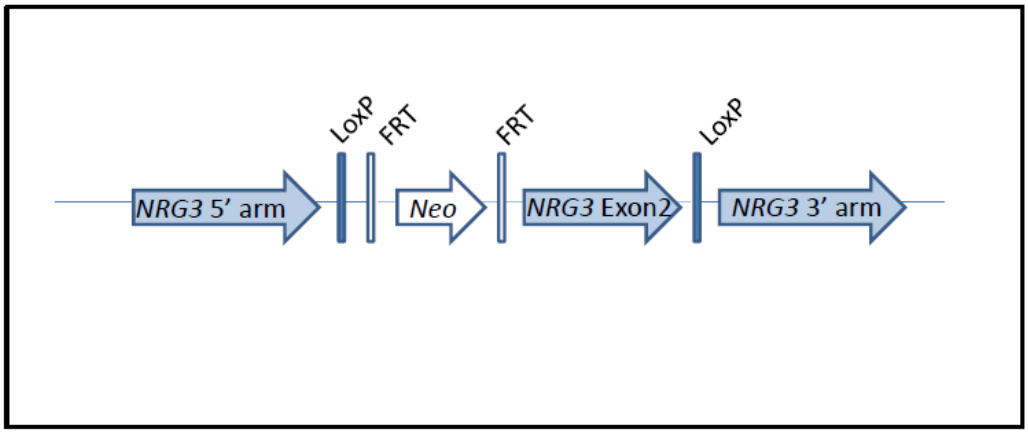

Figure 4-1: Schematic of knockdown strategy. Exon 2 of murine Nrg3 (GRCm38/mm10 Chr14:39,011,969-39,012,099) was targeted for deletion using a Neomycin cassette (Neo) flanked by both FRT and LoxP sites (see Figure 1), as well as genomic regions flanking Exon 2 (5' and 3' arms of murine Nrg3).

Figure 4-2: Northern Blots

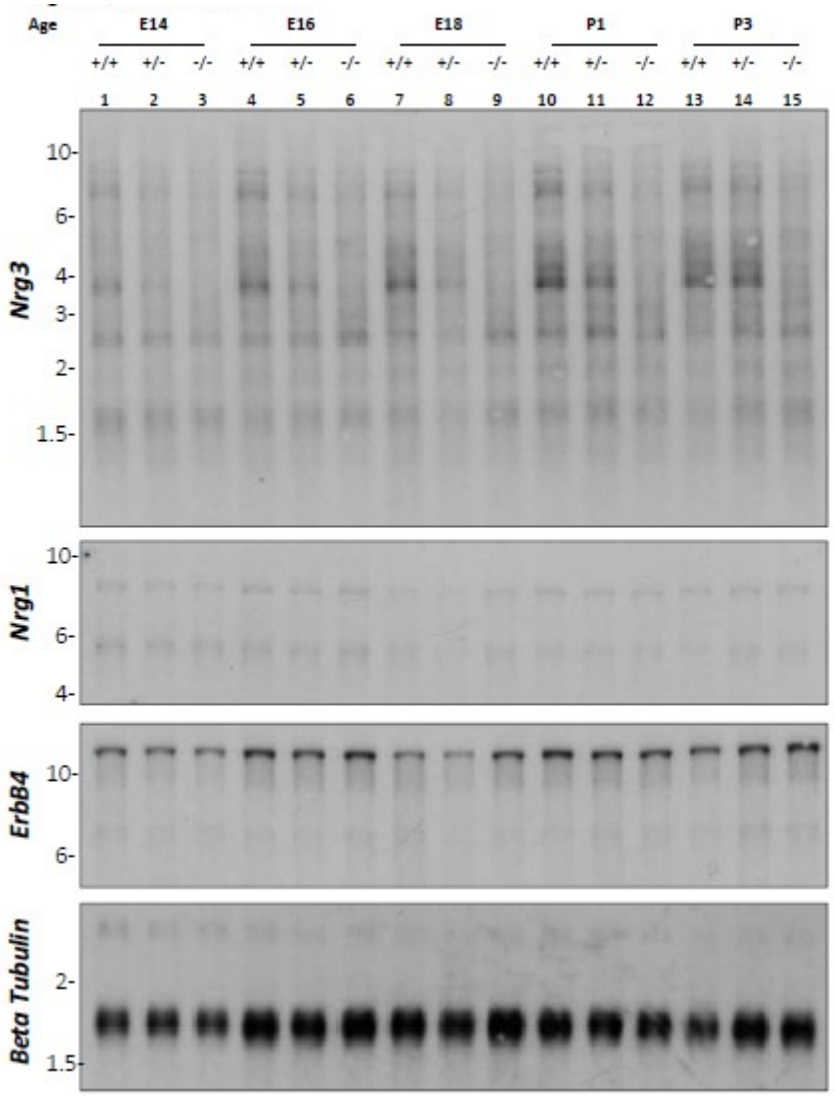

Figure 4-2: Northern Blots. RNA extracted from whole brains of E14 (lanes 1-3), E16 (lanes 4-6), E18 (lanes 7-9), P1 (lanes 10-12) and P3 (13-15) *Nrg3*$^{+/+}$ (lanes 1, 4, 7, 10 and 13), *Nrg3*$^{+/-}$ (lanes 2, 5, 8, 11, and 14) and *Nrg3*$^{-/-}$ (lanes 3, 6, 9, 12 and 15) was probed with *Nrg3*, *Nrg1*, *ErbB4*, and *Beta tubulin* radiolabeled probe.

Figure 4-3: Pre-pulse inhibition of the Startle Response

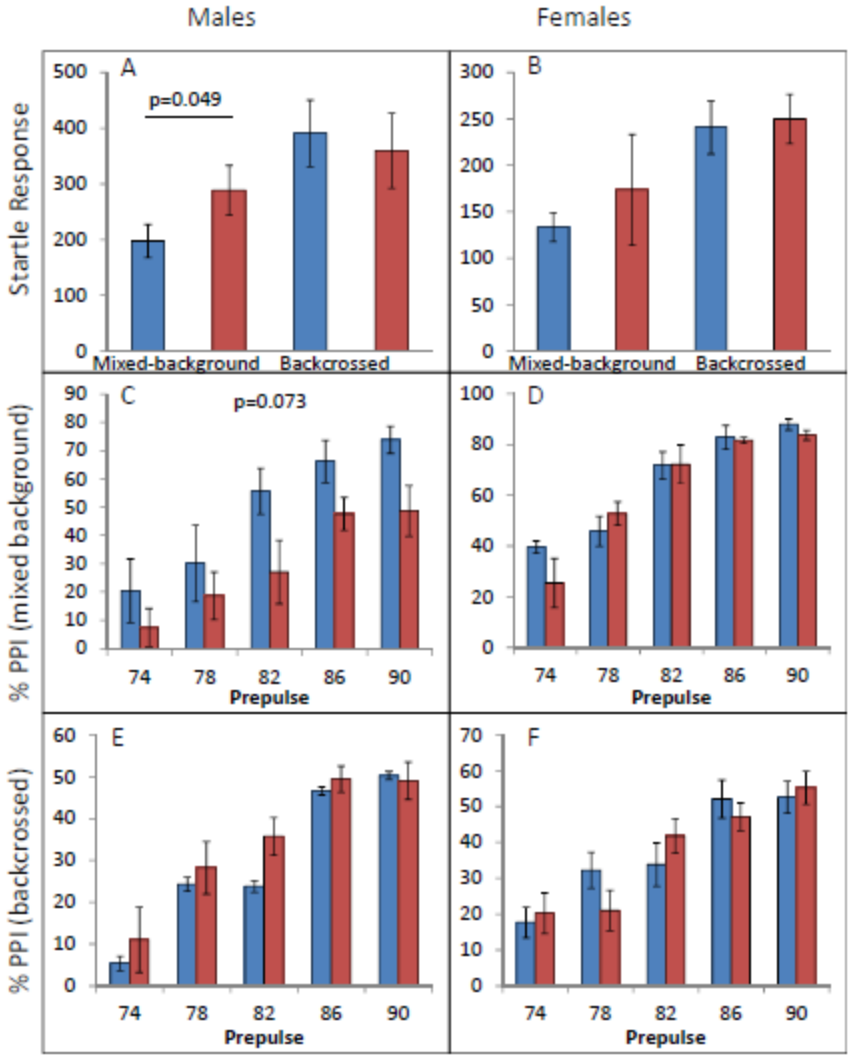

Figure 4-3: Pre-pulse inhibition of the startle response. (A and B) Startle response of mixed-background and backcrossed *Nrg3*$^{-/-}$ and *Nrg3*$^{+/+}$ male (A) and female (B) mice. %PPI was calculated for mixed background (C and D) and backcrossed (E and F) *Nrg3*$^{-/-}$ and *Nrg3*$^{+/+}$ male (C and E) and female (D and F) mice.

Figure 4-4: Fear Conditioning

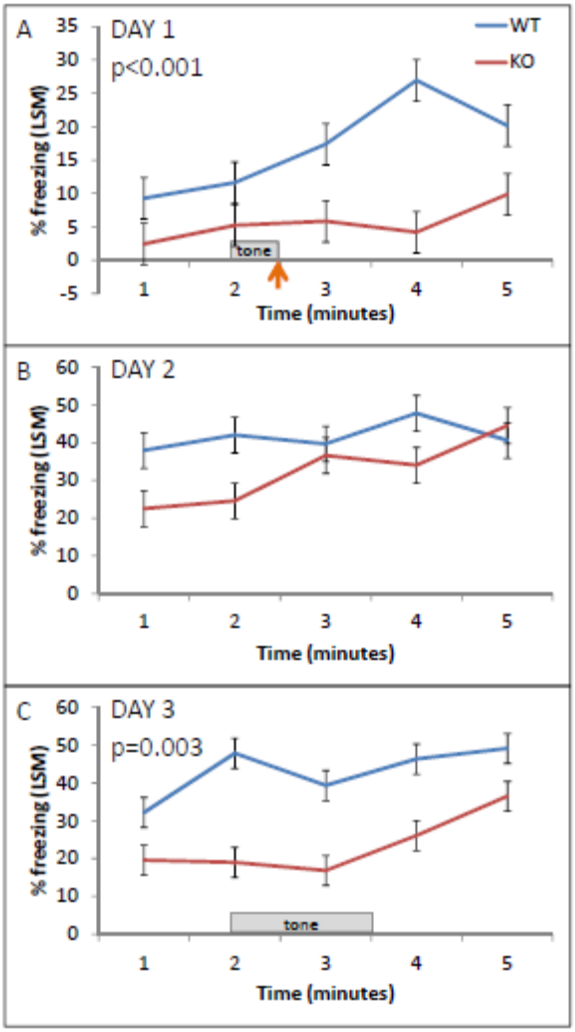

Figure 4-4: Fear Conditioning. Percentage freezing behavior per minute was recorded for Day 1 (A), Day 2 (B) and Day 3 (C) of testing. Grey box denotes interval during which mice were exposed to the tone, and orange arrow denotes shock.

Figure 4-5: Hotplate Nociception Test

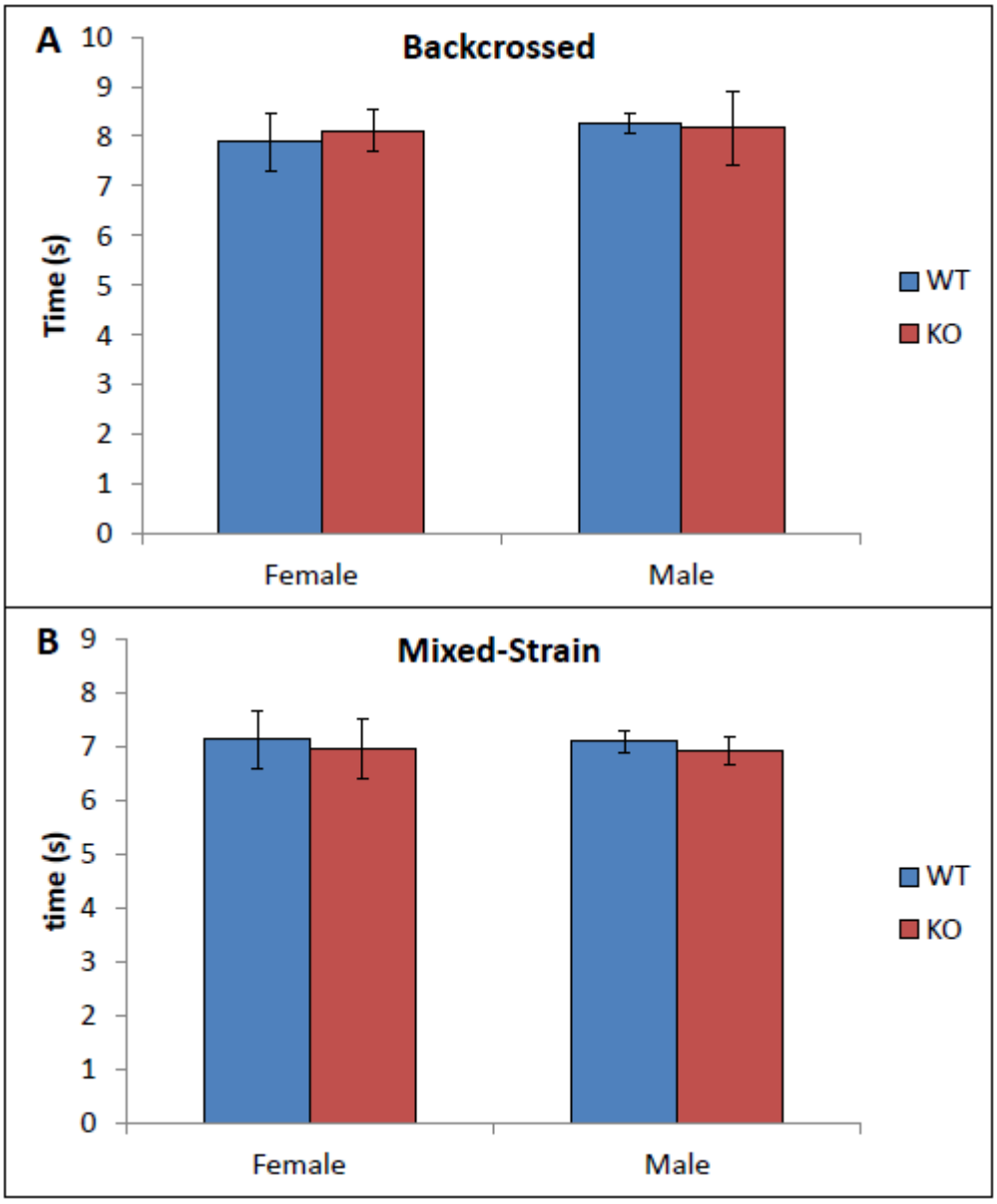

Figure 4-5: Hotplate Nociception Test. *Nrg3*$^{-/-}$ and *Nrg3*$^{+/+}$ mice were tested for nociception by measuring the latency between stimulus and response. Mice tested were either backcrossed (A) or mixed-strain (B).

Figure 4-6: 24-hour Circadian Rhythm

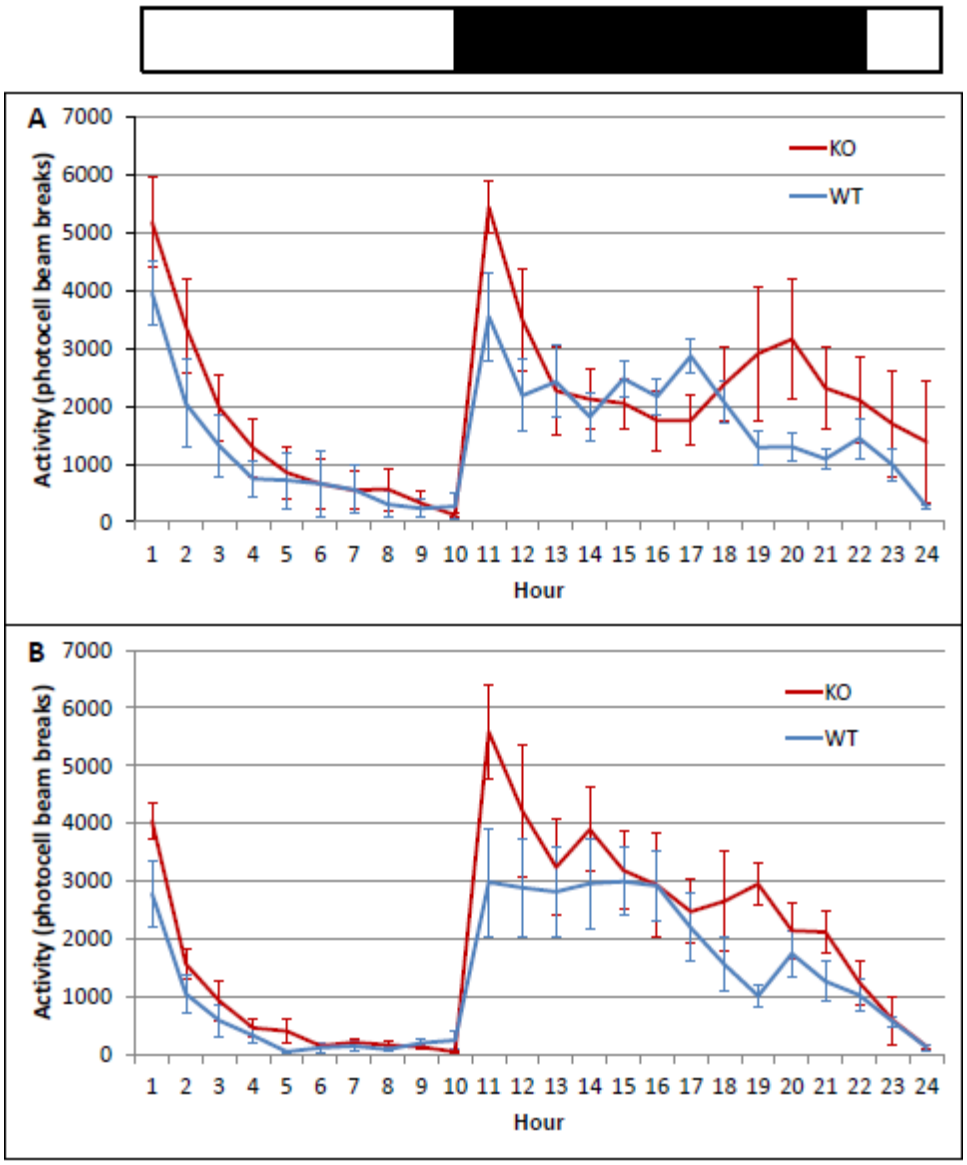

Figure 4-6. 24-hour circadian rhythm. Activity of male (A) and female (B) *Nrg3*$^{-/-}$ and *Nrg3*$^{+/+}$ mice was tested during a 24-hour period by measuring number of photocell beam breaks. Light/dark periods are represented above.

Figure 4-7: Open Field

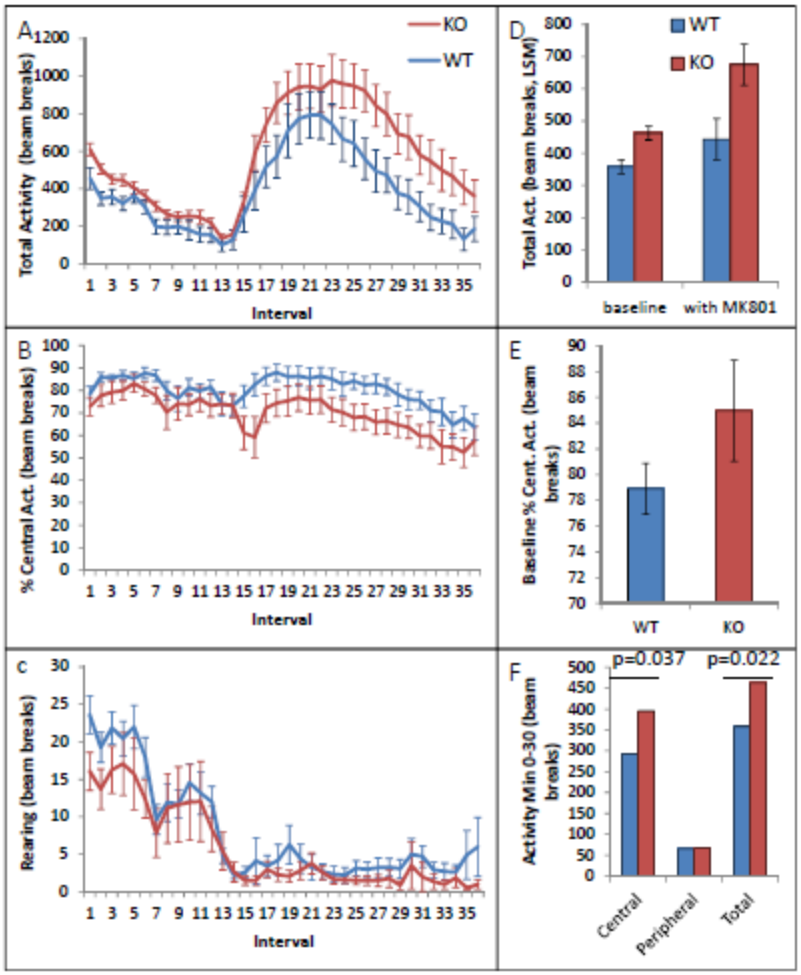

Figure 4-7. Open Field. Total activity (A), percentage central activity (B) and rearing activity (C) of *Nrg3*$^{-/-}$ and *Nrg3*$^{+/+}$ male mice was scored by number of photocell beam breaks per five-minute interval. (D) The least-squares mean of the total activity as measured in beam breaks was calculated for baseline and post-MK801 injection periods. Baseline percentage of central activity (E) was measured according to genotype by recording photocell beam breaks. (F) Total, central and peripheral activity of mice during the first thirty minutes of testing (baseline).

Figure 4-8: MK801 Sensitivity in Open Field

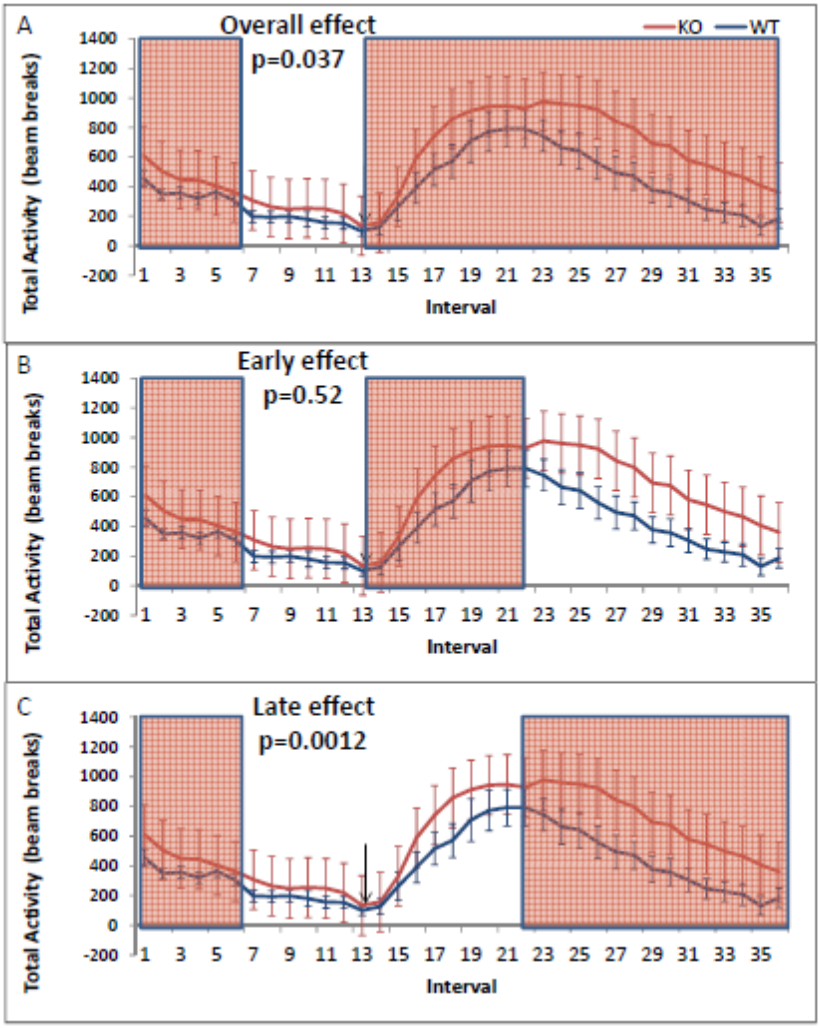

Figure 4-8. MK801 sensitivity during Open Field experiment. Total activity of *Nrg3*$^{-/-}$ and *Nrg3*$^{+/+}$ male mice was scored by number of photocell beam breaks per five-minute interval. Blocks of time shaded in pink were compared to calculate the overall (A), early (B) and late (C) effects of MK801.

Figure 4-9: Elevated Plus Maze

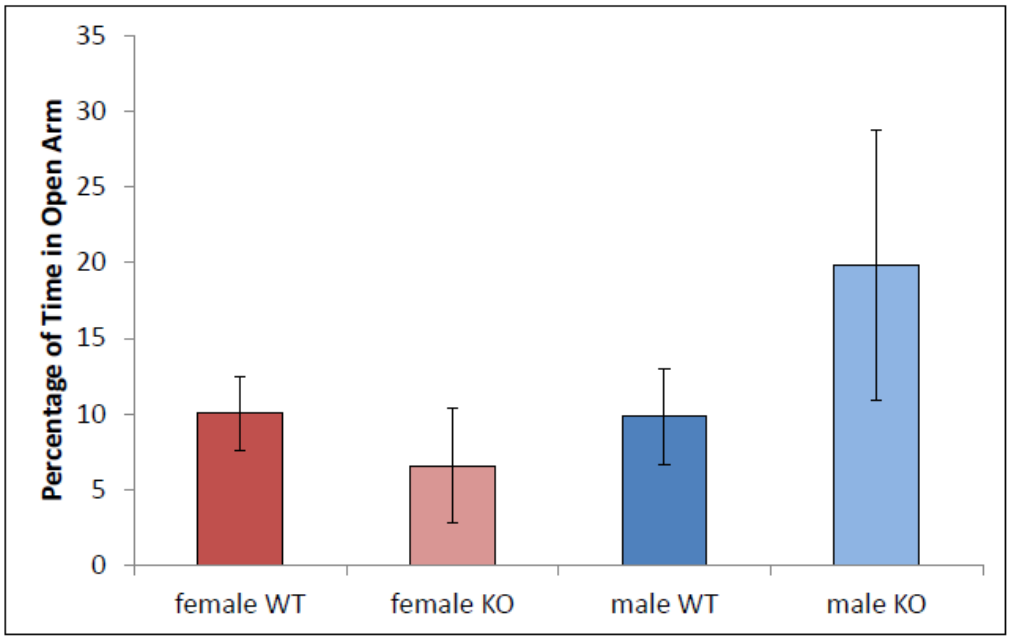

Figure 4-9. Elevated Plus Maze. Percentage of time *Nrg3*$^{-/-}$ and *Nrg3*$^{+/+}$ mice of either sex spent in open arm of elevated plus maze was measured.

Figure 4-10: Y-Maze

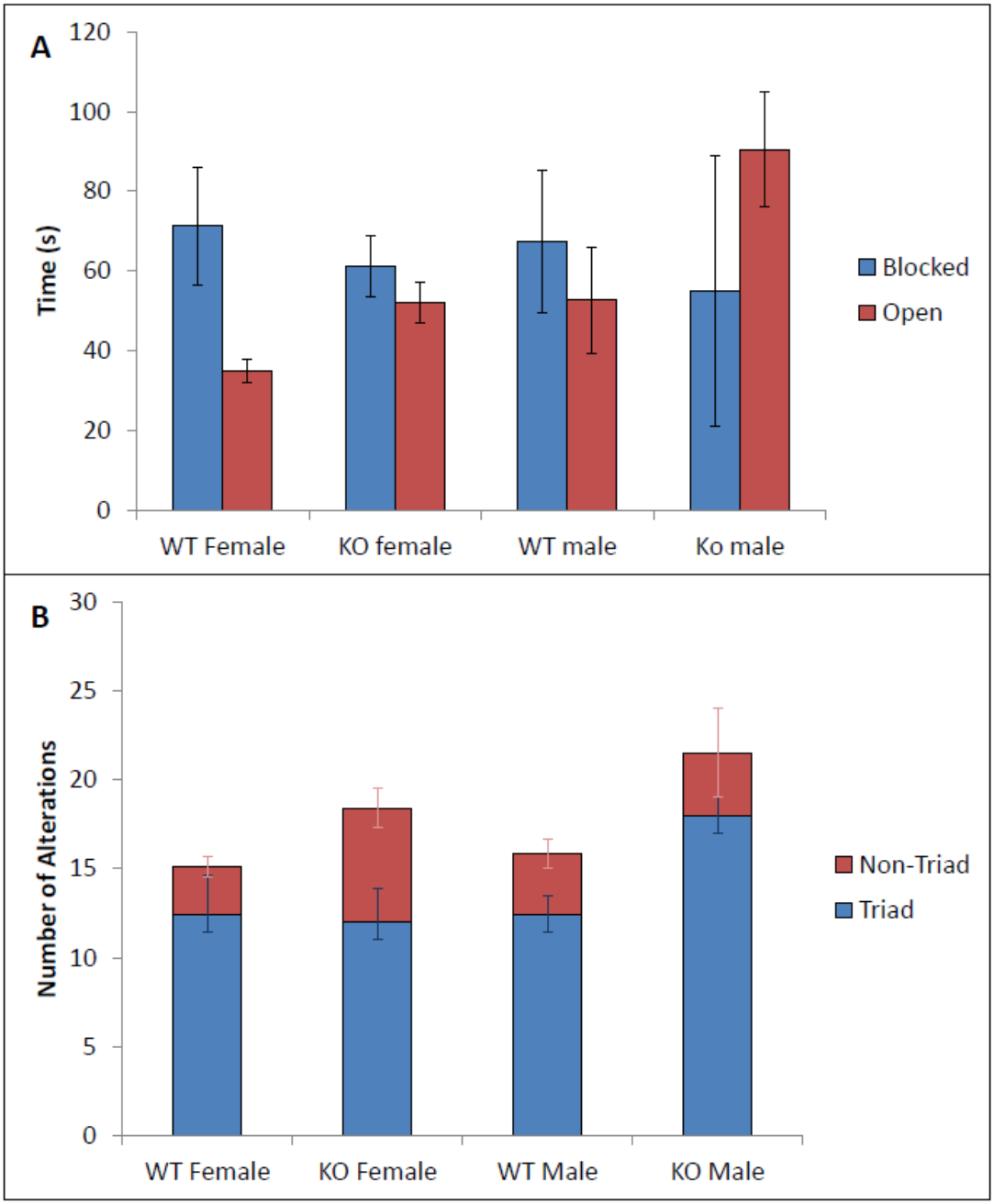

Figure 4-10. Y-Maze. *Nrg3*$^{-/-}$ and *Nrg3*$^{+/+}$ mice of either sex were subjected to a Y Maze. (A) Absolute time (in seconds) spent in blocked and open arms of the Y Maze. (B) Number of triad and non-triad alterations during Y Maze Test.

Figure 4-11: Gross Neuroanatomy of *Nrg3*$^{-/-}$ and *Nrg3*$^{+/+}$ mice

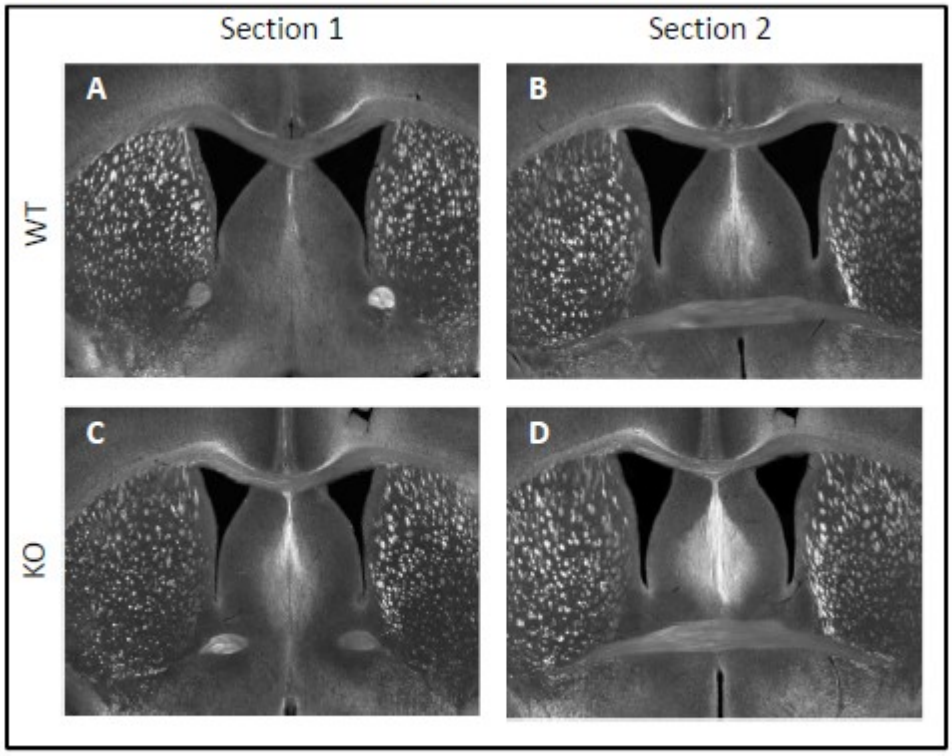

Figure 4-11. Gross Neuroanatomy of *Nrg3*$^{-/-}$ and *Nrg3*$^{+/+}$ mice. Phase contrast microscopy of equivalent vibratome sections from P61 *Nrg3*$^{+/+}$ (WT) and *Nrg3*$^{-/-}$ (KO) mice at two different depths anterior to posterior (Section 1 and Section 2).

Figure 4-12: Cortical Region of Adult and Adolescent Brains

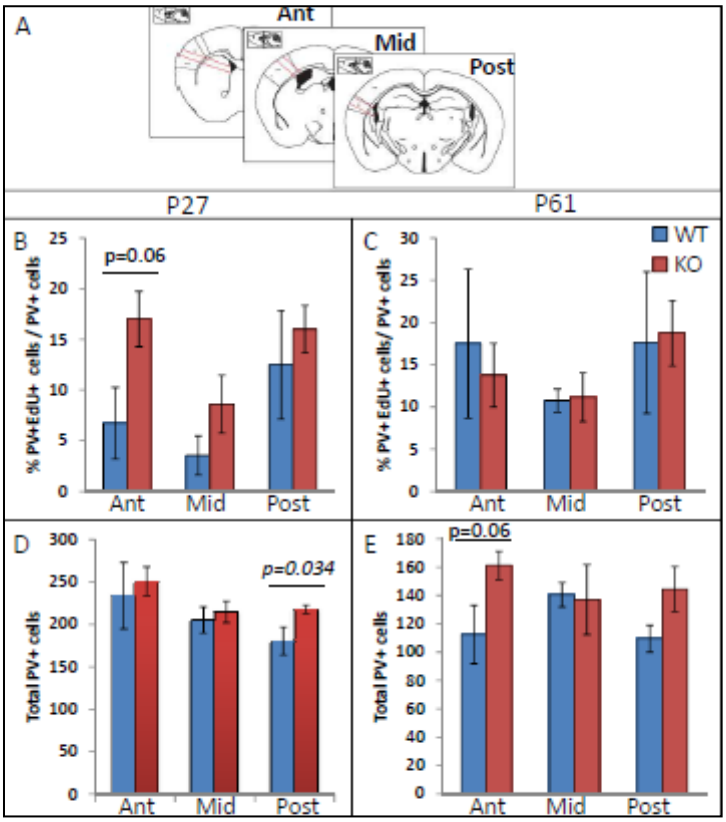

Figure 4-12. Cortical regions of adult and adolescent brains. Microscopic images of cortical regions defined in (A) were examined for (B and C) the percentage of cells staining positive for parvalbumin (PV) that also stained positive for EdU and (D and E) number of cells staining positive for PV. Measurements were performed at Postnatal days (B and D) 27 and (C and E) 61 in *Nrg3*$^{-/-}$ and *Nrg3*$^{+/+}$ mice.

Figure 4-13: Microscopy of Cortical Regions of Adult and Adolescent Brains

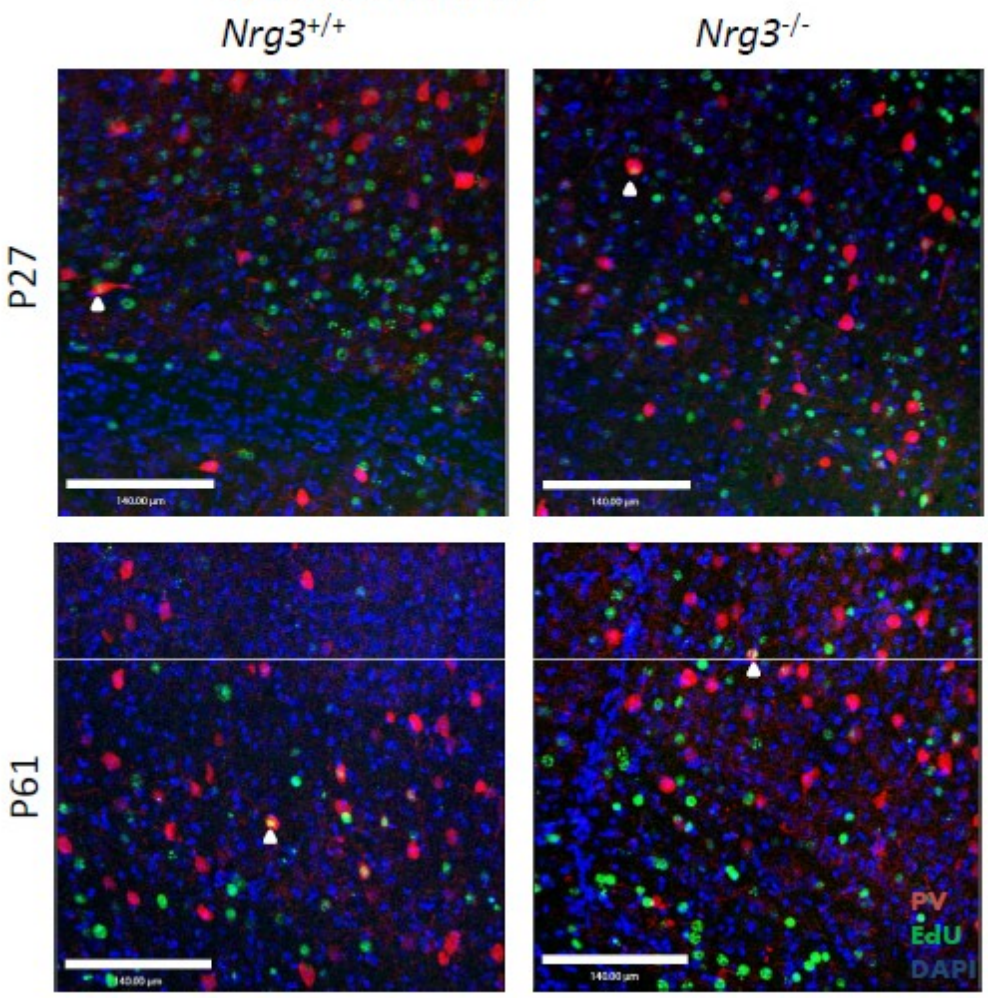

Figure 4-13. Microscopy of cortical regions of adult and adolescent brains. Microscopic images of equivalent regions of cortex in *Nrg3*$^{-/-}$ and *Nrg3*$^{+/+}$ mice at P27 and P61 ages. Arrowhead denotes a cell tallied as double-positive for PV+ and EdU.

Figure 4-14: Subcortical Regions of Adult and Adolescent Brains

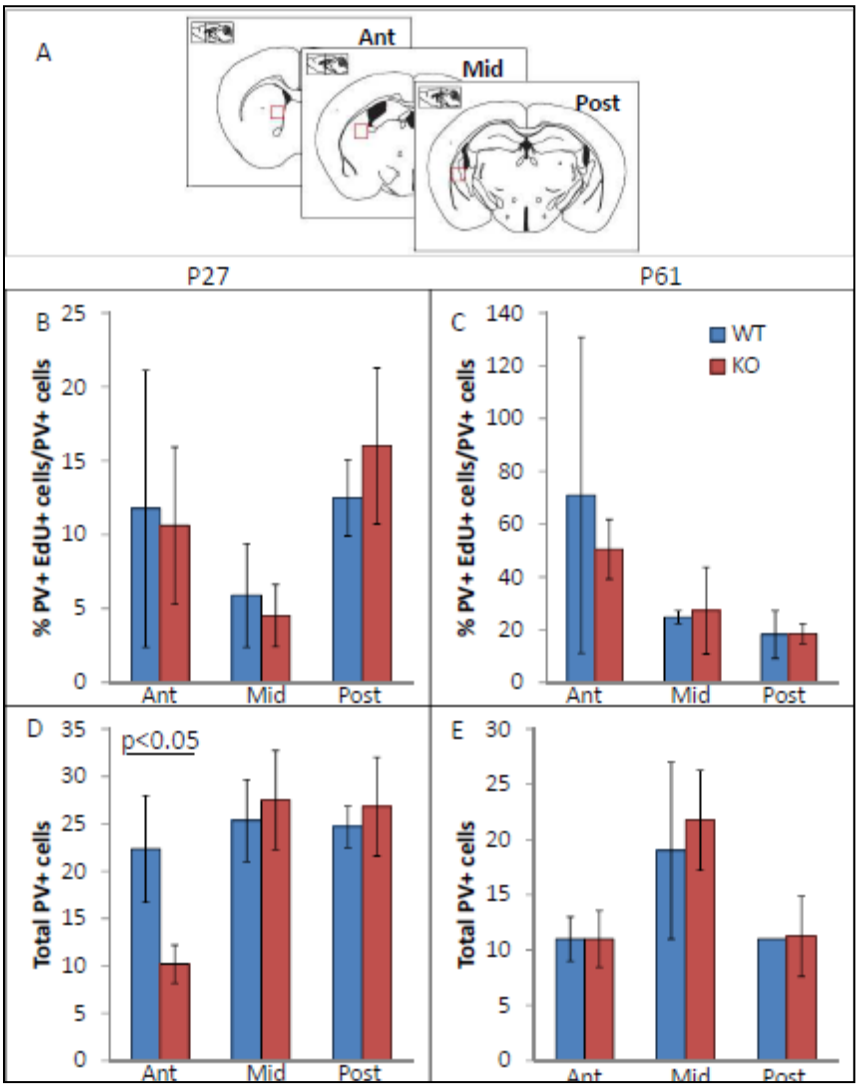

Figure 4-14. Subcortical regions of adult and adolescent brains. Microscopic images of subcortical regions defined in (A) were examined for (B and C) the percentage of cells staining positive for parvalbumin (PV) that also stained positive for EdU and (D and E) number of cells staining positive for PV. Measurements were performed at Postnatal days (B and D) 27 and (C and E) 61 in *Nrg3*$^{-/-}$ and *Nrg3*$^{+/+}$ mice.

Figure 4-15: Cortical Regions of Brain during Embryogenesis

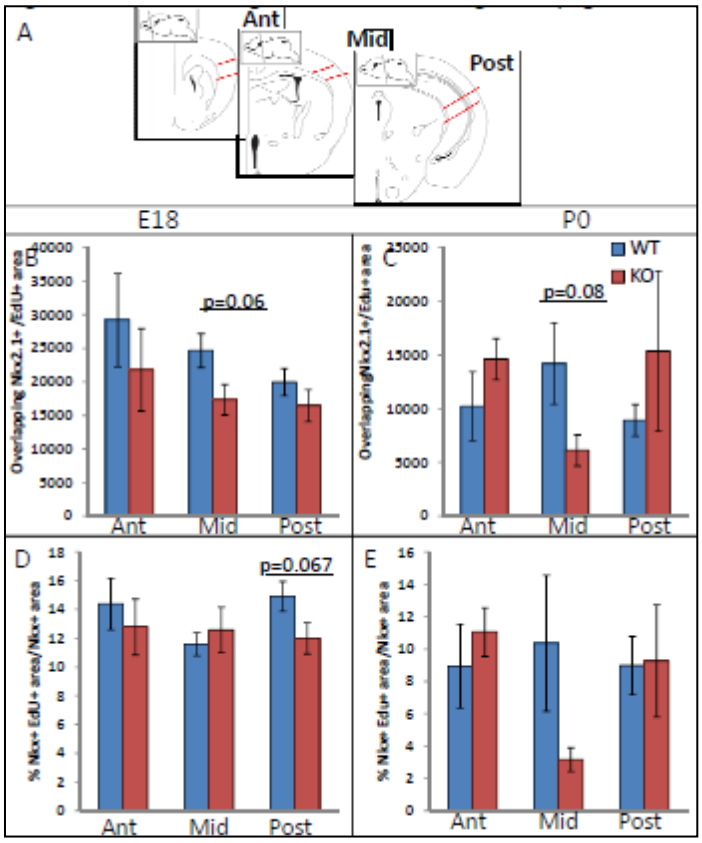

Figure 4-15. Cortical regions of brain during embryogenesis. Microscopic images of cortical regions defined in (A) were examined for (B and C) absolute area staining positive for both Nkx2.1 and EdU, as measured in arbitrary units and (D and E) the percentage of area staining positive for Nkx2.1 that also stained positive for EdU. Measurements were performed for (B and D) embryonic day 18 fetuses and (C and E) early post-natal *Nrg3*$^{-/-}$ and *Nrg3*$^{+/+}$ mice.

Figure 4-16: Subcortical Regions of Brain during Embryogenesis

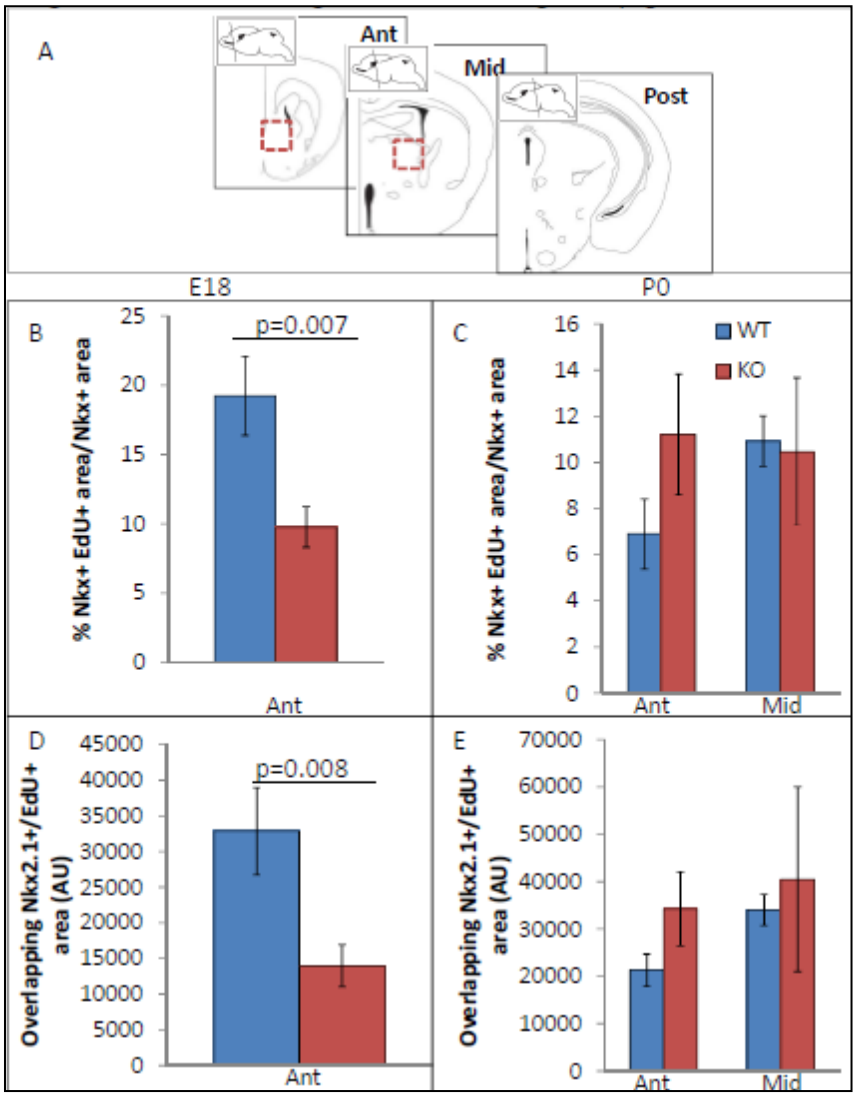

Figure 4-16. Subcortical regions of brain during embryogenesis. Microscopic images of subcortical regions defined in (A) were examined for (B and C) the percentage of area staining positive for Nkx2.1 that also stained positive for EdU and (D and E) absolute area staining positive for both Nkx2.1 and EdU, as measured in arbitrary units. Measurements were performed for (B and D) embryonic day 18 fetuses and (C and E) early post-natal *Nrg3*$^{-/-}$ and *Nrg3*$^{+/+}$ mice.

Table 4-1: Summary of Histological Changes in cortex of *Nrg3*$^{-/-}$ mice

	Anterior		Mid		Posterior	
	%PVEdU/PV	# PV	% PVEdu/PV	#PV	%PVEdU/PV	#PV
P27	↑KO*	-	(↑KO)	-	-	↑KO
P61	-	(↑KO)	-	-	-	(↑KO)

Table 4-1. Summary of histological changes in the cortex of *Nrg3*$^{-/-\ +/+}$ adult and adolescent mice. Observed trends in percentage of parvalbumin (PV)-positive cells that also stained positive for EdU and absolute number of PV-positive cells in the anterior, mid and posterior sections of P27 and P61 mice examined. All trends are in relation to wildtype littermates. Asterisk (*) denotes a statistically-significant difference, parentheses a slight difference, and a dash (-), no observable difference.

Table 4-2: Summary of Histological Changes in striatum of *Nrg3*$^{-/-}$ mice

	Anterior		Mid		Posterior	
	%PVEdU/PV	# PV	% PVEdu/PV	#PV	%PVEdU/PV	#PV
P27	-	↓KO*	-	-	-	-
P61	-	-	-	-	-	(↑KO)

Table 4-2. Summary of histological changes in the striatum of *Nrg3*$^{-/-}$ adult and adolescent mice. Observed trends in percentage of parvalbumin (PV)-positive cells that also stained positive for EdU and absolute number of PV-positive cells in the anterior, mid and posterior sections of P27 and P61 mice examined. All trends are in relation to wildtype littermates. Asterisk (*) denotes a statistically-significant difference, parentheses a slight difference, and a dash (-), no observable difference.

Chapter 5 : Conclusion

Summary

The thesis of my dissertation is that variants in *NRG3* affect the expression and/or splicing of this gene. Regulatory imbalances in *NRG3* absolute levels or relative isoform abundance lead to a predisposition to a subtype of SZ that exhibits more types of delusions. This effect is mediated by improper neural migration during development.

In Chapter 2, I sequenced a 162 Kb LD block covering the 5' end of *NRG3* associated with risk for delusions in the context of SZ and identify those variants driving the association signal. For three of those SNP variants, in a number of cell types, I then show evidence for genotype affecting the regulation of a downstream reporter gene. These SNPs also spear to affect the relative abundance of various transcripts of this gene.

In Chapter 3, I provide evidence that at least one nuclear protein binds each 21-bp probe containing the SNP. In two of the SNPs, the allele of the SNP affects protein binding, by changing the shifting pattern and/or intensity of the observed bands. Bioinformatical analyses reach the same conclusion regarding allele affecting protein binding as our experiments, and suggest possible protein candidates to test for binding. I tested one candidate, CNOT4, by EMSA supershift and conclude that the SNP may be mediating the risk for delusions by preferential binding of this transcription factor complex member. Future experiments are planned for confirmation.

In Chapter 4, I characterize a *Nrg3* knockout mouse through behavioral and neuromigratory experiments. I find a pervasive hyperactive phenotype seen in many other animal models deficient in genes in the same pathway. Additionally, we find a modest deficit in PPI and startle response, as well as decreased anxiety, fear and/or emotional- based learning or memory deficits, and perturbed working memory. I also test the hypothesis that depletion of Nrg3 in the developing brain produces an animal deficient in cortical GABAergic interneurons. I find that although there is evidence for differences in migratory patterns, no cortical depletion of these cells is observed. However, a depletion of PV-positive cells in the striatum suggests a compensatory mechanism that results in altered migration.

Future and Ongoing Work

At the time of publication, a number of experiments are underway that will further inform this thesis.

In order to generate more hypotheses about proteins potentially binding the intronic regions of the SNPs identified in Chapter 2, I have an ongoing protein microarray experiment in which we will probe an array of human transcription factors with labeled probes containing our regions of interest. Observation that CNOT4 binds our probes in an allele-specific fashion will support the evidence presented in Chapter 3. If not, other candidate transcription factors may come out of this experiment that can be tested bioinformatically as well as with EMSA supershift assays.

Finally, we are expanding our mouse colonies in order to increase the number of mice tested for behavioral traits, neuromigratory changes, and gross morphological differences. For those behavioral experiments in which we see a trend, we believe that increasing the number of subjects will help to determine whether the differences we believe we see are statistically significant. We are also expecting to increase the number of P61 mice injected with EdU while *in utero*, in order to assess whether the gross neuromorphological changes described in Chapter 4 are reproducible. We plan to use the same mice to increase the number of subjects in our imaging studies, and perhaps study different regions of the cortex and striatum more systematically.

Another interesting experiment to consider is backcrossing the mixed-strain background to a strain (such as a 129 strain[80]) that has a naturally high startle response. This may uncover the deficit in PPI that may have been obscured due to the low startle response of C57BL/6J strain.[80]

Contributions

In my dissertation, I have specifically contributed:

- New, inclusive nomenclature of all known exons of *NRG3*
- Identification of causative variants in the association of the *NRG3* gene with the delusion factor in SZ
- Evidence of the regulatory effect of intronic SNPs in *NRG3*
- Exploration of putative transcription factors that bind regulatory SNPs and thus mediate the effect of *NRG3* on SZ

- Characterization of neurodevelopmental phenotype of a *Nrg3* knockout mouse
- Analysis of results of behavioral experiments conducted on a *Nrg3* knockout mouse

As a whole, my thesis takes an unconventionally deep approach to association studies. I begin with a region (162 kb LD block) associated with a trait (delusion), I identify all variants in our cohort, rank those variants by strength of association, and demonstrate a regulatory role for three of them. I then explore the mechanism whereby those SNPs appear to be modifying the SZ phenotype in patients, testing for preferential binding and relative transcript abundance changes influenced by genotype at those SNPs. I attempt to identify the protein I surmise to be binding our region of interest by a combined bioinformatics and experimental approach.

Studies such as these, where we follow up association results to find causative variants, are going to become increasingly more important in helping us identify specific polymorphisms that modulate SZ risk, as opposed to genes that mediate risk for the disease. In an age of genomics and whole genome sequencing, better understanding *how* each of the many SZ risk genes mediates its effect on the phenotype is going to become crucial in counseling patients that harbor variants of unknown significance in SZ risk genes.

Additionally, focusing on specific phenotypic traits, such as our delusion factor, rather than a binary diagnostic classification, can help to reduce the noise introduced by empirically-determined diagnostic categories and may provide more power to studies with limited subjects. This approach may also be

important in helping us understand the pathways and mechanisms involved in the components of this disease. This approach should better identify key biomarkers for detecting risk of specific symptoms, may improve our ability to generate and tailor drugs for the individual patient's presenting symptoms (rather than for a "textbook case" of SZ) and will help us better understand the normal mechanisms that go awry in SZ and other psychiatric diseases in a way that studying SZ as a binary entity has not. This "endophenotype" approach has recently been espoused by the National Institutes of Mental Health[81].

My thesis also contributes to the field by describing a *Nrg3* mouse model for SZ. Behavioral tests conducted demonstrate a number of relevant phenotypes, most noticeably hyperactivity, consistent with other mouse models of this pathway. I suspect that the *Nrg3*$^{-/-}$ mouse does have abnormal interneuron migratory patterns, but the end result of this defect is a comparable or greater number of GABAergic interneurons in the cortex. These abnormalities may explain why the mouse is not as debilitated as one might expect. Nonetheless, we believe that this mouse strain is a valuable mouse model for SZ.

Bibliography

1. Sawa A SS. Schizophrenia: Diverse Approaches to a Complex Disease. *Science.* 2002;296:692-695.

2. Insel T. Rethinking schizophrenia. *Nature.* 2010;468:187-193.

3. Eaton W. Epidemiology of schizophrenia. *Epidemiol Rev.* 1985;7:105-126.

4. Bilder RM MS, Rieder RO, Pandurangi AK. Symptomatic and Neuropsychological Components of Defect States. *Schizophr Bull.* 1985;11:409-419.

5. Gottesman II. *Schizophrenia Genesis: The Origin of Madness.* New York: Freeman; 1991.

6. Shih RA BP, Zandi PP. A review of the evidence from family, twin and adoption studies for a genetic contribution to adult psychiatric disorders. *International Review of Psychiatry.* 2004;16(4):260-283.

7. Tsuang M. Schizophrenia: genes and environment. *Biol. Psychiatry.* 2000;47:210-220.

8. Lencz T MT, Athanasiou M, Dain B, Reed CR, Kane JM, Kucherlapati R, Malhotra AK. Converging evidence for a pseudoautosomal cytokine receptor gene locus in schizophrenia. *Molecular Psychiatry.* 2007;12:572-580.

9. O'Donovan MC CN, Norton N, Williams H, Peirce T, Moskvina V, Nikolov I, Hamshere M, Carroll L, Georgieva L, Dwyer S, Holmans P, Marchini JL, Spencer CC, Howie B, Leung HT, Hartmann AM, Moller HJ, Morris DW, Shi Y, Feng G, Hoffmann P..... Identification of loci associated with schizophrenia by genome-wide association and follow-up. *Nature Genetics.* 2008;40:1053-1055.

10. Shifman S JM, Bronstein M, Chen SX, Collier DA, Craddock NJ, Kendler KS, Li T, O'Donovan M, O'Neill FA, Owen MJ, Walsh D, Weinberger DR, Sun C, Flint J, Darvasi A.

Genome-wide association identifies a common variant in the reelin gene that increases the risk of schizophrenia only in women. *PLoS Genetics.* 2008;4.

11. Stefansson H OR, Steinberg S, Andreassen OA, Cichon S, Rujescu D, Werge T, Pietilainen OP, Mors O, Mortensen PB, Sigurdsson E, Gustafsson O, Nyegaard M, Tuulio-Henriksson A, Ingason A, Hansen T, Suvisaari J, Lonnqvist J, Paunio T, Borglum AD.... Common variants conferring risk of schizophrenia. *Nature.* 2009;460:744-747.

12. Athanasiu L MM, Kahler AK, Brown A, Gustafsson O, Agartz I, Giegling I, Muglia P, Cichon S, Rietschel M, Pietilainen OP, Peltonen L, Bramon E, Collier D, Clair DS, Sigurdsson E, Petursson H, Rujescu D, Melle I, Steen VM, Djurovic S.... Gene variants associated with schizophrenia in a Norwegian genome-wide study are replicated in a large European cohort. *Journal of Psychiatric Research.* 2010;44:748-753.

13. Need AC GD, Weale ME, Maia J, Feng S, Heinzen EL, Shianna KV, Yoon W, Kasperaviciute D, Gennarelli M, Strittmatter WJ, Bonvicini C, Rossi G, Jayathilake K, Cola PA, McEvoy JP, Keefe RS, Fisher EM, St Jean PL, Giegling I, Hartmann AM, Moller HJ..... A genome-wide investigation of SNPs and CNVs in schizophrenia. *PLoS Genetics.* 2009;5.

14. Kirov G ZI, Georgieva L, Moskvina V, Nikolov I, Cichon S, Hillmer A, Toncheva D, Owen MJ, O'Donovan MC. A genome-wide association study in 574 schizophrenia trios using DNA pooling. *Molecular Psychiatry.* 2009;14:796-803.

15. Purcell SM WN, Stone JL, Visscher PM, O'Donovan MC, Sullivan PF, Sklar P. Common polygenic variation contributes to risk of schizophrenia and bipolar disorder. *Nature.* 2009;460:748-752.

16. Shi J LD, Duan J, Sanders AR, Zheng Y, Pe'er I, Dudbridge F, Holmans PA, Whittemore AS, Mowry BJ, Olincy A, Amin F, Cloninger CR, Silverman JM, Buccola NG, Byerley WF, Black DW, Crowe RR, Oksenberg JR, Mirel DB, Kendler KS, Freedman R, Gejman PV. Common

variants on chromosome 6p22.1 are associated with schizophrenia. *Nature.* 2009;460:753-757.

17. Sullivan PF LD, Tzeng JY, van den Oord E, Perkins D, Stroup TS, Wagner M, Lee S, Wright FA, Zou F, Liu W, Downing AM, Lieberman J, Close SL. Genomewide association for schizophrenia in the CATIE study : results of stage 1. *Molecular Psychiatry.* 2008;13:570-584.

18. The Schizophrenia Psychiatric Genome-Wide Association Study (GWAS) Consortium RS, Sanders AR, Kendler KS, Levinson DF, Sklar P, Holmans PA, Lin DY, Duan J, Ophoff RA, Andreassen OA, Scolnick E, Cichon S, St Clair D, Corvin A, Gurling H, Werge T, Ruj. Genome-wide association study identifies five new schizophrenia loci. *Nat Genet.* Sept 18 2011;43(10):969-976.

19. G Silberberg AD, R Pinkas-Kramarski, R Navon. The involvement of ErbB4 with schizophrenia: association and expression studies. *Am J Med Genet B Neuropsychiatr Genet.* 2006:142-148.

20. Hatzimanolis A MJ, Wang R, Li T, Wong PC, Nestadt G *et al*. Multiple variants aggregate in the neuregulin signaling pathway in a subset of schizophrenia patients. *Transl Psychiatry.* 2013;3:e264.

21. AJ Law JK, DR Weinberger, CS Weickert. Disease-associated intronic variants in the ErbB4 gene are related to altered ErbB4 splice-variant expression in the brain in schizophrenia. *Human Molecular Genetics.* 2008;16(2):129-141.

22. Zhang D SM, Mark M, Frantz G, Akita R, Sun Y, Hillan K, Crowley C, Brush J, Godowski PJ. Neuregulin-3 (NRG3): A novel neural tissue-enriched protein that binds and activates ErbB4. *Prc. Natl. Acad. Sci. USA.* 1997;94:9562-9567.

23. Stefansson H SE, Steinthorsdottir V, Bjornsdottir S, Sigmundsson T, Ghosh S, et al. Neuregulin 1 and susceptibility to schizophrenia. *Am J Hum Genet.* 2002;71:877-892.

24. Vernon H. unpublished data.

25. Mei L, Xiong W-C. Neuregulin 1 in neural development, synaptic plasticity and schizophrenia. *Nature Reviews Neuroscience.* 2008:437-452.

26. A B. The neuregulin signaling pathway and schizophrenia:from genes to synapses and neural circuits. *Brain Research Bull.* 2010;83:122-131.

27. Buonanno A FG. Neuregulin and ErbB receptor signaling pathways in the nervous system. *Current Opinion in Neurobiology.* 2001;11:287-296.

28. Assimacopoulos S GE, Ragsdale CW. Identification of a Pax6-Dependent Epidermal Growth Factor Family Signaling Source at the Lateral Edge of the Embryonic Cerebral Cortex. *The Journal of Neuroscience.* July 23 2003;23(16):6399-6403.

29. Anton ES GH, Weber JL, McCann C, Fischer TM, Cheung ID, Gassmann M, Messing A, Klein R, Schwab MH, Lloyd KCK, Lai C. Receptor tyrosine kinase ErbB4 modulates neuroblast migration and placement in the adult forebrain. *Nature Neuroscience.* December 2004;7(12):1319-1328.

30. H Li SC, T Hamasaki, CG Perez-Garcia, D DM O'Leary. Neuregulin repellent signaling via ErbB4 restricts GABAergic interneurons to. *Neural Development.* Feb 29 2012;7(10).

31. Fallin DM LV, Wolyniec PS, McGrath JA, Nestadt G, Valle D, Liang KY, Pulver AE. Genomewide Linkage Scan for Schizophrenia Susceptibility Loci among Ashkenazi Jewish Families Shows Evidence of Linkage on Chromosome 10q 22. *Am. J. Hum. Genet.* 2003;73:601-611.

32. Wang YC CJ, Chen ML, Chen CH, Lai IC, Chen TT, Hong CJ, Tsai SJ, Liou YJ. Neuregulin 3 Genetic Variations and Susceptibility to Schizophrenia in a Chinese Population. *Biol. Psychiatry.* 2008;64:1093-1096.

33. McGrath JA AD, Lasseter VK, Wolyniec PS, Fallin MD, Liang K, Nestadt G, Thornquist MH, Luke JR, Chen P, Valle D, Pulver AE. Familiality of Novel Factorial Dimensions of Schizophrenia. *Arch Gen Psychiatry.* June 2009;66(6):591-600.

34. Chen PL AD, Lasseter VK, McGrath JA, Fallin DM, Liang KY, Nestadt G, Feng, N, Steel G, Cutting AS, Wolyniec P, Pulver AE, Valle D. Fine Mapping on Chromosome 10q22-q23 Implicates Neuregulin 2 in Schizophrenia. *Am. J. Hum. Genet. .* 2009;84:21-34.

35. J Wing JN. Discriminating symptoms in schizophrenia. A report from the international pilot study of schizophrenia. *Arch. Gen. Psychiatry.* 1975.

36. Kao WT WY, Kleinman JE, Lipska BK, Hyde TM, Weinberger DR, Law AJ. Common genetic variation in Neuregulin 3 (NRG3) influences risk for schizophrenia and impacts NRG3 expression in human brain. *PNAS.* 2010;107(35):15619-15624.

37. Morar B DM, Waters FAV, Chandler D, Kalaydjieva L, Jablensky A. Neuregulin 3 (NRG3) as a susceptibility gene in a schizophrenia subtype with florid delusions and relatively spared cognition. *Molecular Psychiatry.* 2010:1-7.

38. AE Pulver PW, D Housman, HH Kazazian, SE Antonarakis, G Nestadt, VK Lasseter, JA McGrath, B Dombroski, M Karayiorgou, C Ton, JL Blouin, L Kempf. The Johns Hopkins University Collaborative Schizophrenia Study: an epidemiologic-genetic approach to test the heterogeneity hypothesis and identify schizophrenia susceptibility genes. *Cold Spring Harb Symp Quant Biol.* 1996;61:797-814.

39. Li H DR. Fast and accurate short read alignment with Burrows-Wheeler Transform. *Bionformatics.* 2009;25:1754-1760.

40. McKenna A HM, Banks E, Sivachenko A, Cibulskis K, Kernytsky A, Garimella K, Altshuler D, Gabriel S, Daly M, DePristo MA. The Genome Analysis Toolkit: a MapReduce framework for analyzing next-generation DNA sequencing data. *Genome Res.* Sep 2010;20(9):1297-1303.

41. Li H HB, Wysoker A, Fennell T, Ruan J, Homer N, Marth G, Abecasis H, Durbin R, 1000 Genome Project Data Processing Subgroup. The Sequence alignment/map (SAM) format and SAMtools. *Bioinformatics.* 2009;25:2078-2079.

42. Dudbridge F. Likelihood-Based Association Analysis for Nuclear Families and Unrelated Subjects with Missing Genotype Data. *Human Heredity.* 2008;66:87-98.

43. McGaughey D, Vinton R, Huynh J, Al-Said A, Beer M, McCallion A. Metrics of sequence constraint overlook regulatory sequences in an exhaustive analysis at phox2b. *Genome Res.* 2008:252-260.

44. Grice EA, Rochelle ES, Green ED, Chakravarti A, McCallion AS. Evaluation of the RET regulatory landscape reveals the biological relevance of a HSCR-implicated enhancer. *Human Molecular Genetics.* 2005:3837-3845.

45. Adamczyk A KA, Czapski GA, Strosznajdeer JB. alpha-synuclein induced cell death in mouse hippocampal (HT22) cells is mediated by nitric oxide-dependent activation of caspase-3. *FEBS Letters.* July 16 2010;584:3504-3508.

46. Ishizuka K KA, Oh EC, Kanki H, Seshadri S, Robinson JF, Murdoch H, Dunlop AJ, Kubo K, Furukori K, Huang B, Zeledon M, Hayashi-Takagi A, Okano H, Nakajima K, Houslay MD, Katsanis N, Sawa A. DISC1-dependent switch from progenitor proliferation to migration in the developing cortex. *Nature.* May 05 2011;473(7345):92-96.

47. Szymanski M WR, Bassett SS, Avramopoulos D. Alzheimer's risk variants in the clusterin gene are associated with alternative splicing. *Transl Psychiatry.* 2011;1:1-7.

48. Harismendy O NP, Strausberg RL, Wang X, Stockwell TB, Beeson KY, Schork NJ, Murray SS, Topol EJ, Levy S, Frazer KA. Evaluation of next generation sequencing platforms for population targeted sequencing studies. *Genome Biology.* March 27 2009;10.

49. Leff P MM, Canseco J, Calva JC, Flores A, Salazar A et al. . Cloning of a full-length Homo sapiens mRNA coding for a neuregulin 3 (NGR-3)-like protein. EMBL GenBank DDBJ databases2005.

50. Ye J. Gel Shift/EMSA Protocol. http://labs.pbrc.edu/generegulation/documents/Gelshift_001.pdf, 2011.

51. Lee D KR, Beer MA. Discriminative prediction of mammalian enhancers from DNA sequence. *Genome Res.* 2011;21(12):2167-2180.

52. Mulder KW WG, Timmers HThM. DNA damage and replication stress induced transcription of RNR genes is dependent on the Ccr4-Not complex. *Nucleic Acids Research.* 2005;33(19):6384-6392.

53. Winkler GS MK, Bardwell VJ, Kalkhoven E, Timmers HThM. Human Ccr4-Not complex is a ligand-dependent repressor of nuclear receptio-mediated transcription. *The EMBO Journal.* 2006;25:3089-3099.

54. Hanzawa H dRM, Albert TK, van der Vliet PC, Timmers HT and Boelens R The structure of the C4C4 RING finger of human NOT4 reveals features distinct from those of C3HC4 RING fingers. *J Biol Chem.* 2001;276:10185-10190.

55. Jaaro-Peled H AY, Pletnikov MV, Sawa A. Review of pathological hallmarks of schizophrenia: comparisons of genetic models with patients and nongenetic models. *Schizophr Bull.* 2010;36(2):301-313.

56. Mitchell KJ HZ, Moghaddam B, Sawa A. Following the genes: a framework for animal modeling of psychiatric disorders. *BMC Biol.* 2011;9(76).

57. P B. Of rats and schizophrenia. *J Psychiatry Neurosci.* 2007;32(1):8-10.

58. Powell CM MT. Schizophrenia-relevant behavioral testing in rodent models: a uniquely human disorder? *Biol. Psychiatry.* 2006;59:1198-1207.

59. van den Buuse M. Modeling the Positive Symptoms of Schizophrenia in Genetically Modified Mice: Pharmacology and Methodology Aspects. *Schizophr Bull.* 2010;36(2):246-270.

60. Geyer MA MK, Paylor R. Mouse genetic models for prepulse inhibition: an early review. *Mol Psychiatry.* 2002;7(10):1039-1053.

61. Flames N LJ, Garratt AN, Fischer TM, Gassmann M, Birchmeier C, Lai C, Rubenstein JL, Marin O. Short- and long-range attraction of cortical GABAergic interneurons by neuregulin-1. *Neuron.* 2004;44:251-261.

62. Sambrook J FE, Maniatis T, Fritsch EF, Maniatis T, Maniatis T. *Molecular cloning: A laboratory manual.* Cold Spring Harbor, NY: Cold Spring Harbor Laboratory Press; 1989.

63. Zhang L KC, Obie C, Abidi F, Schwartz CE, Stevenson RE, Valle D, Wang T. X chromosome cDNA microarray screening identifies a functional PLP2 promoter polymorphism enriched in patients with X-linked mental retardation. *Genome Res.* 2007;17(5):641-648.

64. Pletnikov MV AY, Nikolskaia O, Xu Y, Ovanesov MV, Huang H, Mori S, Moran TH, Ross CA. Inducible expression of mutant human DISC1 in mice is associated with brain and behavioral abnormalities reminiscent of schizophrenia. *Molecular Psychiatry.* 2008;13:173-186.

65. AdAmczyk A MR, Takamiya K, Yocum J, Krasnova IN, Calderon J, Cadet JL, Huganir RL, Pletnikov MV, Wang T. GluA3-deficiency in mice is associated with increased social and aggressive behavior and elevated dopamine in striatum. *Behavioural Brain Research.* 2012;229(1):265-272.

66. Pletnikov MV SZ, Sherstnev VV. Relationship between memory and fear: Developmental and pharmacological stuies. *Pharmacology Biochemistry and Behavior.* 1996;54(1):93-98.

67. Ayhan Y AB, Nomura J, Kim R, Ladenheim B, Krasnova IN, Sawa A, Margolis RL, Cadet JL, Mori S, Vogel MW, Ross CA, Pletnikov MV Differential effects of prenatal and postnatal expressions of mutant human DISC1 on neurobehavioral phenotypes in transgenic mice: evidence for eurodevelopmental origin of majot psychiatric disorders. *Molecular Psychiatry.* 2010;16(3):293-306.

68. Eddy NB LD. Synthetic analgesics. II. Dithienylbutenyl- and dithienylbutylamines. *J Pharmacol Exp Ther.* 1953;107(3):385-393.

69. Ouagazzal A-MR, David; Romand, Raymond. Effects of age-related hearing loss on startle reflex and prepulse inhibition in mice on pure and mixed C57BL and 129 genetic background. *Behavioural Brain Research.* 2006;172:307-315.

70. J.W. Rudy NCH, P. Matus-Amat. Understanding contextual fear conditioning: insights from a two-process model. *Neuroscience and Behavioral Reviews.* 2004;28:675-685.

71. Bailey KR CJ. Anxiety-Related Behaviors in Mice. In: JJ B, ed. *Methods of Behavior Analysis in Neuroscience 2nd Edition*. Boca Raton, FL: CRC Press; 2009.

72. Gerlai R PP, Erickson S. Heregulin, but not ErbB2 or ErbB3, heterozygous mutant mice exhibity hyperactivity in multiple behavioral tests. *Behavioural Brain Research.* 1999;109(2000):219-227.

73. Golub MS GS, Kent Lloyd KC. Behavioral characteristics of a nervous system-specific ErbB4 knock-out mouse. *Behavioural Brain Research.* 2004;153:159-170.

74. Wen L LY-S, Z X-H, Li X-M, Woo R-S, Chen Y-J, Yin D-M, Lai C, Terry AV, Vazdarjanova A, Xiong W-C, Mei L. Neuregulin 1 regulates pyramidal neuron activity via ErbB4 in parvalbumin-positive interneurons. *PNAS.* 2009;107(3):1211-1216.

75. Hu X HW, Diaconu C, Tang X, Kidd GJ, Macklin WB, Trapp BD, Yan R. Genetic deletion of BACE1 in mice affects remyelination of sciatic nerves. *FASEB J.* 2008;22(8):2970-2980.

76. Savonenko AV MT, Laird FM, Stewart K-A, Price DL, Wong PC. Alteration of BACE1-dependent NRG1/ErbB4 signaling and schizophrenia-like phenotypes in *BACE1*-null mice. *PNAS.* 2008;105(14):5585-5590.

77. Barros CS CB, Chamero P, Roberts AJ, Korzus E, Lloyd K, Stowers L, Mayford M, Halpain S, Muller U. Impaired maturation of dendritic spines without disorganization of cortical cell layers in mice lacking NRG1/ErbB signaling in the central nervous system. *PNAS.* 2009;106(11):4507-4512.

78. Nakazawa K ZV, Jiang Z, Nakao K, Kolata S, Zhang S, Belforte JE. GABAergic interneuron origin of schizoprhenia pathophysiology. *Neuropharmacology.* 2011:1-10.

79. Yee BK KR, von Boehmer L, Studer R, Benke D, Hangenbuch N, Dong Y, Malenka RC, Fritschy J-M, Bluethmann H, Feldon J, Mohler H, Rudolph U. A schizophrenia-related sensorimotor deficit links alpha3-containing $GABA_A$ receptors to a dopamine hyperfunction. *PNAS.*102(47):17154-17159.

80. Paylor R CJ. Inbred strain differences in prepulse inhibition of the mouse startle response. *Psychopharmacology (Berl).* 1997;132(2):169-180.

81. Insel T CBGM, Heinssen R, Pine DS, Quinn K, Sanislow C, Wang P. Research domain criteria (RDoC): toward a new classification framework for research on mental disorders. *Am J Psychiatry.* 2010;167(7):748-751.

Curriculum Vitae: Mariela Angela Zeledón A.

Address: 310 Crescent Village Circle Apt 1440, San José, CA 95134

Email: marielazeledon@gmail.com

Phone: (412) 841-9176

Citizenship: Dual citizen: USA and Costa Rica

Education

Johns Hopkins School of Medicine, Baltimore, MD

Doctor of Philosophy, Predoctoral Training Program in Human Genetics and Molecular Biology August 2008-January 2014

Advisors: David Valle and Akira Sawa

Carnegie Mellon University, Pittsburgh, PA

Bachelor of Science in Biological Sciences with a minor in Religious Studies, Science and Humanities Scholars Program, August 2004- May 2000

with University Honors

with College Honors from Mellon College of Science

with Departmental Honors from Department of Biological Sciences

Concentrations: Genetics and Molecular Biology

GPA: overall, 3.82; major, 3.94

Country Day School, San José, Costa Rica

Elementary School, Middle School and High School Diplomas, August 1991- June 2004

Salutatorian

National Honor Society Member

Relevant Coursework

Graduate:

Molecules and Cells*	Molecular Mechanisms of Disease
Fundamentals of Genetics	Teaching at the University Level
Cell Structure and Dynamics	Computational Biology and Informatics
Pathways and Regulation	Lectures in Pathology & Pathophysiology*
Molecular Biology and Genomics	Ethical, Legal and Social Issues in Genetics
Advanced Topics in Human Genetics	Organ Systems (Histology)*
Introduction to Neuroscience	Nonprofit Governance & Executive Leadership

*= medical school curriculum

Undergraduate:

Modern Biology	Modern Chemistry I and II	Genes and Diseases	Genetics
Biochemistry	Organic Chemistry I and II	Abnormal Psychology	Adv. Genetics
Cell Biology	Statistics for Lab Sciences	Adv. Molecular Biology	Physiology

Chemistry Laboratory 1: Introduction to Chemical Analysis

Chemistry Laboratory 2: Organic Synthesis and Analysis

Biology Laboratory 1: Experimental Techniques in Genetics and Molecular Biology

Biology Laboratory 2: Experimental Techniques in Cell and Developmental Biology

Technical Skills

Computer: MS Office Suite, Minitab, PageMaker, Metrowerks CodeWarrior, Adobe Suite, Basic programming in Java, CodonCode Aligner, UNPHASED, Volocity

Language: native Spanish, fluent English

Activities

Teaching Assistant, Evolution of the Concept of the Gene, Johns Hopkins School of Medicine:

Fall 2010

Teaching Assistant, Genetics, Carnegie Mellon University: Fall 2007

Carnegie Mellon University Judicial Board: Member, 2007-2008

Mellon College of Science Diversity Sub-committee: Member, 2007-2008

Lambda Sigma: Service and Honor Society for Sophomores: Vice President, Fall 2005; President,

Spring 2006

Research

Valle and Sawa Laboratories, Johns Hopkins School of Medicine. Thesis work on *NRG3* and its

role in mental illness and neurodevelopment. May 2009-November 2013

Avramopoulos and Michaelis Labs, Johns Hopkins School of Medicine. Rotations in Oct 2008-May 2009

Jones Laboratory (genetics), Carnegie Mellon. Spring 2006-May 2008 on *PBN1* project

Supported by Howard Hughes Medical Institute undergraduate support and Scholars program (Summer 2007), Small Undergraduate Research Grants

CIBCM (Center for Cellular & Molecular Biology Research), Universidad de Costa Rica

Internship, Genetics of Alcoholism, Genetics of Bipolar Disorder, Summer 2006

Mentoring and Volunteer Activities

Incentive Mentoring Program, Paul Laurence Dunbar High School: 2008-2013

*Development Officer 2012- 2013: *led a group of volunteers in fundraising annual budget goals through grantwriting and donor development. With the CEO, planned Development strategy. Responsible for organizing Baltimore Kitchen Cabinet event.*

Ensured fundraising strategies were deeply rooted in program values. Raised over $1 million.

*Baltimore Kitchen Cabinet moderator, June 2012: *facilitated discussion about teenage substance abuse with foundation and community leaders.*

*Development Committee member, 2011-2012: *wrote and edited grants, sent recognition to donors and assisted with seasonal projects*

*Brain Trust presenter, May 2011: *presented current Development strategy to a group of high-profile advisors from Baltimore community in order to gather ideas for future efforts.*

*GrandParent, 2010-2012: *Guided, supported and coordinated efforts of 5-7 Heads of Households and their mentors in supporting 5-7 at-risk students.*

*Head of Household, 2009-2010: *Coordinated and supported a group of mentors in customizing support for an at-risk student*

*Mentor, 2008-2013

*Recipient of the Excellence in Leadership Award

COMPASS program for coaching minority students in the sciences: Mentor, 2007-2008

Honors, Scholarships and Fellowships

2013 ASHG/Charles J. Epstein Trainee Award for Excellence in Human Genetics Research –

Semifinalist.

National Science Foundation Graduate Research Fellowship Program, May 2008-2013

Dr. J. Paul Fugassi and Linda E. Monteverde Award, 2008

Phi Beta Kappa, Honor Society, Spring 2008-present; active 2008-2009

Phi Kappa Phi, Honor Society, Spring 2007-present; active 2007-2008

Mortar Board Honor Society for Seniors, 2007-2008

Small Undergraduate Research Grant, Spring and Fall 2007, Spring 2008

Howard Hughes Medical Institute Scholars Program, Summer 2006

Mellon College of Science Dean's List, Fall 2004 and 2006; with High Honors, Spring/Fall 2005,

Spring 2006, Spring/Fall 2007 and Spring 2008

Science and Humanities Scholar Program, 2004-2008

Lambda Sigma Honor Society for Sophomores, 2005-2006

Carnegie Mellon full-tuition scholarship for 2004-2008

Publications

Identification and functional studies of regulatory variants responsible for the association of *NRG3* with a delusion phenotype in schizophrenia. **Zeledón M.**, Taub M., Eckart N., Vernon H., Szymanski M., Wang R., Chen P., Nestadt G., McGrath J.A., Sawa, A., Pulver A.E., Avramopoulos, D., Valle, D. Under review.

Zeledón M., Taub M., Eckhart N., Beer M., Wang R., Szymanski M., Chen P., Pulver A., McGrath J.A., Wolyniec P., Avramopoulos, D., Sawa, A., Valle, D. Variants in NRG3 associated with delusion have regulatory potential and differentially bind to nuclear proteins; (Abstract/Program # 58). Presented at the 63rd Annual Meeting of The American Society of Human Genetics, October 23, 2013, Boston, MA.

Synapse-specific contributions in the cortical pathology of schizophrenia. Seshadri, S., **Zeledón, M.**, Sawa, A. Neurobiol Dis. Epub 2013 Jan 18 PMID:23336981

Zeledón M., Taub M., Eckhart N., Wang R., Szymanski M., Chen P., Pulver A., McGrath J.A., Avramopoulos, D., Sawa, A., Valle, D. Delusion-associated SNPs in *NRG3* show regulatory potential, dysregulate *NRG3* splicing and differentially bind to nuclear proteins; (Abstract/Program # 2461T). Presented at the 62nd Annual Meeting of The American Society of Human Genetics, November 8, 2012, San Francisco, CA.

Zeledón M., Taub M., Eckhart N., Szymanski M., Wang R., Chen P., Pulver A., Avramopoulos, D., Sawa, A., Valle, D. Variants in *NRG3* at 10q23.1 correlated with a subtype of schizophrenia with severe delusions; (Abstract/Program # 552W). Presented at the 12th International Congress of Human Genetics/61st Annual Meeting of The American Society of Human Genetics, October 12, 2011, Montreal, Canada.

Zeledón M., Taub M., Chen P., Pulver A., Avramopoulos, D., Sawa, A., Valle, D. Microdeletion in 10q23.1 correlated with a subtype of Schizophrenia with severe delusions; Presented at the XIXth World Congress of Psychiatric Genetics, September 12, 2011, Washington, DC.

DISC1-dependent switch from progenitor proliferation to migration in the developing cortex. Ishizuka K, Kamiya A, Oh EC, Kanki H, Seshadri S, Robinson JF, Murdoch H, Dunlop AJ, Kubo KI, Furukori K, Huang B, **Zeledón M**, Hayashi-Takagi A, Okano H, Nakajima K, Houslay MD, Katsanis N, Sawa A. Nature. 2011 May 5 PMID:21471969

A novel balanced chromosomal translocation found in subjects with schizophrenia and schizotypal personality disorder: altered L-serine level associated with disruption of PSAT1 gene expression. Ozeki Y, Pickard BS, Kano SI, Malloy MP, **Zeledón M**, Sun DQ, Fujii K, Wakui K, Shirayama Y, Fukushima Y, Kunugi H, Hashimoto K, Muir WJ, Blackwood DH, Sawa A. Neurosci Res. 2010 Oct 15. PMID: 20955740